

A chaotic lattice field theory in two dimensions

P Cvitanović and H Liang

Center for Nonlinear Science, School of Physics, Georgia Institute of Technology,
Atlanta, GA 30332-0430, USA

E-mail: predrag.cvitanovic@physics.gatech.edu

Draft as of February 16, 2024

Abstract.

We describe spatiotemporally chaotic (or turbulent) field theories discretized over d -dimensional lattices in terms of sums over their multi-periodic orbits. ‘Chaos theory’ is here recast in the language of statistical mechanics, field theory, and solid state physics, with the traditional periodic orbits theory of low-dimensional, temporally chaotic dynamics a special, one-dimensional case.

In the field-theoretical formulation, there is no time evolution. Instead, treating the temporal and spatial directions on equal footing, one determines the spatiotemporally periodic orbits that contribute to the partition sum of the theory, each a solution of the system’s defining deterministic equations, with sums over time-periodic orbits of dynamical systems theory now replaced by sums of d -periodic orbits over d -dimensional spacetime geometries, the weight of each orbit given by the Hill determinant of its spatiotemporal orbit Jacobian matrix. Each weight can be computed by application of the Bloch theorem to evaluation of the spectrum of periodic orbit’s Jacobian operator. The weights are multiplicative, leading to a spatiotemporal zeta function formulation of the theory in terms of prime orbits. The shadowing of large periodic orbits by smaller ones then ensures that the predictions of the theory are dominated by the shortest spatiotemporal periods field configurations.

PACS numbers: 02.20.-a, 05.45.-a, 05.45.Jn, 47.27.ed

A temporally chaotic system is exponentially unstable with time: double the time, and exponentially more orbits are required to cover its strange attractor to the same accuracy. For a system of large spatial extent, the complexity of the spatial shapes also needs to be taken into account; double the spatial extent, and exponentially as many distinct spatial patterns will be required to describe the repertoire of system’s shapes to the same accuracy. Systems whose temporal and spatial correlations decay sufficiently fast, and whose ‘physical’ dimension [43, 64] grows linearly with system’s spacetime volume, are said to be ‘spatiotemporally chaotic.’

Our goal here is to make this ‘spatiotemporal chaos’ tangible and precise, in a series of papers that introduce its theory and its implementations. The companion paper I [93] focuses on the $1d$ chaotic lattice field theory, and a novel treatment of time-reversal invariance. In this paper, paper II, we develop the theory of $2d$ spatiotemporal chaotic systems; and in the companion paper III [146] we apply the theory to nonlinear

field theories. As our intended audience spans many, usually disjoint specialties, from fluid dynamics to field theory, the exposition entails much pedagogical detail, so let us start by stating succinctly what the central novelty of our theory is.

There are two ways of studying translationally-invariant systems:

(i) In the textbook ‘QM-in-a-box’ approach, one starts by confining a system to a *finite* box, then takes the box size to infinity. In dynamical systems this point of view leads to the Gutzwiller-Ruelle [40, 73, 126] periodic orbit formulation of chaotic dynamics. This approach is hampered by one simple fact that complicates everything: the periodic orbit weight is *not* multiplicative for its repeats,

$$\det(\mathbf{1} - \mathbb{J}_p^r) \neq [\det(\mathbf{1} - \mathbb{J}_p)]^r .$$

(ii) A crystallographer or field theorist starts with an *infinite* lattice or continuous spacetime. The approach –as we show here– yields weights that are multiplicative for repeats of spatiotemporally periodic solutions,

$$\text{Det } \mathcal{J}_{rp} = (\text{Det } \mathcal{J}_p)^r .$$

This fact simplifies everything, and yields the main result of this paper, a zeta function for field theories in two spatiotemporal dimensions (section 7).

Analysis of a temporally chaotic dynamical system typically starts with establishing that a temporal flow (perhaps reduced to discrete time maps by Poincaré sections) is locally stretching, globally folding. Its state space is partitioned, the partitions labeled by an alphabet, and the qualitatively distinct solutions classified by their temporal symbol sequences [40].

We do not do this here: instead, we find that the natural language to describe ‘spatiotemporal chaos’ and ‘turbulence’ is the formalism of field theory. Furthermore – just as the discretization of time by Poincaré sections aids analysis of temporal chaos– we find it convenient to discretize both time and space. Spatiotemporally steady turbulent flows offer one physical motivation for considering such models: a rough approximation to such flows is obtained discretizing them into spatiotemporal cells, with each cell turbulent, and cells coupled to their nearest neighbors. Lattices also arise naturally in many-body problems, such as many-body quantum chaos models studied in [1, 2, 52, 121]. The observation that for spatiotemporally chaotic systems space and time should be considered on the same footing goes back to the ‘chronotopic’ program of Politi and collaborators [63, 88, 89, 119] who, in their studies of propagation of spatiotemporal disturbances in extended systems, discovered that the spatial stability analysis can be combined with the temporal stability analysis. For someone versed in fluid dynamics or atomic physics the most disconcerting aspect of the field-theoretic perspective is that time is just one of the coordinates over which a field configuration is defined: each field-theoretic solution is a ‘static’ solution over the infinite spacetime. There is *no* ‘evolution in time’.

We start our formulation of chaotic field theory (section 1) by defining the field theory partition sums in terms of spatiotemporally periodic states (section 1.1), and emphasizing throughout the paper the importance of carrying out calculations on the

reciprocal lattice (section 1.4). In section 1.7 we explain the connection between the work presented here and Gutzwiller’s semiclassical quantization, and why the semiclassical field theory, given by the WKB approximation to quantum field theory, has support on the same set of solutions as the *deterministic field theory* (section 1.8). While the formulation provides a framework for studying the quantum behavior of deterministically chaotic spatiotemporal systems, we focus in this triptych of papers only on the structure of the deterministically chaotic field theories. Their building blocks are spatiotemporally periodic solutions of system’s defining equations, which we refer to as *periodic states* (section 1.9).

In section 2 we introduce the field theories studied here, in particular the simplest of chaotic field theories, the spatiotemporal cat [70, 71] that captures the essence of spatiotemporal chaos (section 2.1; for its history, see Appendix A). Spatiotemporal cat is a discretization of the compact boson Klein-Gordon equation,

$$(-\square + \mu^2)\Phi - \mathbf{M} = 0,$$

a deterministic field theory with an unstable ‘anti-harmonic cat’ ϕ_z of mass μ at each lattice site z , a ‘cat’ who, when pushed, gives rather than pushes back. Crucial to ‘chaos’ is the notion of stability: in section 3 we describe spatiotemporal stability of above field theories’ periodic states in terms of their orbit Jacobian operators.

Periodic orbit theory for a time-evolving dynamical system on a one-dimensional temporal lattice is organized by grouping orbits of the same period together [40, 60, 73, 93, 126]. For systems characterized by several translational symmetries, one has to take care of multiple periodicities, in the language of crystallography, organize the periodic orbit sums by corresponding *Bravais lattices*, or, in the language of field theory, by the ‘sum over *geometries*’. In sections 4 and 5 we enumerate and construct spacetime geometries, or $d = 2$ Bravais lattices $[L \times T]_S$, of increasing spacetime periodicities. The classification of periodic states proceeds in two steps. On the coordinate level, periodicity is imposed by the hierarchy of Bravais lattices of increasing periodicities (section 4.1). On the field-configuration level, the key to the spatiotemporal periodic orbit theory is the enumeration and determination of *prime orbits*, the basic building blocks of periodic orbit theory (section 5.4).

The likelihood of each solution is given by the Hill determinant, the determinant of its spatiotemporal orbit Jacobian matrix. Compared to the temporal-evolution chaos theory, the Hill determinant is the central innovation of our field-theoretic formulation of chaotic field theory, so we return to it throughout the paper. We discuss its computation in section 6. In section 6.4 we define the stability exponent of a periodic state over spatiotemporally infinite Bravais lattice, and show how to compute it on the reciprocal lattice. For spatiotemporal cat we evaluate and cross-check Hill determinants by two methods, either on the reciprocal lattice (section 6.3), or by the ‘fundamental fact’ evaluation (Appendix C).


Having enumerated all Bravais lattices (section 4), determined periodic states over each (section 5), computed the weight of each periodic state (section 6), we can now write

down the deterministic field theory partition function as a sum over all spatiotemporal solutions of the theory (section 7). In section 7.1 we reexpress the partition function in terms of prime orbits, and in section 7.2 we construct the spatiotemporal zeta function and explain how it can be used to compute expectation values of observables in deterministic chaotic field theories. What makes these resummations possible is the multiplicative property of Hill determinants announced at the start of this introduction, provided by their evaluation over the spatiotemporally infinite Bravais lattice (section 6.4), rather than being approximated by finite-dimensional matrices.

How is this global, high-dimensional orbit stability related to the stability of the conventional low-dimensional, forward-in-time evolution? The two notions of stability are related by Hill's formulas, relations that rely on higher-order derivative equations being rewritten as sets of first order ODEs, formulas equally applicable to energy conserving systems, as to viscous, dissipative systems. We derive them in [93, 94]. From the field-theoretic perspective, Hill determinants are fundamental, forward-in-time evolution (a transfer matrix method) is merely one of the methods for computing them.

Finally, we know that cycle-expansions' convergence is accelerated by shadowing of long orbits by shorter periodic orbits [10]. In section 8 we check numerically that spatiotemporal cat periodic states that share finite spatiotemporal mosaics shadow each other to exponential precision. This shadowing property ensures that the predictions of the theory are dominated by the shortest period prime orbits.

This completes our generalization [41, 70, 93, 146] of the temporal-evolution deterministic chaos theory [40, 60] to spatiotemporal chaos / turbulence, and recasts both in the formalism of conventional solid state physics, field theory, and statistical mechanics.

Our results are summarized and open problems discussed in section 9. Appendices contain calculations omitted from the main body of the text. Icon  on the margin links a block of text to a supplementary online video. For additional material -online talks and related papers- see ChaosBook.org/overheads/spatiotemporal. We refer the reader to Appendix A of paper I for an in-depth review of the historical context of our formulation of chaotic field theory.

1. Lattice field theory

In a d -dimensional hypercubic discretization of a Euclidean space, the d continuous Euclidean coordinates $x \in \mathbb{R}^d$ are replaced by a hypercubic integer lattice [107, 111]

$$\mathcal{L} = \left\{ \sum_{j=1}^d z_j \mathbf{e}_j \mid z \in \mathbb{Z}^d \right\}, \quad \mathbf{e}_j \in \{\mathbf{e}_1, \mathbf{e}_2, \dots, \mathbf{e}_d\}, \quad (1)$$

spanned by a set of orthogonal unit vectors \mathbf{e}_j , with lattice spacing $a_j = |\mathbf{e}_j| = \Delta x_j$ along the direction of unit vector \mathbf{e}_j . We shall use lattice units, almost always setting

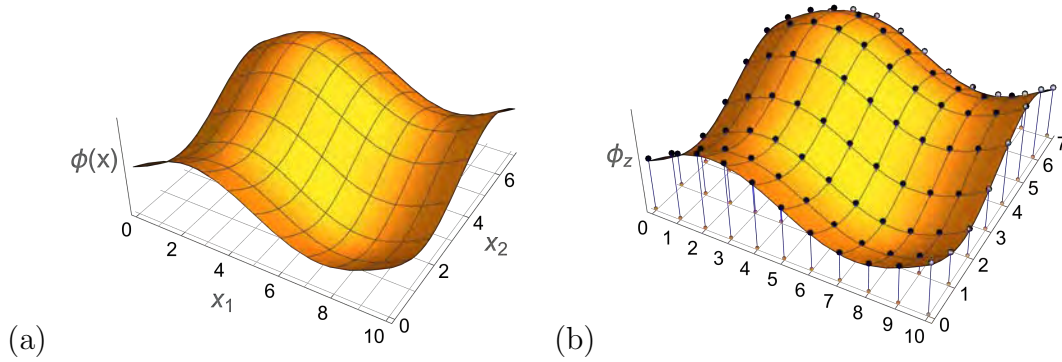


Figure 1. (Color online) Discretization of a field over two-dimensional spacetime. (a) A periodic scalar field configuration $\phi(x)$ over a primitive cell of spatial period L , temporal period T , plotted as a function of continuous coordinates $x \in \mathbb{R}^2$. (b) The corresponding discretized field configuration (3) over primitive cell $[10 \times 7]_0$, with the field value ϕ_z at the lattice site $z \in \mathbb{Z}^2$ indicated by a dot.

$a_j = 1$ (for another choice, see (88)). A field $\phi(x)$ over d continuous coordinates x_j is represented by a discrete array of field values over lattice sites

$$\phi_z = \phi(x), \quad x_j = a_j z_j = \text{lattice site}, \quad z \in \mathbb{Z}^d, \quad (2)$$

as sketched in figure 1. A lattice *field configuration* is a d -dimensional array of field values (in what follows, illustrative examples will be presented in one or two spatiotemporal dimensions)

$$\Phi = \begin{array}{ccccccc} \cdots & \cdots & \cdots & \cdots & \cdots & \cdots & \cdots \\ \cdots & \phi_{-2,1} & \phi_{-1,1} & \phi_{0,1} & \phi_{1,1} & \phi_{2,1} & \cdots \\ \cdots & \phi_{-2,0} & \phi_{-1,0} & \phi_{0,0} & \phi_{1,0} & \phi_{2,0} & \cdots \\ \cdots & \phi_{-2,-1} & \phi_{-1,-1} & \phi_{0,-1} & \phi_{1,-1} & \phi_{2,-1} & \cdots \\ \cdots & \cdots & \cdots & \cdots & \cdots & \cdots & \cdots \end{array} . \quad (3)$$

A field configuration is a *point* in system's *state space*

$$\mathcal{M} = \{ \Phi \mid \phi_z \in \mathbb{R}, z \in \mathbb{Z}^d \}, \quad (4)$$

the totality of ‘states’ Φ , given by all possible values of site fields, where ϕ_z can be a single scalar field, or a multiplet of real or complex fields.

While we refer here to such discretization as a lattice field theory, the lattice might arise naturally from a many-body setting with the nearest neighbors interactions, such as many-body quantum chaos models studied in [1, 2, 52, 121], with a multiplet of fields at every site [71].

1.1. Periodic field configurations

A lattice field configuration is \mathcal{L}_Λ -periodic if

$$\phi_{z+r} = \phi_z \quad (5)$$

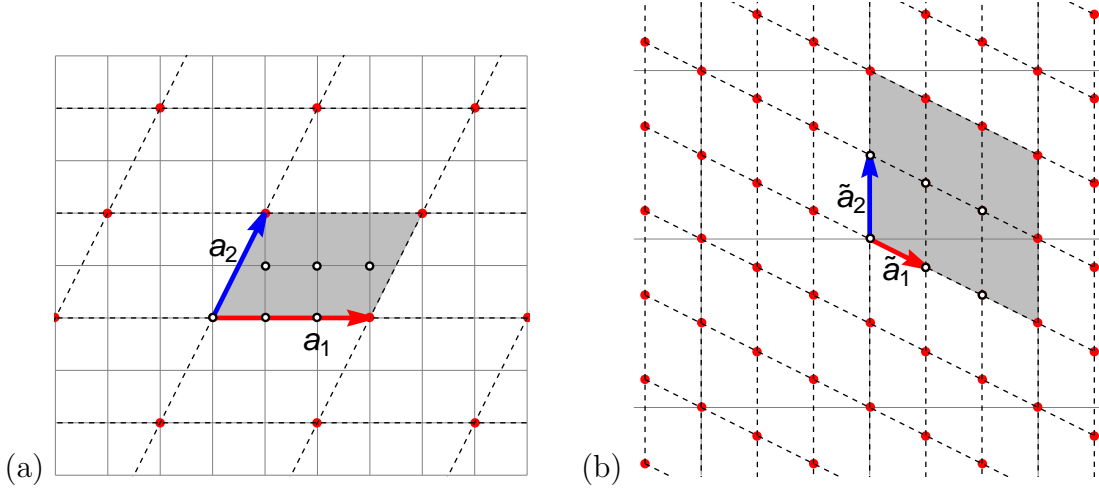


Figure 2. (Color online) (a) The intersection points z of the light grey lines form the integer square lattice (2). The primitive vectors $\mathbf{a}_1 = (3, 0)$ and $\mathbf{a}_2 = (1, 2)$ form the primitive cell $\mathbb{A} = [3 \times 2]_1$ (see (6) and (87)), whose translations tile the Bravais lattice $\mathcal{L}_{\mathbb{A}}$ (red points). (b) The intersection points k of the light grey lines form the reciprocal square lattice. Translations of reciprocal primitive vectors $\tilde{\mathbf{a}}_1$ and $\tilde{\mathbf{a}}_2$ (see (18) and (95)) generate the reciprocal lattice $\mathcal{L}_{\tilde{\mathbb{A}}}$ (red points). (Shaded) The reciprocal primitive cell $\tilde{\mathbb{A}}$. A wave vector outside this region is equivalent to a wave vector within it by a reciprocal lattice translation. Note that the number of lattice sites within the reciprocal primitive cell $\tilde{\mathbb{A}}$ equals the number of sites within the spatiotemporal primitive cell \mathbb{A} . Continued in figure 6.

for any discrete translation $\mathbf{r} = n_1 \mathbf{a}_1 + n_2 \mathbf{a}_2 + \cdots + n_d \mathbf{a}_d$ in the *Bravais lattice*

$$\mathcal{L}_{\mathbb{A}} = \left\{ \sum_{j=1}^d n_j \mathbf{a}_j \mid n_j \in \mathbb{Z} \right\}, \quad (6)$$

where the $[d \times d]$ matrix $\mathbb{A} = [\mathbf{a}_1, \mathbf{a}_2, \dots, \mathbf{a}_d]$ formed from primitive lattice vectors $\{\mathbf{a}_j\}$ defines a d -dimensional *primitive cell* [14, 37] (see figure 2(a)).

Primitive cell \mathbb{A} field configuration lattice-site fields (3) take values in the $N_{\mathbb{A}}$ -dimensional state space

$$\mathcal{M}_{\mathbb{A}} = \{ \Phi \mid \phi_z \in \mathbb{R}, z \in \mathbb{A} \}. \quad (7)$$

If the lattice spacing (2) is set to 1, the *volume* of Bravais lattice $\mathcal{L}_{\mathbb{A}}$ equals the number of lattice sites $z \in \mathbb{A}$ within the primitive cell (see figures 2 and 6):

$$N_{\mathbb{A}} = |\text{Det } \mathbb{A}|. \quad (8)$$

For example, repeats of the $N_{\mathbb{A}} = 15$ -dimensional $[5 \times 3]$ primitive cell field configuration

$$\Phi = \begin{bmatrix} \phi_{-2,1} & \phi_{-1,1} & \phi_{0,1} & \phi_{1,1} & \phi_{2,1} \\ \phi_{-2,0} & \phi_{-1,0} & \phi_{0,0} & \phi_{1,0} & \phi_{2,0} \\ \phi_{-2,-1} & \phi_{-1,-1} & \phi_{0,-1} & \phi_{1,-1} & \phi_{2,-1} \end{bmatrix} \quad (9)$$

tile periodically the doubly-infinite state space (3). For details, see section 4.

1.2. Orbits

Consider a one-dimensional primitive cell \mathbb{A} , defined by a single primitive vector $\mathbf{a}_1 = n$ in (6). One-lattice-spacing shift operator

$$\mathbf{r}_{zz'} = \delta_{z+1,z'}, \quad \mathbf{r} = \begin{pmatrix} 0 & 1 & & & \\ & 0 & 1 & & \\ & & \ddots & \ddots & \\ & & & 0 & 1 \\ 1 & & & & 0 \end{pmatrix}, \quad (10)$$

is a cyclic permutation operator that translates a field configuration by one lattice site,

$$\begin{aligned} \Phi &= [\phi_0 \phi_1 \phi_2 \phi_3 \cdots \phi_{n-1}] \\ \mathbf{r}\Phi &= [\phi_1 \phi_2 \phi_3 \cdots \phi_{n-1} \phi_0], \quad \text{or} \quad (\mathbf{r}\Phi)_z = \phi_{z+1}, \\ &\dots \\ \mathbf{r}^{n-1}\Phi &= [\phi_{n-1} \phi_0 \phi_1 \phi_2 \cdots \phi_3], \\ \mathbf{r}^n\Phi &= [\phi_0 \phi_1 \phi_2 \phi_3 \cdots \phi_{n-1}], \quad \text{so} \quad \mathbf{r}^n\Phi = \Phi. \end{aligned} \quad (11)$$

While each field configuration $\mathbf{r}^j\Phi$ might be a distinct point in the primitive cell's state space (7), they are equivalent, in the sense that they all consist of the same set of lattice site fields $\{\phi_z\}$, up to a cyclic relabelling of lattice sites.

In this way actions of a group of relabelling permutations $g \in G$ on field configurations over a multi-periodic primitive cell \mathbb{A} foliate the state space into a union

$$\mathcal{M}_{\mathbb{A}} = \{\Phi\} = \cup \mathcal{M}_p \quad (12)$$

of *orbits*,

$$\mathcal{M}_p = \{g\Phi_p \mid g \in G\} \quad (13)$$

each a set of equivalent field configurations, labelled p , or perhaps by Φ_p , one of the configurations in the set. By construction, each orbit is a fixed point of G , as for any element $g\mathcal{M}_p = \mathcal{M}_p$. The number of distinct field configurations in the orbit is known as the *index* of orbit \mathcal{M}_p . It can be as large as $|G|$, the number of elements in G , or as small as 1, if the field configuration is a $\phi_z = \phi$ steady state (for further details, see section 5.1).

1.3. Prime orbits

Consider a period-6 field configuration (11) over a primitive cell $2\mathbb{A}$ obtained by a repeat of a primitive cell \mathbb{A} period-3 field configuration,

$$\begin{aligned} \Phi_{2\mathbb{A}} &= [\phi_0 \phi_1 \phi_2 \phi_0 \phi_1 \phi_2], & \Phi_{\mathbb{A}} &= [\phi_0 \phi_1 \phi_2] \\ \mathbf{r}\Phi_{2\mathbb{A}} &= [\phi_1 \phi_2 \phi_0 \phi_1 \phi_2 \phi_0], & \mathbf{r}\Phi_{\mathbb{A}} &= [\phi_1 \phi_2 \phi_0] \\ \mathbf{r}^2\Phi_{2\mathbb{A}} &= [\phi_2 \phi_0 \phi_1 \phi_2 \phi_0 \phi_1], & \mathbf{r}^2\Phi_{\mathbb{A}} &= [\phi_2 \phi_0 \phi_1] \end{aligned} \quad (14)$$

The period of both orbits is 3. If lattice fields ϕ_z do not take the same value (they are not repeats of a period-1, steady state $\phi_z = \phi$), both orbits contain 3 distinct field

configurations. On the Bravais lattice $\mathcal{L}_{\mathbb{A}}$ the period-3 orbit $\mathcal{M}_p = (\Phi_{\mathbb{A}}, r\Phi_{\mathbb{A}}, r^2\Phi_{\mathbb{A}})$ is a *prime orbit*, an orbit whose field configurations are not repeats of shorter period field configurations. On the Bravais lattice $\mathcal{L}_{2\mathbb{A}}$, the period-3 field configuration $\Phi_{2\mathbb{A}}$ is a *repeat* of a prime orbit. This is how ‘prime periodic orbits’ and their repeats work for the one-dimensional, temporal lattice [40]. We shall explain how repeats work for a two-dimensional square lattice in section 5.3.

The totality of field configurations (4) can now be constructed by (i) determining prime orbits for each primitive cell \mathbb{A} , and (ii) including their repeats into field configurations over sublattices $\mathcal{L}_{\mathbb{A}\mathbb{R}}$. Our task is to identify, compute and weigh *the totality* of these prime orbits for a given chaotic field theory.

1.4. Reciprocal primitive cell

Translation invariance of orbits suggests reformulating the theory in a discrete Fourier basis, a discretization approach that goes all the way back to Hill’s 1886 paper [74].

The n consecutive shifts (11) return a period- n field configuration to itself, so acting on a one-dimensional periodic primitive cell, shift operator satisfies the characteristic equation

$$r^n - \mathbb{1} = \prod_{m=0}^{n-1} (r - e^{ik} \mathbb{1}) = 0, \quad (15)$$

with the n -th roots of unity eigenvalues $\{e^{ik}\}$ indexed by integers m

$$k = \frac{2\pi}{n}m, \quad m = 0, 1, \dots, n-1, \quad (16)$$

and n eigenvectors

$$r\varphi(k) = e^{ik}\varphi(k), \quad [\varphi(k)]_z = e^{ikz}. \quad (17)$$

The shift (11)

$$[r\varphi(k)]_z = [\varphi(k)]_{z+1} = e^{ik(z+1)} = e^{ik}[\varphi(k)]_z$$

acts by rotating the eigenvector’s overall phase.

Wave numbers k form a one-dimensional Bravais lattice, called reciprocal lattice,

$$\mathcal{L}_{\tilde{\mathbb{A}}} = \left\{ m\tilde{\mathbf{a}}_1 \mid m \in \mathbb{Z} \right\}, \quad \tilde{\mathbf{a}}_1 \cdot \mathbf{a}_1 = 2\pi,$$

with the primitive reciprocal lattice vector $\tilde{\mathbf{a}}_1 = 2\pi/n$, and the reciprocal primitive cell –the interval $[0, 2\pi)$ – that contains n distinct wave numbers (16).

For a d -dimensional $\mathcal{L}_{\mathbb{A}}$ -periodic Bravais lattice, discrete wave vectors \mathbf{k} form a reciprocal lattice spanned by d reciprocal primitive vectors which satisfy

$$\mathcal{L}_{\tilde{\mathbb{A}}} = \left\{ \sum_{j=1}^d m_j \tilde{\mathbf{a}}_j \mid m_j \in \mathbb{Z} \right\}, \quad \tilde{\mathbf{a}}_i \cdot \mathbf{a}_j = 2\pi\delta_{ij}. \quad (18)$$

Assembling the reciprocal primitive vectors $\{\tilde{\mathbf{a}}_j\}$ into columns of the $[d \times d]$ reciprocal primitive cell matrix $\tilde{\mathbb{A}} = [\tilde{\mathbf{a}}_1, \tilde{\mathbf{a}}_2, \dots, \tilde{\mathbf{a}}_d]$, the reciprocity condition (18) takes form

$$\tilde{\mathbb{A}}^\top \mathbb{A} = 2\pi \mathbb{1}. \quad (19)$$

An example, worked out in section 4.2, is given in figure 2 (b). The reciprocity condition (18) maps a field configuration Φ (7) over the primitive cell \mathbb{A} into the reciprocal field configuration $\tilde{\Phi}$ over $N_{\mathbb{A}}$ reciprocal lattice sites \mathbf{k} within the interior of the reciprocal primitive cell $\tilde{\mathbb{A}}$ (the shaded parallelogram in figure 2 (b)). The reciprocal state space (the space of discrete Fourier coefficients),

$$\mathcal{M}_{\tilde{\mathbb{A}}} = \left\{ \tilde{\Phi} \mid \tilde{\phi}_{\mathbf{k}} \in \mathbb{C}, \mathbf{k} \in \tilde{\mathbb{A}} \right\}, \quad (20)$$

is naturally foliated by orbits: on the reciprocal lattice all field configurations in an orbit such as (11) have the same magnitude $|\tilde{\phi}_{\mathbf{k}}|$ reciprocal lattice site fields, with a translation in j th direction $\Phi \rightarrow \mathbf{r}_j \Phi$ only affecting their phases (17).

1.5. Reciprocal Bravais lattice

Consider next a primitive cell of volume $2N_{\mathbb{A}}$ obtained by joining a primitive cell \mathbb{A} and its repeat. The reciprocal primitive cell is the same, but now there are $2N_{\mathbb{A}}$ reciprocal lattice sites within it. Repeat this in all possible ways (see section 5.3). The result is a tiling of the infinite Bravais lattice $\mathcal{L}_{\mathbb{A}}$ by all repeats of \mathbb{A} , with the infinity of reciprocal lattice sites all within the reciprocal primitive cell $\tilde{\mathbb{A}}$ (the shaded region in figure 2 (b)). The Fourier transform $\tilde{\Phi}(\mathbf{k})$ of an $\mathcal{L}_{\mathbb{A}}$ -periodic field configuration Φ now has the wave vector \mathbf{k} taking a continuum of values within the reciprocal primitive cell.

The key tool that a crystallographer uses next is the Bloch (or Floquet) theorem [14, 25, 56]: A linear operator acting on field configurations with periodicity of Bravais lattice $\mathcal{L}_{\mathbb{A}}$ has continuous spectrum, with the lattice sites z eigenfunctions of form

$$[\varphi^{(\alpha)}(\mathbf{k})]_z = e^{i\mathbf{k} \cdot z} [u^{(\alpha)}(\mathbf{k})]_z, \quad \mathbf{k} \in \mathbb{B}, \quad z \in \mathbb{A}, \quad (21)$$

where $u^{(\alpha)}(\mathbf{k})$ are band-index $\alpha = 1, 2, \dots, N_{\mathbb{A}}$ labelled distinct $\mathcal{L}_{\mathbb{A}}$ -periodic functions, and the continuous wave numbers \mathbf{k} are restricted to a Brillouin zone \mathbb{B} .

1.6. Observables

The field theory is formulated over the set of *all* $\mathcal{L}_{\mathbb{A}} \subset \mathcal{L}$ spatiotemporally *infinite* Bravais sublattices (6) of the hypercubic lattice (1). Periodic field configuration calculations are carried out either over a finite volume primitive cell \mathbb{A} , or over the infinite Bravais lattice. In what follows, suffix $(\dots)_{\mathbb{A}}$ indicates that the calculation is carried out over the $N_{\mathbb{A}}$ primitive cell lattice-site fields.

An example of such calculation is the evaluation of expectation values of an *observable*. An observable ‘ a ’ is a function or a set of field configuration functions $a[\Phi]$, evaluated on each lattice site $a_z = a_z[\Phi]$. For a given $\mathcal{L}_{\mathbb{A}}$ -periodic field configuration Φ , the *Birkhoff average* of observable a is given by the Birkhoff sum A ,

$$\langle a \rangle[\Phi]_{\mathbb{A}} = \frac{1}{N_{\mathbb{A}}} A[\Phi]_{\mathbb{A}}, \quad A[\Phi]_{\mathbb{A}} = \sum_{z \in \mathbb{A}} a_z. \quad (22)$$

For example, if the observable is the field itself, $a_z = \phi_z$, the Birkhoff average over the lattice field configuration Φ is the average ‘height’ of the field in figure 1 (b).

To be able to evaluate expectation values of observables, we need to know the probability amplitude (quantum theory, section 1.7), or the probability (deterministic theory, section 1.8) of field configuration Φ .

For pedagogical reasons, we introduce the two theories by first restricting them to finite-dimensional state space (7) of a primitive cell \mathbb{A} . These finite volumes are not meant to serve as finite approximations to the infinite Bravais lattices $\mathcal{L}_{\mathbb{A}}$: as is standard in solid state physics, the actual calculations are always carried out over the infinite lattice, more precisely (not standard in solid state physics, but necessary to describe a chaotic field theory) over the set of all periodic lattice field configurations (5) over all Bravais lattices $\mathcal{L}_{\mathbb{A}}$ (6), or, in language of field theory [102], as the ‘sum over geometries’.

The reader might prefer to skip the next two, largely motivational sections, go directly to section 2, taking the deterministic partition function (41) as the starting point for what follows.

1.7. Semiclassical field theory

In the path integral formulation of quantum field theory, a field configuration Φ over primitive cell \mathbb{A} occurs with probability *amplitude* density

$$p_{\mathbb{A}}[\Phi] = \frac{1}{Z_{\mathbb{A}}} e^{\frac{i}{\hbar} S[\Phi]}, \quad Z_{\mathbb{A}} = Z_{\mathbb{A}}[0], \quad (23)$$

where $S[\Phi]$ is the action of the field configuration Φ . The $N_{\mathbb{A}}$ -dimensional *partition sum* is the sum over all field configurations over primitive cell \mathbb{A}

$$Z_{\mathbb{A}}[J] = \int d\Phi_{\mathbb{A}} e^{\frac{i}{\hbar} (S[\Phi] + \Phi \cdot J)}, \quad d\Phi_{\mathbb{A}} = \prod_{z \in \mathbb{A}} \frac{d\phi_z}{\sqrt{2\pi}}. \quad (24)$$

Here the ‘sources’ $J = \{j_z\}$ are added to the action to facilitate the evaluation of expectation values of field moments (n -point Green’s functions) by applications of d/dj_z to the partition sum (24):

$$\langle \phi_i, \phi_j, \dots, \phi_k \rangle_{\mathbb{A}} = \int d\Phi_{\mathbb{A}} \phi_i \phi_j \dots \phi_k p_{\mathbb{A}}[\Phi], \quad (25)$$

A *semiclassical* (or *WKB*) approximation to the partition sum is obtained by the method of stationary phase. We illustrate this by a 0-dimensional lattice field theory.

1.7.1. Semiclassical field theory, a single lattice site. Consider a Laplace integral of form

$$\langle a \rangle_0 = \int \frac{d\phi}{\sqrt{2\pi}} a(\phi) e^{\frac{i}{\hbar} S(\phi)}, \quad (26)$$

with a real-valued positive parameter \hbar , a real-valued function $S(\phi)$, and an observable $a(\phi)$. Laplace estimate of this integral is obtained by determining its extremal point ϕ_c , given by the stationary phase condition

$$\frac{d}{d\phi} S(\phi_c) = 0, \quad (27)$$

and approximating the action to second order,

$$S(\phi) = S(\phi_c) + \frac{1}{2}S''(\phi_c)(\phi - \phi_c)^2 + \dots .$$

The contribution of the quadratic term is given by the Fresnel integral

$$\frac{1}{\sqrt{2\pi}} \int_{-\infty}^{\infty} d\phi e^{-\frac{\phi^2}{2ib}} = \sqrt{ib} = |b|^{1/2} e^{i\frac{\pi}{4} \frac{b}{|b|}}, \quad b = \hbar/S''(\phi_c), \quad (28)$$

with phase depending on the sign of $S''(\phi_c)$, so for a lattice with a single site the *semiclassical* approximation to the partition sum formula (26) for the expectation value is

$$\langle a \rangle_0 = \int \frac{d\phi}{\sqrt{2\pi}} a(\phi) e^{i\hbar S(\phi)} \approx a(\phi_c) \frac{e^{i\hbar S(\phi_c) \pm i\frac{\pi}{4}}}{|S''(\phi_c)/\hbar|^{1/2}}, \quad (29)$$

with \pm for positive/negative sign of $S''(\phi_c)$.

1.7.2. Semiclassical lattice field theory. The semiclassical approximation to the lattice field theory partition sum (24) is a $N_{\mathbb{A}}$ -dimensional generalization of the above Laplace-Fresnel integral. The stationary phase condition (27)

$$\frac{\delta S[\Phi_c]}{\delta \phi_z} = 0 \quad (30)$$

is system's Euler-Lagrange equation, whose global *deterministic* solution or solutions Φ_c satisfy this local extremal condition on every lattice site z ; in system's state space (7) Φ_c is a stationary *point* of the action $S[\Phi]$.

In the *WKB approximation*, the action near the point Φ_c is expanded to quadratic order,

$$S[\Phi] \approx S[\Phi_c] + \frac{1}{2}(\Phi - \Phi_c)^\top \mathcal{J}_c (\Phi - \Phi_c), \quad (31)$$

where we refer to the matrix of second derivatives

$$(\mathcal{J}_c)_{z'z} = \left. \frac{\delta^2 S[\Phi]}{\delta \phi_{z'} \delta \phi_z} \right|_{\Phi=\Phi_c} \quad (32)$$

as the *orbit Jacobian matrix*. The Fresnel integral (28) is now a multidimensional integral over $N_{\mathbb{A}}$ lattice sites state-space neighborhood \mathcal{M}_c of a deterministic solution Φ_c approximated by a Gaussian

$$\int d\Phi_{\mathbb{A}} e^{\frac{i}{2\hbar} \Phi^\top \mathcal{J}_c \Phi} = \frac{1}{|\text{Det}(\mathcal{J}_c/\hbar)|^{1/2}} e^{im_c}, \quad d\Phi_{\mathbb{A}} = \prod_z^{\mathbb{A}} \frac{d\phi_z}{\sqrt{2\pi}}, \quad (33)$$

where the Maslov index m_c is a sum of phases (28), with signs determined by the signs of eigenvalues of \mathcal{J}_c .

Our semiclassical d -dimensional spatiotemporal quantum *field* theory is a generalization of Gutzwiller [73] semiclassical approximation to quantum *mechanics* (temporal quantum evolution of a classically low-dimensional mechanical system, no



TURBULENT FIELD THEORY

quantum chaos:

$$\langle a \rangle \approx \sum_c a[\Phi_c] \frac{e^{\frac{i}{\hbar} S[\Phi_c] + im_c}}{|\text{Det}(\mathcal{J}_c/\hbar)|^{1/2}}$$

deterministic chaos:

$$\langle a \rangle = \sum_c a[\Phi_c] \frac{1}{|\text{Det} \mathcal{J}_c|}$$

Figure 3. A bird's eye view of the action landscape. The stationary points (39) –the set of all deterministic solutions $\{\Phi_c\}$ – form the skeleton on which the partition sums of both quantum chaos and deterministic chaos / turbulence are evaluated. They share the set of deterministic solutions as their common backbone, but with different weights. For a deterministic theory the probabilities that form the partition function (41) are *exact*. For a quantum theory, the semiclassical partition function (35) is an approximation, with quantum probability amplitudes phases given by deterministic solutions' actions, and stability weights given by square roots of the deterministic ones.

infinite spatial directions). It assigns a *quantum* probability amplitude to a *deterministic* solution Φ_c [90, 91, 140, 142]

$$p_c(\Phi) \approx \frac{1}{Z_{\mathbb{A}}} \frac{e^{\frac{i}{\hbar} S[\Phi_c] + im_c}}{|\text{Det}(\mathcal{J}_c/\hbar)|^{1/2}}, \quad Z_{\mathbb{A}} = Z_{\mathbb{A}}[0], \quad (34)$$

with the partition sum (24) having support on the set of *deterministic periodic solutions* Φ_c over primitive cell \mathbb{A} ,

$$Z_{\mathbb{A}}[J] \approx \sum_c \frac{e^{\frac{i}{\hbar} S[\Phi_c] + im_c + i\Phi_c \cdot J}}{|\text{Det}(\mathcal{J}_c/\hbar)|^{1/2}}. \quad (35)$$

We could have equally well derived the Onsager-Machlup-Freidlin-Wentzell [58] weak noise saddle-point approximation, and arrived to the same conclusion: stochastic partition sums also have support on the set of deterministic periodic solutions.

To summarize: The backbone of semiclassical *quantum* theory is the set of *deterministic* solutions of system's Euler-Lagrange equations (30), with the leading exponential contribution given by action evaluated on the deterministic solution, while the next-to-leading prefactor is the determinant of the operator describing quantum fluctuations about the classical solution. For chaotic (or 'turbulent') systems deterministic solutions form a fractal set of saddles, sketched in figure 3.

1.8. Deterministic lattice field theory

In Euclidean field theory a field configuration Φ over primitive cell \mathbb{A} occurs with probability density

$$p_{\mathbb{A}}[\Phi] = \frac{1}{Z_{\mathbb{A}}} e^{-S[\Phi]}, \quad Z_{\mathbb{A}} = Z_{\mathbb{A}}[0], \quad (36)$$

with $Z_{\mathbb{A}}$ is a normalization factor, given by the partition function

$$Z_{\mathbb{A}}[\beta] = e^{N_{\mathbb{A}}W_{\mathbb{A}}[\beta]} = \int d\Phi_{\mathbb{A}} e^{-S[\Phi] + N_{\mathbb{A}}\beta \cdot a_{\mathbb{A}}[\Phi]}, \quad d\Phi_{\mathbb{A}} = \prod_z^{\mathbb{A}} d\phi_z, \quad (37)$$

where the action $S[\Phi]$ defines the system under consideration, and $\langle a \rangle_{\mathbb{A}}[\Phi]$ is the Birkhoff average (22) of observable $a[\Phi]$.

Square brackets $[\dots]$ in quantities such as $Z[J]$ are a convention inherited from [quantum field theory](#) [38], where the spacetime coordinates are continuous, fields are functions $\phi(x)$, and Z 's are functionals. Here we retain these conventions to emphasize that these are spatiotemporal *field* theories, rather than temporal dynamics of a few degrees of freedom.

Instead of probing the field ϕ_z at each lattice site using the sources $\mathbf{J} \cdot \Phi$, as in partition function (24), here we multiply by a parameter (or a set of parameters) β the Birkhoff average over the primitive cell (22) of an observable (or a set of observables), in order to evaluate its expectation value by applying a $\partial/\partial\beta$ derivative to the partition function:

$$\langle a \rangle_{\mathbb{A}} = \left. \frac{\partial}{\partial\beta} W_{\mathbb{A}}[\beta] \right|_{\beta=0} = \int d\Phi_{\mathbb{A}} a_{\mathbb{A}}[\Phi] p_{\mathbb{A}}[\Phi]. \quad (38)$$

Thus, motivated by either a semiclassical quantum or a stochastic theory, or by deterministic chaos / turbulence, one is led to the *deterministic* field theory, where a field configuration Φ_c contributes only if it satisfies the stationary point condition (30), i.e., only if the Euler-Lagrange equation

$$F[\Phi_c]_z = \frac{\delta S[\Phi_c]}{\delta\phi_z} = 0$$

(for example, eqs. (54)-(56) below) is satisfied on every lattice site. If the system (for example, Navier-Stokes equations) does not have a Lagrangian formulation, we take the Euler-Lagrange equation

$$F[\Phi_c]_z = 0 \quad (39)$$

as the defining equation of the system.

To summarize: For a deterministic field theory, the probability density is non-vanishing only at the *exact* solutions of the Euler-Lagrange equations (that's what we mean by determinism),

$$p[\Phi] = \frac{1}{Z} \delta(F[\Phi]), \quad (40)$$

where the $N_{\mathbb{A}}$ -dimensional Dirac delta function $\delta(\dots)$ enforces Euler-Lagrange equation, with the primitive cell \mathbb{A} *deterministic partition function* (37) given by the sum over periodic states:

$$Z_{\mathbb{A}}[\beta] = \sum_c \int_{\mathcal{M}_c} d\Phi_{\mathbb{A}} \delta(F[\Phi]) e^{N_{\mathbb{A}}\beta \cdot a_{\mathbb{A}}[\Phi]} = \sum_c \frac{1}{|\text{Det}\mathcal{J}_c|} e^{N_{\mathbb{A}}\beta \cdot \langle a \rangle_c}, \quad (41)$$

where \mathcal{M}_c is an infinitesimal neighborhood of periodic state Φ_c , and

$$\langle a \rangle_c = \frac{1}{N_{\mathbb{A}}} \sum_{z \in \mathbb{A}} a_z[\Phi_c] \quad (42)$$

is the Birkhoff average (22) of observable a over periodic state Φ_c . We refer to

$$(\mathcal{J}_c)_{z'z} = \frac{\delta F[\Phi_c]_{z'}}{\delta \phi_z} \quad (43)$$

evaluated as an $[N_{\mathbb{A}} \times N_{\mathbb{A}}]$ matrix over the primitive cell \mathbb{A} , as *orbit Jacobian matrix*, to the linear operator (43), evaluated over infinite Bravais lattice $\mathcal{L}_{\mathbb{A}}$, as *orbit Jacobian operator*, and to the orbit Jacobian matrix determinant $\text{Det}\mathcal{J}_c$, the probability weights in (41), as *Hill determinant* [74, 116, 139, 140].

The Hill determinant is the central ingredient of our formulation of spatiotemporal chaos, so we discuss its evaluation at length in sections 3, 6, and Appendix C.

1.9. Periodic states, mosaics

The backbone of a *deterministic* chaotic system is thus the set of all spatiotemporal solutions of system's Euler-Lagrange equations (39) that we here refer to as *periodic states*, or, on occasion, as (multiply-) *periodic orbits*. Depending on the application, in literature they appear under many other names. For example, Gutkin and Osipov [71] refer to a two-dimensional periodic state Φ_c as a ‘many-particle periodic orbit’, with each lattice site field ϕ_{nt} ‘doubly-periodic’, or ‘closed’.

A periodic state is a $\mathcal{L}_{\mathbb{A}}$ -periodic set of field values $\Phi_c = \{\phi_z\}$ over the d -dimensional lattice $z \in \mathbb{Z}^d$ that satisfies the Euler-Lagrange equation on every lattice site. As any field configuration Φ is a *point* in $N_{\mathbb{A}}$ -dimensional state space (7), so is a periodic state Φ_c . Furthermore, just as a temporal evolution period n periodic point is a fixed point of n th iterate of the dynamical time-forward map, every periodic state is a *fixed point* of a set of symmetries of the theory (see section 5). A periodic state is a fixed spacetime pattern: the ‘time’ direction is just one of the coordinates. If you insist on visualising solutions as evolving in time, a periodic state is a video, not a snapshot of the system at an instant in time (that these are merely different visualizations is proven in [94]).

System's Euler-Lagrange equations are the law everyone must obey: look at your left neighbor, right neighbor, remember who you were, make sure you fit in just right. The set $\{\Phi_c\}$ of all possible periodic states is system's ‘Book of Life’ - a catalogue of all possible ‘lives’, possible spatiotemporal patterns that the law allows, each life a *point* in system's infinite-dimensional state space, each life's likelihood given by its Hill

determinant. For a chaotic (or ‘turbulent’) system they form a fractal set of saddles sketched in figure 3.

Throughout this paper we make the *hyperbolicity assumption*: we consider only cases where there is one isolated unstable solution Φ_c in a sufficiently small open state-space neighborhood \mathcal{M}_c in (41), and its orbit Jacobian matrix \mathcal{J}_c has no zero eigenvalues. For field theories studied here, one can partition the values of a lattice site field ϕ_z into a set of $|\mathcal{A}|$ disjoint intervals, and label each interval by a letter $m_z \in \mathcal{A}$ drawn from an alphabet \mathcal{A} , let’s say

$$\mathcal{A} = \{1, 2, \dots, |\mathcal{A}|\}. \quad (44)$$

This associates a d -dimensional ‘*mosaic*’ \mathbf{M}_c to a periodic state Φ_c over d -dimensional lattice [32, 33, 100, 101]

$$\mathbf{M}_c = \{m_z\}, \quad m_z \in \mathcal{A}. \quad (45)$$

A mosaic serves both as a proxy (a ‘name’) for the periodic state Φ_c , and its visualization as color-coded symbol array \mathbf{M}_c (for examples, see figure 10 and figure 11).

If there is only one, distinct mosaic \mathbf{M}_c for each periodic state Φ_c , the alphabet is said to be *covering*. While each periodic state thus gets assigned a unique mosaic that paginates its location in the Book of Life, the converse is in general not true. If a given mosaic \mathbf{M} corresponds to a periodic state, it is *admissible*, otherwise \mathbf{M} has to be deleted from the list of mosaics. In the temporal-evolution setting there is a variety of methods of finding grammar rules that eliminate the inadmissible mosaics. Such rules for 2- or higher-dimensional lattice field theories remain, in general, not known to us.

We construct the field theory’s deterministic partition function (section 7) by first enumerating all Bravais lattices or geometries $\mathcal{L}_{\mathbb{A}}$ (section 4.1), determining prime orbits over each (section 2), computing the weight of each (section 3), and then (section 7.1) adding together the contributions of periodic states for each. The potentials may be bounded (ϕ^4 theory) or unbounded (ϕ^3 theory), or the system may be energy conserving or dissipative, as long as the set of its periodic states Φ_c is bounded in system’s state space (3). To get a feel for how all this works, we illustrate the theory by applying it to four lattice field theories that we now introduce.

2. Examples of spatiotemporal lattice field theories

A field theory is defined either by its action, for example a lattice sum over the Lagrangian density for a discretized scalar d -dimensional Euclidean ϕ^k theory [4–6, 47, 59, 92, 110],

$$S[\Phi] = \sum_z \left\{ \frac{1}{2} \sum_{\mu=1}^d (\partial_{\mu}\phi)_z^2 + V(\phi_z) \right\}, \quad (46)$$

with a local potential $V(\phi)$ the same for every lattice site z , or, if lacking a variational formulation, by its Euler-Lagrange equation $F[\Phi]_z = 0$. For what follows, it is convenient

to define a ‘lattice momentum’ operator in j th lattice direction as the forward lattice difference operator,

$$p_j = r_j - \mathbb{1}, \quad (47)$$

where r is the shift operator (11), lattice spacing is set to 1, and the d -dimensional lattice Laplacian is the lattice momentum operator squared,

$$\square = - \sum_{j=1}^d p_j^\top p_j = \sum_{j=1}^d (r_j - 2 \mathbb{1} + r_j^{-1}). \quad (48)$$

The discrete Euler-Lagrange equations (39) now take form of a second-order difference equations

$$-\square \phi_z + V'(\phi_z) = 0. \quad (49)$$

In lattice field theory ‘locality’ means that a field at site z interacts only with its neighbors. To keep the exposition as simple as possible, we treat here the spatial and temporal directions on equal footing, with the graph Laplace operator [35, 66, 97, 120]

$$\square \phi_z = \sum_{z' \mid \|z'-z\|=1} (\phi_{z'} - \phi_z) \quad \text{for all } z, z' \in \mathbb{Z}^d \quad (50)$$

comparing the field on lattice site z to its $2d$ nearest neighbors. For example, the two-dimensional square lattice Laplace operator is given by

$$\square = r_1 + r_2 - 4 \mathbb{1} + r_2^{-1} + r_1^{-1}, \quad (51)$$

where r_1, r_2 shift operators (see (83) for a group-theoretical perspective)

$$(r_1)_{nt, n't'} = \delta_{n+1, n'} \delta_{tt'}, \quad (r_2)_{nt, n't'} = \delta_{nn'} \delta_{t+1, t'} \quad (52)$$

translate a field configuration Φ ,

$$(r_1 \phi)_{nt} = \phi_{n+1, t}, \quad (r_2 \phi)_{nt} = \phi_{n, t+1},$$

by one lattice spacing (11) in the spatial, temporal direction, respectively.

Here, and in papers I and III [93, 146] we investigate spatiotemporally chaotic lattice field theories using as illustrative examples the d -dimensional hypercubic lattice (2) discretized Klein-Gordon free-field theory, spatiotemporal cat, spatiotemporal ϕ^3 theory, and spatiotemporal ϕ^4 theory, defined respectively by Euler-Lagrange equations (39)

$$-\square \phi_z + \mu^2 \phi_z = 0, \quad \phi_z \in \mathbb{R}, \quad (53)$$

$$-\square \phi_z + \mu^2 \phi_z - m_z = 0, \quad \phi_z \in [0, 1) \quad (54)$$

$$-\square \phi_z + \mu^2 (1/4 - \phi_z^2) = 0, \quad (55)$$

$$-\square \phi_z + \mu^2 (\phi_z - \phi_z^3) = 0. \quad (56)$$

For free-field theory the sole parameter μ^2 is known as the Klein-Gordon (or Yukawa) mass. The anti-integrable form [15, 16, 134] of the spatiotemporal ϕ^3 (55) and spatiotemporal ϕ^4 (56) Euler-Lagrange equations, and a rescaling away of other ‘coupling’ parameters, is explained in the companion paper III [146].

Spatiotemporal cat (54) we derive next, as it will be used throughout the paper to illustrate our field-theoretic formulation of spatiotemporal chaos. The spatiotemporal cat is arguably the simplest example of a chaotic (or ‘turbulent’) deterministic field theory for which the local degrees of freedom are hyperbolic (anti-harmonic, ‘inverted pendula’) rather than oscillatory (‘harmonic oscillators’). For its history, see [Appendix A](#).

2.1. Spatiotemporal cat

While a free-field theory teaches us much about how a field theory works, it is not an example of a chaotic field theory: its Euler-Lagrange equation (53) is linear, with a single deterministic solution, the steady state $\phi_z = 0$. For that reason one goes to a ‘compact boson’ (or ‘compact scalar’) [31, 53] formulation (54), and compactifies the lattice site field values to a circle,

$$(-\square + \mu^2) \phi_z = m_z, \quad z \in \mathbb{Z}^d, \quad \phi_z \in [0, 1). \quad (57)$$

with the circle $\phi_z \pmod{1}$ condition enforced by integers m_z , called ‘winding numbers’ [85], or, as they shepherd stray points back into the state space unit hypercube, ‘stabilising impulses’ [115]. As this is a linear equation, for a primitive cell \mathbb{A} we can write it in a finite matrix form,

$$F[\Phi_{\mathbb{M}}] = \mathcal{J}_{\mathbb{A}} \Phi_{\mathbb{M}} - \mathbb{M} = 0, \quad \Phi_{\mathbb{M}} \in [0, 1)^{N_{\mathbb{A}}}, \quad (58)$$

where $\mathcal{J}_{\mathbb{A}} = -\square + \mu^2 \mathbb{1}$ is the orbit Jacobian matrix (43) with primitive cell \mathbb{A} periodic boundary conditions (see (97), for example).

We refer to the one-dimensional *temporal* lattice, three-term recurrence case of this equation

$$-\phi_{t+1} + s\phi_t - \phi_{t-1} = m_t, \quad t \in \mathbb{Z}, \quad \phi_t \in [0, 1), \quad (59)$$

with the ‘stretching parameter’ s related to the Klein-Gordon mass by $\mu^2 = s - 2$, as ‘*temporal cat*’, and to the Euler-Lagrange equation (57) in higher spatiotemporal dimensions as the ‘*spatiotemporal cat*’. In two spacetime dimensions, the Euler-Lagrange equation (57) is a five-term recurrence relation

$$-\phi_{j,t+1} - \phi_{j,t-1} + 2s\phi_{jt} - \phi_{j+1,t} - \phi_{j-1,t} = m_{jt}, \quad \mu^2 = 2(s - 2), \quad (60)$$

where, in the matrix format (58), the orbit Jacobian operator can be expressed in terms of shift operators (51),

$$\mathcal{J} = -r_1 - r_2 + 2s \mathbb{1} - r_2^{-1} - r_1^{-1}. \quad (61)$$

We study the one-dimensional temporal cat (59) in some depth in companion paper I [93]. In this paper we focus on the $d = 2$ spatiotemporal cat (60).

Computation of spatiotemporal cat periodic states. Euler-Lagrange equation (58) is linear, and, given a primitive cell \mathbb{A} and a mosaic \mathbf{M} (45) over it, always has a unique solution $\Phi_{\mathbf{M}}$. We solve it by reciprocal lattice diagonalization (section 6.3), by direct determinant evaluation (Appendix C), or by matrix inversion:

$$\phi_z = \sum_{z' \in \mathbb{Z}^D} g_{zz'} m_{z'}, \quad g_{zz'} = \left[\frac{1}{-\square + \mu^2} \right]_{zz'}, \quad (62)$$

where $g_{zz'}$, the inverse of the orbit Jacobian operator, is the spatiotemporal cat (57) Green's function. In literature, $g_{zz'}$ is known as the Green's function for the d -dimensional discretized screened Poisson equation, see Appendix A.

The solution $\Phi_{\mathbf{M}}$ is a periodic state, and the mosaic \mathbf{M} is said to be *admissible*, if and only if all lattice-site field values ϕ_z of $\Phi_{\mathbf{M}}$ lie in the compact boson state space (57)

$$\mathcal{M} = \{ \Phi \mid \phi_z \in [0, 1), z \in \mathbb{Z}^d \}. \quad (63)$$

So we need to define the range of integers m_z , and, if possible, the grammar of admissible mosaics \mathbf{M} .

Spatiotemporal cat mosaics. ‘Letter’ m_z is the integer part of the LHS of (57) that enforces the circle (mod 1) condition for field ϕ_z on lattice site z . Its range depends on the Klein-Gordon mass-squared μ^2 , and the lattice dimension d . If all nearest neighbor fields are as large as allowed, $\phi_{z'} = 1 - \epsilon$, in two spatiotemporal dimensions the integer part of the LHS of (60) can be as low as -3 , for $\phi_z = 0$, or as high as $2s - 1$, for $\phi_z = 1 - \epsilon$, hence the covering alphabet $\mathcal{A} = \{m_z\}$ is

$$\mathcal{A} = \{ \underline{3}, \underline{2}, \underline{1}; 0, \dots, \mu^2; \mu^2 + 1, \mu^2 + 2, \mu^2 + 3 \}, \quad (64)$$

where symbol \underline{m}_z denotes m_z with the negative sign, i.e., ‘ $\underline{3}$ ’ stands for symbol ‘ -3 ’. As a mosaic \mathbf{M} corresponds to a unique periodic state $\Phi_{\mathbf{M}}$, the periodic state can be visualized as the color-coded symbol array.

If all nearest neighbor fields are as small as allowed, $\phi_{z'} = 0$, the Laplacian does not contribute, and the integer part of the LHS of (57) ranges from 0, for $\phi_z = 0$, to μ^2 , for $\phi_z = 1$, hence the $\mu^2 + 7$ letter alphabet (64) can be divided into two subsets, the interior and the exterior alphabets \mathcal{A}_0 and \mathcal{A}_1 , respectively.

$$\mathcal{A}_0 = \{0, \dots, \mu^2\}, \quad \mathcal{A}_1 = \{ \underline{3}, \underline{2}, \underline{1} \} \cup \{ \mu^2 + 1, \mu^2 + 2, \mu^2 + 3 \}. \quad (65)$$

If all m_z of a mosaic \mathbf{M} belong to the interior alphabet \mathcal{A}_0 , the mosaic \mathbf{M} is admissible [70]. However, the grammar rules that would determine what spatiotemporal cat mosaic \mathbf{M} are admissible are -except in the $d = 1$ case [93]- not known to us, so we solve the equations for all possible mosaics, and then discard those for which $\Phi_{\mathbf{M}}$ lies outside the unit hypercube (63).

3. Spatiotemporal stability of a periodic state

For field theories (49) considered here, the orbit Jacobian operators (43) are of form

$$\mathcal{J}_{zz'} = -\square_{zz'} + V''(\phi_z) \delta_{zz'}, \quad (66)$$

with the free field (53) and spatiotemporal cat (54), ϕ^3 (55), ϕ^4 (56) orbit Jacobian operators

$$\mathcal{J}_{zz'} = -\square_{zz'} + \mu^2 \delta_{zz'}, \quad (67)$$

$$\mathcal{J}_{zz'} = -\square_{zz'} - 2\mu^2 \phi_z \delta_{zz'}, \quad (68)$$

$$\mathcal{J}_{zz'} = -\square_{zz'} + \mu^2(1 - 3\phi_z^2) \delta_{zz'}. \quad (69)$$

Sometimes it is convenient to lump the diagonal terms of the discrete Laplace operator (51) together with the site potential $V''(\phi_z)$. In that case, the orbit Jacobian operator takes the $2d + 1$ banded form

$$\mathcal{J}[\Phi] = \sum_{j=1}^d (-r_j + s_z \mathbb{1} - r_j^{-1}), \quad s_z = V''(\phi_z)/d + 2, \quad (70)$$

where r_j shift operators (52) translate the field configuration by one lattice spacing in the j th hypercubic lattice direction, and we refer to s_z as the *stretching factor* at lattice site z . For the free field and spatiotemporal cat (67), ϕ^3 (68), ϕ^4 (69) theories the stretching factor s_z is, respectively,

$$s = \mu^2/d + 2, \quad (71)$$

$$s_z = -2\mu^2 \phi_z/d + 2, \quad (72)$$

$$s_z = \mu^2(1 - 3\phi_z^2)/d + 2. \quad (73)$$

What can we say about the spectra of above orbit Jacobian operators? In the anti-integrable limit [15, 16, 134] the ‘potential’ term in (66) dominates, and one treats the Laplacian (‘kinetic energy’) as a perturbation. In particular, for the free field and spatiotemporal cat (67), in the anti-integrable limit all eigenvalues of the orbit Jacobian operator tend to the Klein-Gordon mass-squared,

$$\mathcal{J} \approx \mu^2 \mathbb{1}, \quad \mu^2 \text{ large}, \quad (74)$$

in any spacetime dimension. Analogous limits apply to ϕ^3 and ϕ^4 field theories as well, see the companion paper III [146].

In what follows, it is crucial to distinguish the $[N_{\mathbb{A}} \times N_{\mathbb{A}}]$ orbit Jacobian matrix, evaluated over a finite volume primitive cell \mathbb{A} , from the orbit Jacobian operator (70) that acts on the infinite Bravais lattice $\mathcal{L}_{\mathbb{A}}$.

3.1. Primitive cell stability

The orbit Jacobian (70) evaluated over a *finite volume* primitive cell \mathbb{A} is an $[N_{\mathbb{A}} \times N_{\mathbb{A}}]$ matrix, with $N_{\mathbb{A}}$ discrete eigenvalues.

As an example, consider a periodic state c over the one-dimensional primitive cell of period n , discussed in section 1.2. For a periodic state Φ_c , the orbit Jacobian matrix

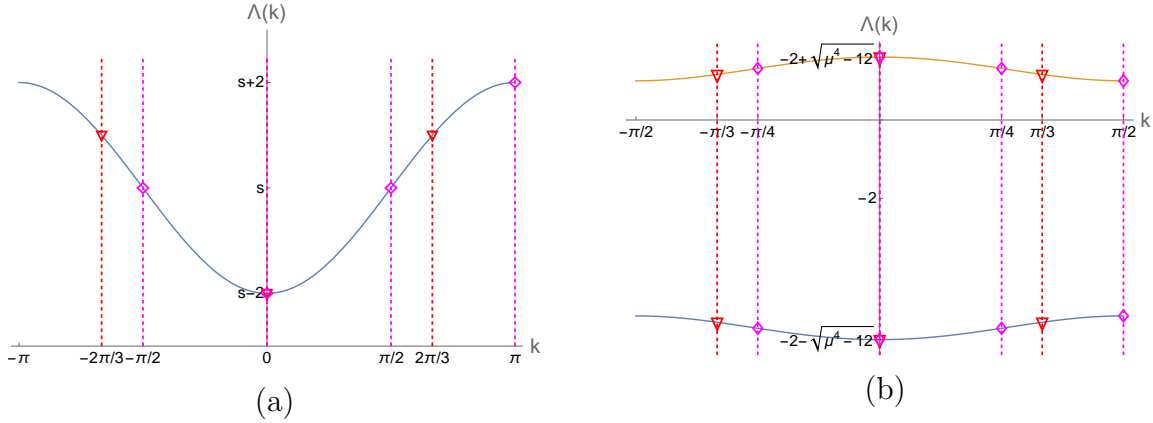


Figure 4. (Color online) One-dimensional lattice orbit Jacobian operator spectra, as functions of the reciprocal lattice wave number k . For time-reversal invariant systems the spectra are $k \rightarrow -k$ symmetric. (a) The free-field $\Lambda(k)$ spectrum (77). Any period- n primitive cell (75) orbit Jacobian matrix spectrum consists of n discrete points embedded into $\Lambda(k)$, for example period-3 (red triangles) and period-4 (magenta diamonds) eigenvalues. (b) The nonlinear ϕ^3 theory $\Lambda_{LR,\pm}(k)$ spectrum (D.2) of the Bravais lattice \mathcal{L}_{LR} tiled by the period-2 periodic state $\Phi_{LR} = \{\phi_L, \phi_R\}$, together with the eigenvalues of 3rd repeat (red triangles) and 4th repeat (magenta diamonds) primitive cells. See Appendix D.1. From [93].

is

$$\mathcal{J}_{\mathbb{A},c} = \begin{pmatrix} s_0 & -1 & 0 & \cdots & 0 & -1 \\ -1 & s_1 & -1 & \cdots & 0 & 0 \\ 0 & -1 & s_2 & \cdots & 0 & 0 \\ \vdots & \vdots & \vdots & \ddots & \vdots & \vdots \\ 0 & 0 & 0 & \cdots & s_{n-2} & -1 \\ -1 & 0 & 0 & \cdots & -1 & s_{n-1} \end{pmatrix}, \quad (75)$$

where the shift operators (10) in (70) are the off-diagonals.

The free-field theory orbit Jacobian operator (67), with no lattice site dependence, $s_z = s$, is diagonalized by going to the reciprocal lattice. For example, for a one-dimensional primitive cell \mathbb{A} of period n , the Fourier transform (17) of Laplacian (48),

$$\begin{aligned} \mathcal{J}_{\mathbb{A}} \varphi_k &= (-\square + \mu^2 \mathbb{1}) \varphi_k = (p^2 + \mu^2) \varphi_k \\ p &= 2 \sin(k/2), \quad k = \frac{2\pi}{n} m, \quad m = 0, 1, \dots, n-1, \end{aligned} \quad (76)$$

expresses the Fourier-diagonalized lattice Laplacian as the square of the lattice momentum p (47),

$$(\tilde{\mathcal{J}}_{\mathbb{A}})_{mm'} = (p^2 + \mu^2) \delta_{mm'}, \quad (77)$$

with n eigenvalues $\Lambda_m = p^2 + \mu^2$ indexed by the integer m . The ‘cord function’ $\text{crd}(\theta) = 2 \sin(\theta/2)$ was used already by Hipparchus cc. 130 BC in the same context, as a discretization of a circle by approximating n arcs by n cords [22, 144].

Evaluate, as an example, the spectrum of orbit Jacobian matrix for a temporal cat period-3 state. The wave-numbers (76) are $k = (0, 2\pi/3, 4\pi/3)$, with lattice momentum

values $p(0) = 0$, $p(2\pi/3) = p(4\pi/3) = \sqrt{3}$. The lattice momentum square \mathbf{p}^2 in (77) is a field over the $N_{\mathbb{A}} = 3$ lattice sites of the reciprocal primitive cell $\tilde{\mathbb{A}}$, indexed by integer reciprocal lattice-site labels $m = 0, 1, 2$:

$$\mathbf{p}_{\tilde{\mathbb{A}}}^2 = \boxed{\mathbf{p}_0^2 \mid \mathbf{p}_1^2 \mid \mathbf{p}_2^2} = \boxed{0 \mid 3 \mid 3}. \quad (78)$$

Then the $\mathcal{J}_{\mathbb{A}}$ eigenvalues are

$$\Lambda_m = (\mu^2, 3 + \mu^2, 3 + \mu^2).$$

The ‘brick’ outline in (78) will be explained in (98), when we compute $\mathbf{p}_{\tilde{\mathbb{A}}}^2$ for a two-dimensional lattice. The corresponding Hill determinant is the product of the $\mathcal{J}_{\mathbb{A}}$ eigenvalues (see tables B1 and B2).

Discrete Fourier transforms diagonalize the hypercubic lattice free-field orbit Jacobian matrix over a periodic, ‘rectangular’ primitive cell in any spatiotemporal dimension,

$$\tilde{\mathcal{J}}_{\mathbb{A}} = (\mathbf{p}^2 + \mu^2) \mathbb{1}, \quad \mathbf{p}^2 = \sum_{j=1}^d p_j^2, \quad p_j = 2 \sin \frac{k_j}{2}, \quad k_j = \frac{2\pi}{L_j} m_j, \quad (79)$$

where \mathbf{p} denotes the ‘momentum measured in lattice units’ (48), p_j is the lattice momentum in j th direction, and L_j is the period of the primitive cell \mathbb{A} in j th direction, with $N_{\mathbb{A}}$ orbit Jacobian matrix eigenvalues $\Lambda_m = \mathbf{p}^2 + \mu^2$ taking values on the reciprocal lattice sites \mathbf{k} , indexed by integers $m = m_1 m_2 \cdots m_d$. $1/(\mathbf{p}^2 + \mu^2)$ is known as the lattice free-field theory propagator.

This is almost everything there is to a primitive cell stability, except that the ‘rectangle’ periodic boundary conditions are only a special case of spacetime periodicity: we describe the general, Bravais lattice periodicity case in section 4.1.

3.2. Bravais lattice stability

The linear orbit Jacobian *operator* acts on the *infinite* Bravais lattice $\mathcal{L}_{\mathbb{A}}$, for example the orbit Jacobian operator a periodic state Φ_c over the one-dimensional Bravais lattice of a period n ,

$$\mathcal{J}_c = \begin{pmatrix} \cdots & \cdots & \cdots & \cdots & \cdots & \cdots & \cdots & \cdots & \cdots \\ \cdots & s_0 & -1 & 0 & 0 & 0 & 0 & 0 & \cdots \\ \cdots & -1 & s_1 & -1 & 0 & 0 & 0 & 0 & \cdots \\ \cdots & 0 & -1 & s_2 & -1 & 0 & 0 & 0 & \cdots \\ \vdots & \vdots & \vdots & \ddots & \ddots & \ddots & \vdots & \vdots & \\ \cdots & 0 & 0 & 0 & -1 & s_{n-2} & -1 & \cdots & \\ \cdots & 0 & 0 & 0 & 0 & -1 & s_{n-1} & \cdots & \\ \cdots & \cdots & \cdots & \cdots & \cdots & \cdots & \cdots & \cdots & \cdots \end{pmatrix}, \quad (80)$$

is an infinite matrix, with the block $s_0 s_1 \cdots s_{n-1}$ infinitely repeated along the diagonal. By Bloch theorem, section 1.5, the Bravais lattice eigenvalue spectrum consists of n continuous Brillouin zone bands $\Lambda(k)$ and Bloch eigenfunctions (21).

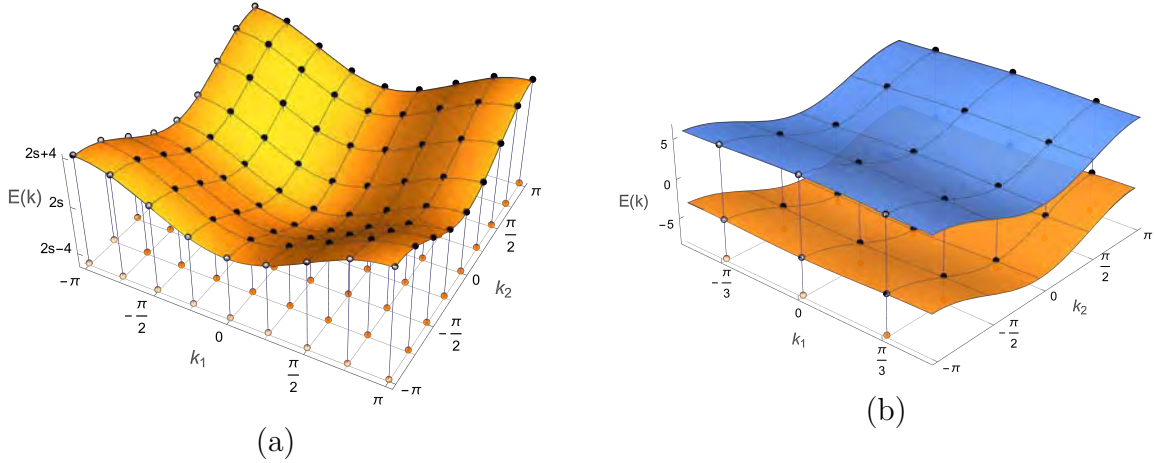


Figure 5. (Color online) Square spatiotemporal lattice orbit Jacobian operator spectra, as functions of the wave vectors (k_1, k_2) . For time and space-reflection and interchange invariant Euclidean theories the spectra are $k_1 \rightarrow -k_1$, $k_2 \rightarrow -k_2$ and $k_1 \leftrightarrow k_2$ symmetric. (a) The free-field theory $\Lambda(\mathbf{k})$ Bloch band (81) as a function of the wave vector \mathbf{k} . Black dots are eigenvalues of the orbit Jacobian matrix of periodic states over primitive cell with periodicity $[8 \times 8]_0$. (b) The spatiotemporal ϕ^4 lattice field theory spectra of the Bravais lattice $\mathcal{L}_{[2 \times 1]_0}$ periodic state (D.3). Black dots are eigenvalues of the orbit Jacobian matrix of a $[6 \times 4]_0$ primitive cell tiled by 12 repeats of a prime $[2 \times 1]_0$ periodic state, with $\Lambda_{\pm}(\mathbf{k})$ Bloch bands computed in Appendix D.2.

The free-field theory orbit Jacobian operator (67), with no periodic state dependence, can be diagonalized by going to the reciprocal lattice. The calculation is essentially the same as the above primitive cell calculation, leading to the hypercubic lattice free-field orbit Jacobian operator (79) in any spatiotemporal dimension as the inverse propagator

$$\tilde{\mathcal{J}} = (\mathbf{p}^2 + \mu^2) \mathbf{1}, \quad \mathbf{p}^2 = \sum_{j=1}^d p_j^2, \quad p_j = 2 \sin \frac{k_j}{2}, \quad (81)$$

with eigenvalues $\Lambda(\mathbf{k}) = \mathbf{p}^2 + \mu^2$, except that the Bloch wave numbers are continuous, only restricted to 2π intervals, conventionally to the centered hypercubic ‘1st Brillouin zone’

$$k_1, k_2, \dots, k_d \in (-\pi, \pi]. \quad (82)$$

The relation between the discrete and the continuous spectra is illustrated by figure 4(a) which shows the spectra of the one-dimensional free-field theory orbit Jacobian matrices, and figure 5(a) of the two-dimensional free-field theory as a function of the wave vector(s) k , or $k = k_1 k_2$, in the one-, or two-dimensional Brillouin zone \mathbb{B} , respectively.

For the free-field theory and spatiotemporal cat, $s_z = s$, orbit Jacobian operator (67) is 1-step translation (11) invariant along all lattice dimensions. Its stability is the stability of a constant state, with any primitive cells \mathbb{A} tiled by repeats of the unit hypercube (1) primitive cell periodic state. In this case, a unit hypercube primitive

cell periodic state is the prime orbit, a *prime* steady state (section 1.3), all other orbit Jacobians over larger primitive cells are repeats of the unit hypercube orbit Jacobian (see section 5.3).

4. Bravais lattices

Periodic orbit theory for a time-evolving dynamical system on a one-dimensional temporal lattice is organized by grouping orbits of the same period together [40, 60, 73, 93, 126]. For systems characterized by several translational symmetries, one has to take care of multiple periodicities, or, in the language of crystallography, organize the periodic orbit sums by corresponding *Bravais lattices* (introduced in section 1.1).

In crystallography the set of all transformations that overlay a lattice over itself is called the *space group* G . For case at hand, the unit cell (1) tiles the hypercubic lattice under action of translations \mathbf{r}_j (52) in d spatiotemporal directions, called ‘shifts’ for infinite Bravais lattices, ‘rotations’ for finite periodic primitive cells. They form the abelian translation group

$$T = \{\mathbf{r}_1^{m_1} \mathbf{r}_2^{m_2} \cdots \mathbf{r}_d^{m_d} \mid m_j \in \mathbb{Z}\}. \quad (83)$$

The cosets a space group G by its translation subgroup T form the group G/T , isomorphic to a *point group* g . For example, the square lattice space group $G = T \rtimes D_4$ is the semi-direct product of translations (83), and the point group g of right angle rotations, time reversal, spatial reflection, and space-time interchanges. In addition, there might also be internal symmetries, such as the invariance of spatiotemporal cat equations (54) under inversion of the field though the center of the $0 \leq \phi_z < 1$ unit interval:

$$\phi_z \rightarrow 1 - \phi_z \text{ for all } z \in \mathbb{Z}^d. \quad (84)$$

Already in the case of chaotic lattice field theory over one-dimensional temporal integer lattice \mathbb{Z} there is a sufficient amount of group-theoretical detail to merit the stand-alone companion paper I [93], which treats in detail the time reversal invariance for $G = D_\infty$ dihedral space group of translations and reflections. Here we focus only the two-dimensional square lattice *translations*, as a full symmetry treatment would distract the reader from the main trust of the paper, the construction of the spatiotemporal zeta function (section 7).

4.1. Bravais lattices of the square lattice

Consider a $[2 \times 2]$ integer matrix (6)

$$\mathbb{A} = [\mathbf{a}_1, \mathbf{a}_2] = \begin{bmatrix} a_{1,1} & a_{2,1} \\ a_{1,2} & a_{2,2} \end{bmatrix}, \quad \mathbf{a}_j = \begin{bmatrix} a_{j,1} \\ a_{j,2} \end{bmatrix}, \quad (85)$$

formed from a pair of two-dimensional integer lattice primitive vectors $\mathbf{a}_1, \mathbf{a}_2$. A two-dimensional *Bravais lattice*, figure 6,

$$\mathcal{L}_{\mathbb{A}} = \{\mathbb{A}\mathbf{n} \mid \mathbf{n} \in \mathbb{Z}^2\} \quad (86)$$

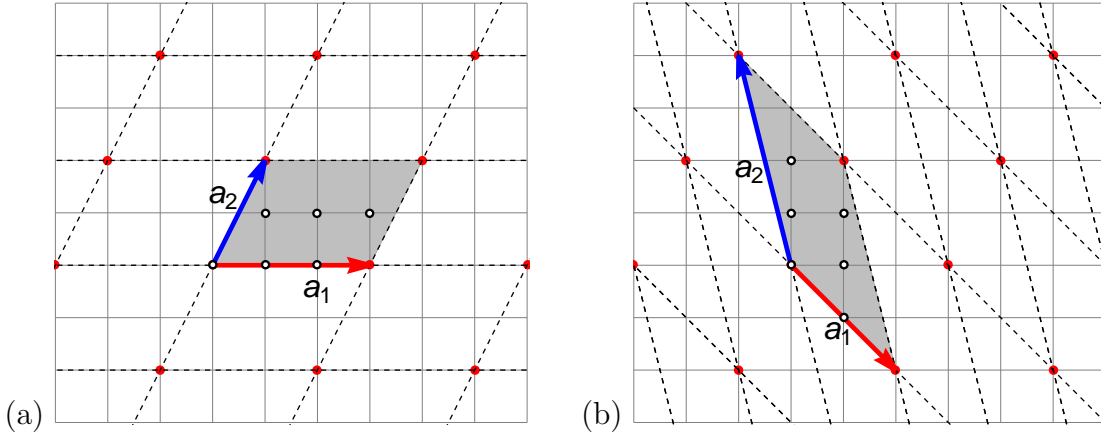


Figure 6. (Color online) The intersections of the light grey lines -lattice sites $z \in \mathbb{Z}^2$ form the integer square lattice (2). (a) Translations of the primitive cell $\mathbb{A} = [3 \times 2]_1$ spanned by primitive vectors $\mathbf{a}_1 = (3, 0)$ and $\mathbf{a}_2 = (1, 2)$ define the Bravais lattice $\mathcal{L}_{\mathbb{A}}$. (b) The primitive vectors $\mathbf{a}_1 = (2, -2)$ and $\mathbf{a}_2 = (-1, 4)$ form a primitive cell \mathbb{A}' equivalent to (a) by a unimodular transformation. The intersections (red points) of either set of dashed lines form the same Bravais lattice $\mathcal{L}_{\mathbb{A}} = \mathcal{L}_{\mathbb{A}'}$. The volume (8) of either primitive cell is $N_{\mathcal{L}} = 6$, the number of integer lattice sites within the cell, with the tips of primitive vectors and tiles' outer boundaries belonging to the neighboring tiles. Continued in figure 7.

of lattice points generated by all discrete translations $\mathbb{A}\mathbf{n}$ is a sublattice of the integer lattice \mathbb{Z}^2 .

As in a discretized field theory the fields are defined only on the hypercubic integer lattice, not on a continuum, we define the *primitive cell* (7) as the set of lattice sites within the parallelepiped (85) illustrated by figure 6. The tips of primitive vectors and parallelepiped's outer boundaries belong, by translation, to the neighboring tiles; this yields the correct lattice volume (8), $N_{\mathbb{A}}$ the number of lattice sites within the primitive cell \mathbb{A} .

A primitive cell is not unique [129]: the Bravais lattice $\mathcal{L}_{\mathbb{A}'}$ defined by basis \mathbb{A}' is the same as the Bravais lattice $\mathcal{L}_{\mathbb{A}}$ defined by basis $\mathbb{A} = \mathbb{A}'\mathbb{U}$ if the two are related by a $[2 \times 2]$ unimodular, volume preserving matrix $\mathbb{U} \in \text{SL}(2, \mathbb{Z})$ transformation [29, 87, 150], see figure 6(b). This equivalence underlies many of the properties of elliptic functions and modular forms. While we make no use of this mathematics (reader might enjoy Ghys and Leys [62] visual introduction to the subject), the Dedekind eta function $\eta(\tau)$ will come to play a key role in section 7.2.

Constructing *all* Bravais lattices (geometries) is straightforward, as each such infinite family of equivalent primitive cells contains a single, unique *Hermite normal form* primitive cell, with upper-triangular basis [36] primitive vectors $\mathbf{a}_1 = (L, 0)$, $\mathbf{a}_2 = (S, T)$,

$$\mathbb{A} = \begin{bmatrix} L & S \\ 0 & T \end{bmatrix}, \quad N_{\mathbb{A}} = LT, \quad (87)$$

where L, T are the spatial, temporal lattice periods, respectively, and $N_{\mathbb{A}}$ is the lattice volume (8). The 'tilt' [112] $0 \leq S < L$ imposes 'relative-periodic shift' boundary

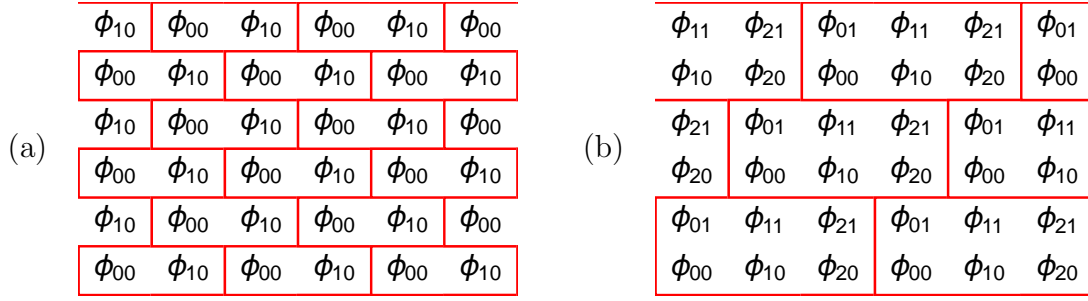


Figure 7. Examples of $[L \times T]_S$ field configurations (87) or ‘bricks’, together with their spatiotemporal Bravais lattice tilings, visualized as brick walls. (a) $[2 \times 1]_1$, primitive vectors $\mathbf{a}_1 = (2, 0)$, $\mathbf{a}_2 = (1, 1)$; (b) $[3 \times 2]_1$ of figure 6 (a), primitive vectors $\mathbf{a}_1 = (3, 0)$, $\mathbf{a}_2 = (1, 2)$. Rectangles enclose the primitive cell and its Bravais lattice translations. Continued in figure 8.

conditions [40]. In the literature these are also referred to as ‘helical’ [95], ‘toroidal’ [79], ‘screw’ [46], S -corkscrew [33], ‘twisted’ [78] or ‘twisting factor’ [95] boundary conditions. Parenthetically, in the theory of elliptic functions [133] the primitive cell is represented by a complex modular parameter τ , with spatial period L taken as the lattice spacing constant, primitive vectors $\mathbf{a}_1 = (1, 0)$, $\mathbf{a}_2 = (\tau_1, \tau_2)$, so $T \rightarrow \tau_2 = T/L$, $S \rightarrow \tau_1 = S/L$, and

$$\mathbb{A} = \begin{bmatrix} 1 & \tau_1 \\ 0 & \tau_2 \end{bmatrix}, \quad N_{\mathbb{A}} = \tau_2. \quad (88)$$

If the corresponding torus is visualised as a glueing of a unit square into a tube, τ parameterizes how the tube is stretched and twisted before its edges are stitched together.

Here we refer to a particular Bravais lattice by its Hermite normal form (87), as

$$\mathcal{L}_{\mathbb{A}} = [L \times T]_S, \quad (89)$$

and to the set of lattice sites within the primitive parallelogram \mathbb{A} as its primitive cell. In terms of lattice site fields, a field configuration $\phi_{z_1 z_2}$ (5), $z_1 z_2 \in \mathbb{Z}^2$, satisfies the S -corkscrew boundary condition [33],

$$\begin{aligned} \text{horizontally:} \quad & \phi_{z_1 z_2} = \phi_{z_1 + L, z_2} \\ \text{vertically:} \quad & \phi_{z_1 z_2} = \phi_{z_1 + S, z_2 + T}, \end{aligned} \quad (90)$$

see figure 7. Notation $[L \times T]_S$ refers to primitive cell being a rectangle of spatial width L , temporal height T , with the primitive cell above it shifted by S , see for example the $[3 \times 2]_1$ primitive cell shown in figure 7 (b).

If an operator, in case at hand the orbit Jacobian operator (66), is invariant under spacetime translations, its eigenvalue spectrum and Hill determinant can be efficiently computed using tools of crystallography. However, as explained in section 3.2, it is crucial that we distinguish the *finite* primitive cell orbit Jacobian *matrix* from the *infinite* Bravais lattice orbit Jacobian *operator* in such calculations.

4.2. Reciprocal primitive cell

In two spatiotemporal dimensions, the reciprocal Bravais lattice (18) is given by

$$\mathcal{L}_{\tilde{\mathbb{A}}} = \{m_1 \tilde{\mathbf{a}}_1 + m_2 \tilde{\mathbf{a}}_2 \mid m_i \in \mathbb{Z}\}, \quad (91)$$

where the reciprocal lattice unit vectors $\tilde{\mathbf{a}}_1 = \frac{2\pi}{N_{\mathbb{A}}}(T, -S)$ and $\tilde{\mathbf{a}}_2 = \frac{2\pi}{N_{\mathbb{A}}}(0, L)$ satisfy the reciprocity condition (19), so the reciprocal primitive cell is also of Hermite normal (but lower-triangular) form,

$$\tilde{\mathbb{A}} = \frac{2\pi}{N_{\mathbb{A}}} \begin{bmatrix} T & 0 \\ -S & L \end{bmatrix}, \quad (92)$$

with the reciprocal basis condition (18) satisfied. The components of a reciprocal lattice wave vector $\mathbf{k} = m_1 \tilde{\mathbf{a}}_1 + m_2 \tilde{\mathbf{a}}_2$ (91) are

$$\mathbf{k} = \begin{bmatrix} k_1 \\ k_2 \end{bmatrix} = \frac{2\pi}{LT} \begin{bmatrix} m_1 T \\ -m_1 S + m_2 L \end{bmatrix}. \quad (93)$$

As in the one-dimensional case (16), the wave numbers along each direction of a 2-dimensional square lattice are restricted to $k_j \in [0, 2\pi)$, and it suffices to use the wave vectors $\mathbf{k} = m_1 \tilde{\mathbf{a}}_1 + m_2 \tilde{\mathbf{a}}_2$ with $m_1 = (0, 1, \dots, L-1)$, $m_2 = (0, 1, \dots, T-1)$ to get all $N_{\mathbb{A}} = LT$ distinct wave vectors. This set of reciprocal lattice sites, conveniently indexed by integers $m = m_1 m_2$, forms the *reciprocal primitive cell* $\tilde{\mathbb{A}}$, which contains the same number of lattice sites $\mathbf{k} \in \tilde{\mathbb{A}}$ as the spatiotemporal Bravais lattice primitive cell \mathbb{A} .

Example: A spatiotemporal primitive cell, reciprocal primitive cell.

Primitive vectors $\mathbf{a}_1 = (3, 0)$ and $\mathbf{a}_2 = (1, 2)$ define the primitive cell $[3 \times 2]_1$ drawn in figure 2(a),

$$\mathbb{A} = \begin{bmatrix} 3 & 1 \\ 0 & 2 \end{bmatrix}, \quad N_{\mathbb{A}} = 6. \quad (94)$$

The corresponding reciprocal primitive cell $\tilde{\mathbb{A}}$ (shaded region in figure 2(b)),

$$\tilde{\mathbb{A}} = \frac{2\pi}{6} \begin{bmatrix} 2 & 0 \\ -1 & 3 \end{bmatrix}, \quad (95)$$

satisfies the reciprocal bases condition (19), and contains the same number of reciprocal lattice sites $\mathbf{k} \in \tilde{\mathbb{A}}$ as the Bravais lattice primitive cell \mathbb{A} of figure 2(a).

4.3. Reciprocal primitive cell stability

In section 3.1 we computed the orbit Jacobian matrix eigenvalues for a one-dimensional primitive cell. Here we repeat the calculation for any two-dimensional primitive cell.

As illustrated by figure 2(b), there are $N_{\mathbb{A}} = LT$ discrete reciprocal primitive cell wave vectors in the reciprocal primitive cell $\tilde{\mathbb{A}}$. Substituting wave vector (93) into the

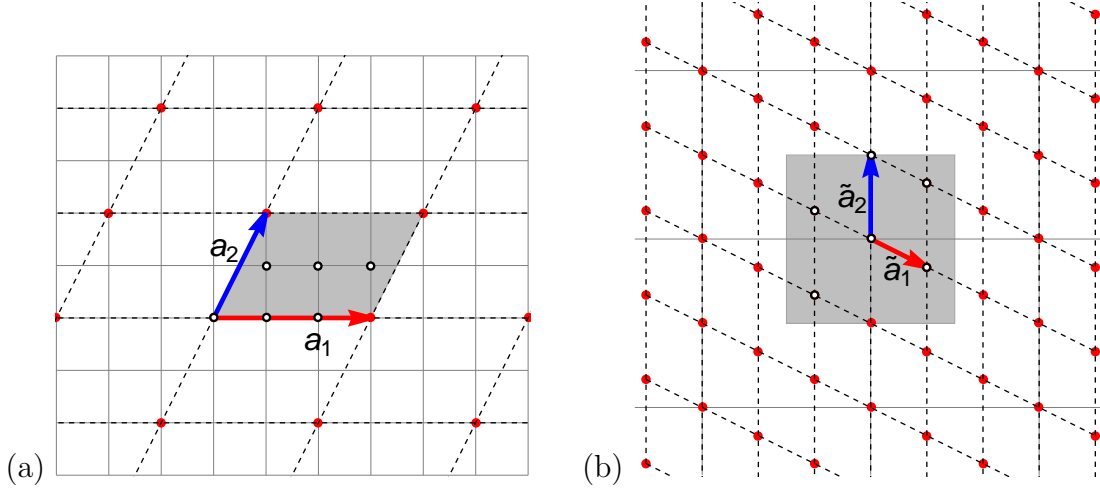


Figure 8. (Color online) (a) As in figure 2(a): translations of the primitive cell $\mathbb{A} = [3 \times 2]_1$ tile the Bravais lattice $\mathcal{L}_{\mathbb{A}}$ (red points). (b) Translations of reciprocal primitive vectors $\tilde{\mathbf{e}}_1, \tilde{\mathbf{e}}_2$ generate the reciprocal lattice $\mathcal{L}_{\tilde{\mathbb{A}}}$ (red points). (Shaded) The Brillouin zone \mathbb{B} , with $k_1, k_2 \in (-\pi, \pi]$. Continued in figure 9.

2-dimensional plane wave (as we did for the one-dimensional case, see (17)), we find that the k th eigenfunction phase evaluated on the lattice site z is

$$[\varphi(\mathbf{k})]_z = e^{i(k_1 z_1 + k_2 z_2)} \quad (96)$$

where

$$\begin{aligned} z &= z_1 z_2 \in \mathbb{A}, & \mathbf{k} &= k_1 k_2 \in \tilde{\mathbb{A}} \\ m &= m_1 m_2, & m_1 &= (0, 1, \dots, L-1), & m_2 &= (0, 1, \dots, T-1) \\ k_1 &= \frac{2\pi}{L} m_1, & k_2 &= \frac{2\pi}{T} (-m_1 S + m_2). \end{aligned}$$

The spatiotemporal orbit Jacobian matrix, $\tilde{\mathcal{J}} = (\mathbf{p}^2 + \mu^2)$, is diagonal on the reciprocal lattice, for any given primitive cell \mathbb{A} . The only subtlety is that, as illustrated by figure 2(b), now the reciprocal primitive vector $\tilde{\mathbf{a}}_1 = \frac{2\pi}{L}(1, -S/T)$ has a slant, resulting in a the diagonalized orbit Jacobian matrix

$$(\tilde{\mathcal{J}}_{\mathbb{A}})_{m_1 m_2} = p(k_1)_{m_1 m_2}^2 + p(k_2)_{m_1 m_2}^2 + \mu^2. \quad (97)$$

The reciprocal lattice orbit Jacobian matrix evaluated above in (79) is the special, tilt $S = 0$, rectangular primitive cell case. As wave-numbers k_j are not integers, but proportional to integers m_j –see (96)– it is convenient to index reciprocal lattice sites (discrete wave-numbers) by integer pairs $m_1 m_2$, while evaluating the RHS of (97) using the corresponding values of wave numbers k_1, k_2 . It's helpful to work out an example to demonstrate that (97) gives us the orbit Jacobian matrix spectrum.

Example: Orbit Jacobian matrix eigenvalues for $[3 \times 2]_1$ primitive cell.

We have $S/T = 1/2$, the wave-number ranges in (96) are $k_1 \in (0, 2\pi/3, 4\pi/3)$, $k_2 \in (0, \pi)$. The lattice momentum square part of the reciprocal lattice orbit

Jacobian matrix (97) is

$$\mathbf{p}^2 = p(k_1)^2 + p(k_2 - k_1/2)^2,$$

so lattice momenta $p(k) = 2 \sin(k/2)$ take values (up to a sign)

$$p(0) = 0, \quad p(\pi/3) = 1, \quad p(2\pi/3) = \sqrt{3}, \quad p(\pi) = 2.$$

A typical reciprocal lattice site evaluation of \mathbf{p}^2 :

$$\mathbf{p}_{11}^2 = p\left(\frac{2\pi}{3}\right)^2 + p\left(\pi - \frac{2\pi}{3} \frac{1}{2}\right)^2 = 3 + 3.$$

The values of the lattice momentum square \mathbf{p}^2 in (97), evaluated on the $N_{\mathbb{A}} = 6$ lattice sites of the reciprocal primitive cell in figure 2(b), indexed by integers $m_1 m_2$ as in (97), are

$$\mathbf{p}_{\mathbb{A}}^2 = \begin{array}{|c|c|c|} \hline \mathbf{p}_{01}^2 & \mathbf{p}_{11}^2 & \mathbf{p}_{21}^2 \\ \hline \mathbf{p}_{00}^2 & \mathbf{p}_{10}^2 & \mathbf{p}_{20}^2 \\ \hline \end{array} = \begin{array}{|c|c|c|} \hline 4 & 6 & 4 \\ \hline 0 & 4 & 6 \\ \hline \end{array}, \quad (98)$$

so, for example, the $(\tilde{\mathcal{J}}_{\mathbb{A}})_{11}$ eigenvalue is

$$\Lambda_{11} = 6 + \mu^2,$$

and so on. The ‘brick’ outlined in (98) is the rectangular primitive cell depicted in figure 7(b), with momentum squared \mathbf{p}^2 taking values on reciprocal lattice sites $m_1 m_2$.

The values of the lattice momentum square happen to be integers only for the few smallest primitive cells: in general their values are expressed in terms of Hipparchus cord functions $\text{crd}(2\pi m_j/L_j)$, or what we today call lattice momenta (76). However, for integer Klein-Gordon masses square μ^2 , the Hill determinants take integer values, so if we are not interested in details of the spectrum, their direct evaluation might be preferable. That we do in Appendix C.

Reciprocal lattice computations of spatiotemporal cat orbit Jacobian matrix spectra are easily automatized and have been carried out for thousands of Bravais lattices. We continue these calculations in section 6.3, with further explicit but not particularly illuminating spatiotemporal cat calculations relegated to Appendix B.

4.4. Reciprocal Bravais lattice stability

As explained in section 3.2, the orbit Jacobian *operator* acts on the *infinite* Bravais lattice $\mathcal{L}_{\mathbb{A}}$ and has a continuum spectrum over reciprocal lattice Brillouin zone. For Bravais lattice $\mathcal{L}_{[LX]_S}$, see (89), the Bloch eigenfunction (21) is a discrete field configuration over square lattice $z \in \mathbb{Z}^2$, with its phase $e^{i\mathbf{k}\cdot z}$ a continuous function of \mathbf{k} over the reciprocal lattice Brillouin zone \mathbb{B} . Any rectangle of area $(2\pi)^2$ can serve as the Brillouin zone, with Bloch eigenfunctions of the propagator (81),

$$\tilde{\mathcal{J}}\varphi(\mathbf{k})_z = (\mathbf{p}^2 + \mu^2) \varphi(\mathbf{k})_z. \quad (99)$$

Conventionally the Brillouin zone is a centered square, see shaded domain in figure 8(b).

5. Prime orbits

The key to the periodic orbit theory of time-evolving dynamical systems is the notion of *prime* periodic orbits [40, 124, 125], defined here in section 1.3. For a one-dimensional, temporal Bravais lattice, the form of the deterministic partition function (107), known as the deterministic trace formula (see [ChaosBook eq. \(21.24\)](#)), is very simple. For every temporal period n , we first determine all *prime orbits* Φ_p (section 1.3), and then sum over their repeats. The partition function takes form

$$Z[\beta, z] = \sum_p Z_p, \quad Z_p = \sum_{r=1}^{\infty} n_p t_p^r = \frac{n_p t_p}{1 - t_p}, \quad (100)$$

with the primitive cell volume $N_p = n_p$ equal to the time period of a prime orbit (see section 5.4) of temporal evolution equation $\phi_{t+1} - f(\phi_t) = 0$.

Then the set of all periodic states contributing to the partition function (41) consists of the n cyclic rotations of Φ_p plus $n_{p'}$ cyclic rotations of all shorter prime orbits $\Phi_{p'}$ whose r th repeat is of period $n = rn_{p'}$. So all we have to do is to determine the *prime orbits* of the translation equivalent periodic states.

5.1. Orbits

If Euler-Lagrange equations (39) keep their form (are ‘equivariant’) under a set of transformations $g \in G$, G is the *symmetry group* of the system. A solution (what we refer to here as a ‘periodic state’, see section 1.9) may satisfy all of system’s symmetries, a subgroup of them, or have no symmetry at all. Typically, a symmetry g acting on periodic state Φ_p generates a distinct periodic state $g\Phi_p$. The totality of symmetry transformations g applied to a periodic state Φ_p generates a set of equivalent periodic states that we refer to as the *orbit* or *G-orbit* of Φ_p ,

$$\mathcal{M}_p = \{g \Phi_p \mid g \in G\}. \quad (101)$$

We label the orbit \mathcal{M}_p by any periodic state Φ_p belonging to it, or by its mosaic M_p (45) (for examples of orbits, their symmetries and their indices, see companion paper I [93].)

The maximal subgroup $G_p \subseteq G$ of actions which permute periodic states within the orbit set \mathcal{M}_p , but leave the set invariant, is the *symmetry group* of \mathcal{M}_p ,

$$G_p = \{g \in G_p \mid g\mathcal{M}_p = \mathcal{M}_p\}. \quad (102)$$

The orbit \mathcal{M}_p is then said to be G_p -symmetric (symmetric, set-wise symmetric). The *index* of orbit \mathcal{M}_p

$$m_p = |G|/|G_p| \quad (103)$$

is the number of distinct periodic states in the orbit (see [Wikipedia \[143\]](#) and Dummit and Foote [48]).

For example, if system’s defining equations are of the same form for all times and everywhere in the space, they retain their form under action of one-lattice-spacing shift

operator r_1, r_2, \dots, r_d (52) in j th lattice direction. A periodic state Φ_p , however, is transformed by 1-step translation into -in general- a distinct periodic state $r_j\Phi_p$, with each translated periodic state Φ'_p having its own, periodic state dependent orbit Jacobian matrix $\mathcal{J}'_p = \mathcal{J}[\Phi'_p]$, with the stretching factor (70) at the lattice site z a function of the periodic state, $s_z = s[\Phi'_p]_z$. Bravais lattices $\mathcal{L}_{\mathbb{A}}$ (section 1.2) are infinite, and their translational symmetries (83) are infinite groups, but the orbit of a Bravais periodic state is always *finite*, generated by the finite cyclic group of translations of the infinite lattice curled up into a $N_{\mathbb{A}}$ -sites periodic primitive cell \mathbb{A} .

5.2. Stability of large primitive cells

In textbook arguments leading to the Bloch theorem (section 1.5), one notes that larger and larger spatiotemporal primitive cells correspond to denser and denser reciprocal primitive cells (see, for example, figure 5 (b)), leading in the infinite primitive cell limit to the parametrization of the 1st Brillouin zone \mathbb{B} by a continuum of values of wave vectors $\mathbf{k} = (k_1, k_2, \dots, k_d)$, $k_j \in (-\pi, \pi]$.

We take no such limit here. Instead, the partition function has a support on *all* Bravais lattices. In illustrating this, the calculation of free-field / spatiotemporal cat primitive cell stability of sections 3.1 and 4.3 is particularly helpful. For both linear and nonlinear field theories, steady states $\phi_z = \phi$, whose primitive cell is the hypercubic unit cell (1), have orbit Jacobian matrices (71)–(73) with a single, constant stretching factor $s_z = s$. For each primitive cell \mathbb{A} , a calculation yields orbit Jacobian matrix's $N_{\mathbb{A}}$ eigenvalues that depend on the primitive cell shape, but for the *orbit Jacobian operator* there is only a single continuous Bloch band. Inspection of figures 4 and 5 makes it clear what all these different orbit Jacobian matrix's spectra are: they are discrete approximations to continuous Bloch bands, with ‘cords’ approximation errors decreasing as the primitive cell volume increases (for the convergence rate of the approximations, see shadowing section 8).

The most important observation for what follows is that while each primitive cell \mathbb{A} has its own distinct orbit Jacobian matrix spectrum, for a steady $\phi_z = \phi$ state there is *only one* continuous orbit Jacobian operator spectrum. Why is that?

5.3. A doubly-periodic prime orbit, and its repeats

For the free-field theory and spatiotemporal cat, $s_z = s$, orbit Jacobian operator (67) is 1-step translation (11) invariant along all lattice dimensions. Its stability is the stability of a steady state, with all other primitive cells \mathbb{A} tiled by repeats of the unit hypercube (1) primitive cell steady state. Here the unit square primitive cell periodic state is the simplest *prime orbit* (section 1.3), a steady state, all larger primitive cells' periodic states are repeats of the unit square prime orbit. In particular, the primitive cell (87) is tiled by L copies of the unit square steady state horizontally, T copies vertically, with $S = 0, 1, \dots, L - 1$ distinct primitive cells for a given T .

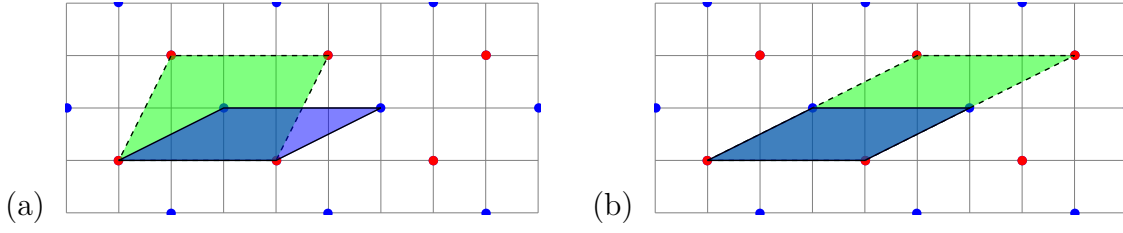


Figure 9. (Color online) (a) Bravais lattice $\mathbb{A} = [3 \times 2]_1$ of figure 6, red dots, is a sublattice of Bravais lattice $\mathbb{A}' = [3 \times 1]_2$, blue and red dots, even though the primitive cell \mathbb{A} (green parallelogram spanned by primitive vectors $(3,0)$ and $(1,2)$) does not appear to be tiled by repeats of the primitive cell \mathbb{A}' (blue parallelogram spanned by primitive vectors $(3,0)$ and $(2,1)$). (b) If we shift the top edge of primitive cell \mathbb{A} by 3 lattice units, to $[3 \times 2]_4 = [3 \times 2]_1$ (green parallelogram spanned by primitive vectors $(3,0)$ and $(4,2)$), the tiling is clear. Continued in figure 10.

Now, view the primitive cell \mathbb{A} as the *unit* square of a square lattice, that supporting a multiplet of $N_{\mathbb{A}}$ fields belonging to a *prime* periodic state, i.e., a periodic state which is not a repeat of a smaller periodicity periodic state. Under Bravais lattice translations, this multiplet is an $N_{\mathbb{A}}$ -dimensional steady state. The same procedure as for the initial lattice unit square repeats applies: a $P_{\mathbb{A}\mathbb{R}}$ primitive cell periodic state is obtained by repeating this tile r_1 times horizontally, r_2 times along the ‘slanted’ primitive vector $\mathbf{a}_2 = (S, T)$, with $0 \leq s < r_1$ doubly-periodic distinct twisted $[r_1 \times r_2]$ tori, each resulting in a periodic state over larger-periodicity Bravais sublattice $\mathcal{L}_{\mathbb{A}\mathbb{R}}$.

Examples are figure 9 (b), and the mosaics of figure 10.

5.4. Prime field configurations

Example: $[2 \times 2]_0$ is a sublattice of $[2 \times 1]_1$.

It is possible that a field configuration with periodicity $[L \times T]_S$ is invariant under the translation of another lattice $[L_p \times T_p]_{S_p}$, if $[L \times T]_S$ is a sublattice of $[L_p \times T_p]_{S_p}$. For example, consider a field configuration over primitive cell $[2 \times 2]_0$:

$$\Phi = \begin{bmatrix} \phi_{10} & \phi_{00} \\ \phi_{00} & \phi_{10} \end{bmatrix}.$$

This is a repeat and shift of the field configuration

$$\Phi_p = \begin{bmatrix} \phi_{00} & \phi_{10} \end{bmatrix}$$

over primitive cell $[2 \times 1]_1$. As shown in figure 7 (a), Bravais lattice $[2 \times 2]_0$ is a sublattice of $[2 \times 1]_1$. From the figure 10 (d) it is clear that over the infinite spacetime Φ and Φ_p are the same field configuration.

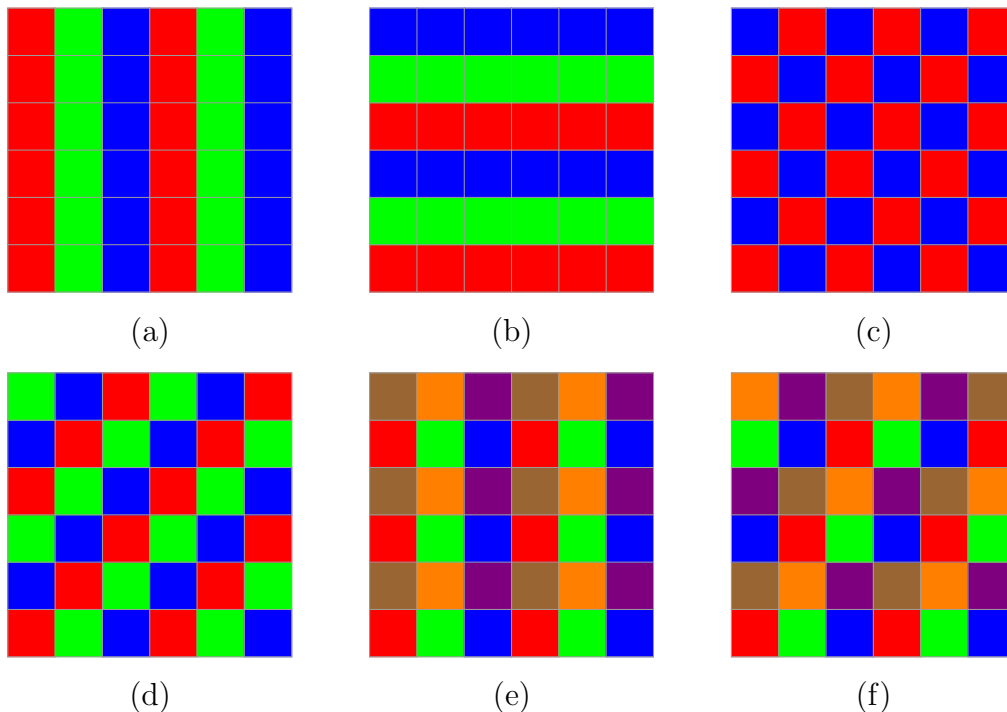


Figure 10. (Color online) Examples of spatiotemporal mosaic tilings (45) of $[6 \times 6]_0$ primitive cell by repeats of smaller prime orbits, Appendix F. (a) $[3 \times 1]_0$ temporally steady state. (b) $[1 \times 3]_0$ spatially steady state. (c) $[2 \times 1]_1$ relative-periodic prime orbit, spatial period-2, temporal period-2; compare with figure 7(a). (d) $[3 \times 1]_1$ relative-periodic prime orbit, spatial period-3, temporal period-3. (e) $[3 \times 2]_0$ spatial period-3, temporal period-2. (f) $[3 \times 2]_1$ of figures 7(b) and 9. It is a relative-periodic prime orbit, of spatial period-3, temporal period-6. See also figure 11.

6. Weight of a periodic state

The deterministic partition sum (41) is the sum over all periodic states c over a primitive cell \mathbb{A} ,

$$Z_{\mathbb{A}}[\beta] = \sum_c \frac{1}{|\text{Det } \mathcal{J}_c|} e^{N_{\mathbb{A}} \beta \cdot \langle a \rangle_c}, \quad (104)$$

where the periodic state's Hill determinant is the weight of its contribution to the partition sum. We now reformulate this partition sum in terms of primitive cell \mathbb{A} *stability exponents* (section 6.1), in order to be able to evaluate it on the spatiotemporally infinite Bravais lattice $\mathcal{L}_{\mathbb{A}}$ (section 6.4).

A Hill determinant of an orbit Jacobian matrix evaluated over a primitive cell \mathbb{A} is a determinant of a finite-dimensional matrix, for example matrix (75). In section 6.3 we show how the Hill determinant of periodic state c , given by the product of orbit Jacobian matrix's eigenvalues,

$$|\text{Det } \mathcal{J}_c| = \prod_{j=1}^{N_{\mathbb{A}}} |\Lambda_{c,j}|, \quad (105)$$

is evaluated on the reciprocal lattice. In [Appendix C](#) we show that one can also visualize and compute a Hill determinant geometrically, as the volume of the orbit Jacobian matrix fundamental parallelepiped.

But what is the ‘Hill determinant’ of an ∞ -dimensional linear operator such as the Bravais lattice operator [\(80\)](#)? A textbook approach to calculation of spectra of such linear operators (for example, quantum-mechanical Hamiltonians) is to compute them in a large primitive cell \mathbb{A} , and then take the infinite box limit. It is crucial to understand that we *do not* do that here. Instead, as in solid state physics and quantum field theory, our calculations are carried out over the *infinite* spatiotemporal Bravais lattice [\[14, 46, 86\]](#) or *infinite* continuous spacetime [\[102\]](#), and the weight [\(105\)](#) is a functional determinant [\[50\]](#).

6.1. Stability exponent of a primitive cell periodic state

To develop some intuition about the Hill determinant [\(105\)](#), consider its evaluation in the anti-integrable limit [\(74\)](#). For the free massive boson theory and the spatiotemporal cat, all $N_{\mathbb{A}}$ orbit Jacobian matrix eigenvalues tend to $\Lambda_{c,j} \rightarrow \mu^2$, so

$$|\text{Det } \mathcal{J}_{\mathbb{A}}| \rightarrow e^{N_{\mathbb{A}}\lambda}, \quad \lambda = \ln \mu^2,$$

where λ is the stability exponent per unit-lattice-volume. This suggests that we assign to each periodic state an average *stability exponent* λ_c per unit-lattice-volume,

$$\frac{1}{|\text{Det } \mathcal{J}_c|} = e^{-N_{\mathbb{A}}\lambda_c}, \quad \lambda_c = \frac{1}{N_{\mathbb{A}}} \sum_{j=1}^{N_{\mathbb{A}}} \ln |\Lambda_{c,j}|, \quad (106)$$

where λ_c is the Birkhoff average [\(22\)](#) of the logs of orbit Jacobian matrix’s eigenvalues. This is a generalization of the temporal periodic orbit Floquet exponent (the periodic orbit ‘Lyapunov’ exponent) to any multi-periodic state, in any spatiotemporal dimension.

Now the deterministic partition sum [\(104\)](#) takes form

$$Z_{\mathbb{A}}[\beta] = e^{N_{\mathbb{A}}W_{\mathbb{A}}[\beta]} = \sum_c t_c, \quad t_c = e^{N_{\mathbb{A}}(\beta \cdot \langle a \rangle_c - \lambda_c)}, \quad (107)$$

where the sum is over all periodic states c with primitive cell periodicity \mathbb{A} , and

$$p_{\mathbb{A}}[\Phi_c] = e^{-N_{\mathbb{A}}\lambda_c} / Z_{\mathbb{A}}[0] \quad (108)$$

is the probability [\(36\)](#) of periodic state Φ_c . What is this partition sum good for? To paraphrase Baxter [\[20\]](#): “We are particularly interested in calculating the partition function [\(107\)](#) per site,

$$e^W = Z^{1/N_{\mathbb{A}}}, \quad N_{\mathbb{A}} = LT,$$

[...]. We expect W to tend to limit when $L, T \rightarrow \infty$. Notation ‘ t_c ’ is a vestige of referring to this weight in the time-periodic orbit, 1-dimensional temporal lattice case, as the ‘little trace’ (see [ChaosBook example 18.12](#)).

As a concrete example, let us derive the formula for the expectation value $\langle \lambda \rangle_{\mathbb{A}}$ of the stability exponent averaged over primitive cell \mathbb{A} . Take as the observable the log of an orbit Jacobian matrix's eigenvalue (106). Its expectation value (38) is obtained by applying a $\partial/\partial\beta$ derivative to the log of partition function, and then setting the auxiliary variable β to zero,

$$\langle \lambda \rangle_{\mathbb{A}} = \left. \frac{\partial}{\partial \beta} W_{\mathbb{A}}[\beta] \right|_{\beta=0} = \frac{1}{Z_{\mathbb{A}}[0]} \sum_c \lambda_c e^{-N_{\mathbb{A}} \lambda_c}. \quad (109)$$

In the one-dimensional, temporal lattice systems case, large time period limit, this is system's Lyapunov exponent: the stability of a periodic solution is characterized by its Floquet exponents, i.e., average expansion rates per unit *time* interval. In our field-theoretic formulation, the corresponding quantity for spatiotemporal systems is the average stability exponent per unit *spacetime volume*, in any spacetime dimension, over a finite primitive cell \mathbb{A} of volume $N_{\mathbb{A}}$.

6.2. Temporal cat

There are many different ways to skin this cat, some discussed in companion paper I [93], where we review the one-dimensional temporal lattice Isola [77] topological zeta function $1/\zeta_{\text{top}}(z)$ and its relation to $T_n(s/2)$, the Chebyshev polynomials of the first kind.

6.3. Spatiotemporal cat: primitive cell stability

In this section, we use 2-dimensional free-field / spatiotemporal cat as an example of computation of the Hill determinants over a finite volume primitive cell \mathbb{A} . For a given $\mathcal{L}_{\mathbb{A}}$ -periodic state, the Hill determinant of the finite volume primitive cell \mathbb{A} orbit Jacobian matrix is given by the product of its eigenvalues (105).

As shown in section 3.1, the free-field theory / spatiotemporal cat orbit Jacobian matrix (67), with no periodic state dependence, $s_z = s$, is diagonalized by going to the reciprocal lattice. For the square-lattice spatiotemporal cat the explicit formula for Hill determinant (105) of the primitive cell \mathbb{A} orbit Jacobian matrix in terms of lattice momenta follows from (97):

$$\begin{aligned} |\text{Det } \mathcal{J}_{\mathbb{A}}| &= \prod_{m_1=0}^{L-1} \prod_{m_2=0}^{T-1} [p(k_1)^2 + p(k_2 - k_1 S/T)^2 + \mu^2] \\ k_1 &= \frac{2\pi}{L} m_1, \quad k_2 = \frac{2\pi}{T} m_2. \end{aligned} \quad (110)$$

Note that all spatiotemporal cat Hill determinants have a μ^2 prefactor. This is due to the fact that for $\mu^2 = 0$ one is looking at a Laplacian, and Laplacian operator (50), which compares a site field to its neighbors, always has a zero eigenvalue for the constant eigenvector φ_{00} .

6.4. Stability exponent of a Bravais periodic state

The field configurations we consider here are not the primitive cell \mathbb{A} periodic states Φ_c with only $N_{\mathbb{A}}$ field values, but the infinite spatiotemporal Bravais lattice states, with each orbit Jacobian operator \mathcal{J}_c an ∞ -dimensional linear operator.

Consider approximating the Bravais lattice $\mathcal{L}_{\mathbb{A}}$ periodic state Φ_c (3) by r repeats (a finite ‘box’) of the primitive cell periodic state (9) in every spacetime direction (here just one), computing the eigenvalues of the $[rN_{\mathbb{A}} \times rN_{\mathbb{A}}]$ orbit Jacobian matrix and taking the $r \rightarrow \infty$ limit,

$$\langle \lambda \rangle_c = \lim_{r \rightarrow \infty} \langle \lambda \rangle_{r\mathbb{A},c} = \lim_{r \rightarrow \infty} \frac{1}{rN_{\mathbb{A}}} \sum_{j=1}^{rN_{\mathbb{A}}} \ln |\Lambda_{c,j}|. \quad (111)$$

But a better way of computing the stability exponent is to find the spectrum of the orbit Jacobian matrix on the reciprocal lattice. We show in section 6.3 that the Birkhoff average $\langle \lambda \rangle_c$ is an average over the Brillouin zone.

Bravais lattice $\mathcal{L}_{\mathbb{A}}$ has continuous (band) spectra of form

$$\ell = \frac{N_{\mathbb{A}}}{(2\pi)^d} \mathbf{k}$$

$$\frac{1}{N_{\mathbb{A}}} \sum_{j=1}^{N_{\mathbb{A}}} \ln |\Lambda_{c,j}| \Rightarrow \langle \lambda \rangle_{c,j} = \frac{1}{(2\pi)^d} \int_{\mathcal{L}_{\mathbb{A}}} d\mathbf{k} \ln |\Lambda_{c,j}(\mathbf{k})|,$$

We now show that the ‘Hill determinant’ of the infinite-dimensional Bravais lattice $\mathcal{L}_{\mathbb{A}}$ orbit Jacobian operator is computed using an integral of the continuous spectra (112).

6.5. Spatiotemporal cat: Bravais lattice stability

The Hill determinant of the infinite spacetime orbit Jacobian operator is not finite. The stability exponent of the periodic states (111) can be computed by integrating the spectrum over the Brillouin zone:

$$\lambda_c = \frac{1}{(2\pi)^2} \int_{-\pi}^{\pi} \int_{-\pi}^{\pi} dk_1 dk_2 \ln (p(k_1)^2 + p(k_2)^2 + \mu^2). \quad (112)$$

The Bravais lattice $\mathcal{L}_{\mathbb{A}}$ orbit Jacobian operators are computed on the infinite spacetime without periodic boundary conditions. Thus for spatiotemporal cat, every periodic state has a same Bravais lattice $\mathcal{L}_{\mathbb{A}}$ orbit Jacobian operator.

The spectrum of the 2-dimensional spatiotemporal cat computed using the Bloch theorem is plotted in figure 5 (a). Eigenvalues of primitive cell \mathbb{A} orbit Jacobian matrices can be found on this spectrum, at the reciprocal lattice sites of their Bravais lattice $\mathcal{L}_{\mathbb{A}}$.

7. Periodic orbit theory

For a one-dimensional, temporal Bravais lattice, the generating function of the deterministic partition function (107) is known as the deterministic trace formula (see

ChaosBook eq. (21.24)),

$$Z[\beta, z] = \sum_p \sum_{r=1}^{\infty} N_p t_p^r = \sum_p \frac{T_p t_p}{1 - t_p}, \quad (113)$$

with the primitive cell volume $N_p = T_p$ equal to the time period of a prime orbit (see section 5.4) of temporal evolution equation $\phi_{t+1} - f(\phi_t) = 0$. As here every periodic state weight contributes with a positive sign, there are no cancelations, and the key property of hyperbolic flow trajectories, that they are shadowed by shorter trajectories (section 8), is here not taken into account. That is accomplished by reorganizing the periodic state contributions into the dynamical zeta function [126],

$$1/\zeta = \prod_p (1 - t_p), \quad (114)$$

whose pseudo-cycle expansion leads to cycle averaging formulas with better convergence than the partition sum (113) (see ChaosBook sect. 23.5). 

An inspiration for construction of the Ruelle dynamical zeta function (114) is the Artin-Mazur zeta function [9, 39, 93],

$$\zeta_{\text{AM}}(z) = \exp\left(\sum_{n=1}^{\infty} \frac{N_n}{n} z^n\right), \quad (115)$$

which *counts* the numbers of the periodic points N_n of a discrete-time dynamical system. In what follows we draw inspiration from Lind's generalization [96] of Artin-Mazur zeta function,

$$\zeta_{\text{Lind}}(z) = \exp\left(\sum_H \frac{N_H}{|G/H|} z^{|G/H|}\right), \quad (116)$$

where in our application, G is the symmetry group (crystallographic space group) of a field theory over a hypercubic lattice \mathbb{Z}^d , H a finite-index $|G/H|$ subgroup of G , and N_H is the number of the periodic states that are invariant under actions of the subgroup H .

In paper I we have derived the Lind-inspired, dihedral-space group $G = D_\infty$ zeta function for time-reversal invariant field theories over temporal one-dimensional integer lattice \mathbb{Z} . Here we assume that the space group is the translation group $G = T$ (no point group of section 4), and focus on the case of a two-dimensional square lattice, with the translation group (83).

7.1. Primitive cell partition sum in terms of prime orbits

As translation symmetry of the theory stratifies the set of all periodic states into prime orbits, i.e., sets of translation-equivalent periodic states (section 1.2), the primitive cell \mathbb{A} deterministic partition function (41) can be

For any primitive cell of a given Bravais lattice, we can compute the corresponding partition function (107). The *deterministic generating partition function* is the generating function of deterministic partition functions $Z_{\mathbb{A}}[\beta]$ (107) over all Bravais

sublattices $\mathcal{L}_{\mathbb{A}}$ of the hypercubic integer lattice \mathbb{Z}^d , i.e. the sum over all periodic states Φ_c over all Bravais lattices

$$\begin{aligned} Z[\beta, z] &= \sum_{\mathbb{A}} Z_{\mathbb{A}}[\beta] z^{N_{\mathbb{A}}} \\ &= \sum_c t_c, \quad t_c = \left(e^{\beta \cdot \langle a \rangle_c - \langle \lambda \rangle_c} z \right)^{N_c}, \end{aligned} \quad (117)$$

where t_c is the observable-weighted probability of periodic state Φ_c , $\langle \lambda \rangle_c$ the stability exponent (111), N_c is the volume (8) of \mathcal{L}_c , and z is a variable that we use to organize generating functions.

We have not actually encountered any such sum over Bravais lattices in solid state literature. In field theory they play a key role [102], so here we refer to them as field theorists do, as ‘sums over geometries’.

A periodic state Φ_c is either prime, or a repeat (section 5.3) of a prime orbit Φ_p with periodicity $\mathcal{L}_{\mathbb{A}}$. A prime orbit Φ_p over its primitive cell of $\mathcal{L}_{\mathbb{A}}$ has the same Hill determinant and Birkhoff sum (22) for the N_p periodic states in its translational group orbit, so its contribution to the deterministic generating partition function (117) is $N_p t_p$, where

$$t_p = \left(e^{\beta \cdot \langle a \rangle_p - \langle \lambda \rangle_p} z \right)^{N_p}, \quad N_p = N_{\mathbb{A}} = L_{\mathbb{A}} T_{\mathbb{A}}. \quad (118)$$

For any periodic state over the infinite spacetime, a prime orbit over its primitive cell \mathbb{A} is the smallest tile that tiles the infinite periodic state. The repeat matrix \mathbb{R} (section 5.3), acting on the unit cell \mathbb{A} generates all distinct $\mathcal{L}_{\mathbb{A}\mathbb{R}}$ Bravais sublattices of $\mathcal{L}_{\mathbb{A}}$.

The wonderful thing about using the stability exponent $\langle \lambda \rangle_p$ over the infinite spacetime (111) (as opposed to the stability exponent over a finite primitive cell (106)) is that it is multiplicative for the prime orbit Φ_p repeated over a larger $\mathbb{A}\mathbb{R}$ primitive cell (section 5.3): the contribution of a repeat to the partition function is

$$N_p \left(e^{\beta \cdot \langle a \rangle_p - \langle \lambda \rangle_p} z \right)^{r_1 r_2 N_p} = N_p t_p^{r_1 r_2}, \quad (119)$$

where $r_1 r_2 N_p$ is the volume of the $\mathbb{A}\mathbb{R}$ primitive cell and $\exp(\beta \cdot \langle a \rangle_c - \langle \lambda \rangle_c)$ is the observable-weighted probability density per lattice site. The sum over all prime orbits Φ_p and their repeats ($\mathbb{A}\mathbb{R}$ primitive cells) yields the deterministic generating partition function $Z[\beta, z]$ (117) expressed in terms of prime orbits Φ_p . For the two-dimensional square lattice this is

$$Z[\beta, z] = \sum_p Z_p[\beta, z], \quad Z_p[\beta, z] = N_p \sum_{r_1=1}^{\infty} \sum_{r_2=1}^{\infty} \sum_{s=0}^{r_1-1} t_p^{r_1 r_2}.$$

The N_p prefactor arises because all periodic states in the group orbit of a prime orbit Φ_p have the same weight. For each width r_1 , height r_2 , the number of Hermite normal form (87) relative periodic primitive cells $[r_1 \times r_2]_s$ is

$$\sum_{s=0}^{r_1-1} 1 = r_1 \quad \text{so} \quad Z_p[\beta, z] = N_p \sum_{r_1=1}^{\infty} \sum_{r_2=1}^{\infty} r_1 (t_p^{r_1})^{r_2}.$$

As the r_2 sum is a geometric series, the deterministic generating partition function (117)

$$Z[\beta, z] = \sum_p N_p \sum_{n=1}^{\infty} \frac{nt_p^n}{1-t_p^n} \quad (120)$$

is expressed as the sum of all prime orbits and their repeats, the two-dimensional spacetime generalization of the temporal deterministic generating partition function (113). The prime orbit repeats sum

$$\begin{aligned} \frac{1}{N_p} Z_p[\beta, z] &= \sum_{n=1}^{\infty} \sigma(n) t_p^n \\ &= t_p + 3t_p^2 + 4t_p^3 + 7t_p^4 + 6t_p^5 + 12t_p^6 + 8t_p^7 + \dots, \end{aligned} \quad (121)$$

was first studied by Euler, where $\sigma(n)$ is the Euler **sum-of-divisors function**.

Now back to the deterministic generating partition function. For Bravais lattices with large primitive cells \mathbb{A} , the deterministic partition function tends to the limit

$$Z_{\mathbb{A}}[0] \rightarrow e^{-N_{\mathbb{A}}\gamma}$$

where γ is the escape rate of the system, and the derivative of the partition function tends to the expectation value of the observable

$$\left. \frac{\partial}{\partial \beta} \ln Z_{\mathbb{A}}[\beta] \right|_{\beta=0} \rightarrow N_{\mathbb{A}} \langle a \rangle.$$

So the escape rate and expectation values of observables are determined by the radius of convergence of (117) as a function of β :

$$z(\beta) = e^{-\beta \cdot \langle a \rangle + \gamma}, \quad (122)$$

and

$$\gamma = \ln z(0), \quad \langle a \rangle = - \left. \frac{\partial}{\partial \beta} \ln z(\beta) \right|_{\beta=0}. \quad (123)$$

Now, in the deterministic generating partition function (117) everything contributes to periodic state weights with positive signs, there are *no shadowing cancellations*. The smart thing is to replace the partition function by the appropriate zeta function.

7.2. Spatiotemporal zeta function

In the spirit of the Lind zeta function, we define the two-dimensional spatiotemporal zeta function, now not as a solution-counting generating function (116), but *probability weighted* by t_p (118),

$$\begin{aligned} \zeta[\beta, z] &= \prod_p \zeta_p[\beta, z], \quad \ln \zeta_p[\beta, z] = \sum_{r_1=1}^{\infty} \sum_{r_2=1}^{\infty} \sum_{s=0}^{r_1-1} \frac{t_p^{r_1 r_2}}{r_1 r_2} = - \sum_{r_1=1}^{\infty} \ln(1 - t_p^{r_1}) \\ 1/\zeta[\beta, z] &= \prod_p \prod_{n=1}^{\infty} (1 - t_p^n). \end{aligned} \quad (124)$$

Our spatiotemporal zeta function - a two-dimensional generalization of the dynamical zeta function (114) - is related to the deterministic generating partition function (120) (two-dimensional generalization of the deterministic trace formula (113)) by the usual logarithmic derivative relation between the partition sum and the zeta function

$$Z[\beta, z] = z \frac{d}{dz} \ln \zeta[\beta, z] = \sum_p N_p \sum_{n=1}^{\infty} \frac{nt_p^n}{1 - t_p^n}, \quad (125)$$

see, for example, [ChaosBook eq. \(18.24\)](#).

The zeros of the zeta function (124) are poles of the deterministic generating partition function (117). So to compute the escape rate and expectation values of observables one can use the leading root $z(\beta)$ of the zeta function $1/\zeta[\beta, z]$:

$$1/\zeta[\beta, z(\beta)] = 0. \quad (126)$$

The escape rate γ and expectation value of observables $\langle a \rangle$ are computed using $z(\beta)$ by (123). Using the implicit equation (126) the expectation value of observable $\langle a \rangle$ can also be computed as:

$$\langle a \rangle = \frac{1}{z} \left(\frac{\partial \zeta[\beta, z]}{\partial \beta} / \frac{\partial \zeta[\beta, z]}{\partial z} \right) \Big|_{\beta=0, z=z(0)}. \quad (127)$$

Much is known about this zeta function, as for each prime orbit $1/\zeta_p[\beta, z]$ is the [Euler function](#) $\phi(t_p)$,

$$1/\zeta_p[\beta, z] = \phi(t_p) = \prod_{n=1}^{\infty} (1 - t_p^n), \quad |t_p| < 1, \quad (128)$$

whose power series in terms of pentagonal number powers of z was given by Euler in 1741 [21]

$$\begin{aligned} \phi(z) = & 1 - z - z^2 + z^5 + z^7 - z^{12} - z^{15} \\ & + z^{22} + z^{26} - z^{35} - z^{40} + z^{51} + z^{57} \\ & - z^{70} - z^{77} + z^{92} + z^{100} + \dots \end{aligned} \quad (129)$$

So, while for one-dimensional temporal lattice contribution (114) of a prime orbit Φ_p is simply $1/\zeta_p[\beta, z] = 1 - t_p$, in 2 spatiotemporal dimensions the prime orbit weight is a special function with an infinite power series expansion, but also many other powerful methods to compute it.

The Euler function can be expressed as the [Dedekind eta function](#) $\eta(\tau)$,

$$\phi(z) = z^{-\frac{1}{24}} \eta(\tau), \quad \text{Im}(\tau) > 0, \quad (130)$$

where the complex phase τ_p , $t_p = e^{i2\pi\tau_p}$ follows from (119),

$$\tau_p = i \frac{N_p}{2\pi} (-\beta \cdot \langle a \rangle_p + \langle \lambda \rangle_p + s), \quad (131)$$

with the periodic state Φ_p probability weight having a pure positive imaginary phase

$$\tau_p = i N_p \langle \lambda \rangle_p / 2\pi.$$

Variants of such partition functions had been derived, by various methods and in different contexts, in [28, 78, 102].

7.2.1. Example: Escape rate of temporal cat

The topological zeta function of temporal cat is [77, 93]:

$$1/\zeta_{AM}(z) = \exp\left(-\sum_{n=1}^{\infty} \frac{N_n}{n} z^n\right) = \frac{1 - sz + z^2}{(1 - z)^2}, \quad (132)$$

where N_n is the number of periodic states with period n . Due to the uniform stretching factor s , the dynamical zeta function of temporal cat has the same form, up to a rescaling:

$$1/\zeta(0, z) = \exp\left(-\sum_{n=1}^{\infty} \frac{N_n z^n}{n \Lambda^n}\right) = 1/\zeta_{AM}(t), \quad t = \frac{z}{\Lambda}, \quad (133)$$

where Λ is the stability multiplier

$$\Lambda = e^\lambda = \frac{1}{2}(s + \sqrt{(s-2)(s+2)}). \quad (134)$$

Solve for the roots of $1/\zeta(z) = 0$, we have:

$$t = \frac{1}{2}(s \pm \sqrt{(s-2)(s+2)}) \rightarrow z = 1 \text{ or } \Lambda^2. \quad (135)$$

The leading root is 1 so the escape rate is 0. The Fredholm determinant is:

$$F(0, z) = \exp\left(-\sum_{n=1}^{\infty} \frac{N_n z^n}{n |\text{Det } \mathcal{J}_n|}\right) = \exp\left(-\sum_{n=1}^{\infty} \frac{z^n}{n}\right) = 1 - z, \quad (136)$$

the escape rate computed from which is also 0.

7.2.2. Lind zeta function and spatiotemporal zeta function of the two-dimensional spatiotemporal cat

The Lind zeta function of the two-dimensional spatiotemporal cat can be computed by substitute the number of the spatiotemporally periodic states (110) to (116):

$$1/\zeta_{Lind}(z) = \exp\left(-\sum_{L=1}^{\infty} \sum_{T=1}^{\infty} \sum_{S=0}^{L-1} \frac{N_{[L \times T]_S}}{LT} z^{LT}\right). \quad (137)$$

We do not know how to compute (137) for the two-dimensional spatiotemporal cat.

Every periodic state of spatiotemporal cat has a same stability exponent $\langle \lambda \rangle$:

$$\langle \lambda \rangle = \frac{1}{(2\pi)^2} \int_{-\pi}^{\pi} dk_1 \int_{-\pi}^{\pi} dk_2 \ln(2s - 2 \cos k_1 - 2 \cos k_2) \quad (138)$$

which can be evaluated numerically. The spatiotemporal zeta function of spatiotemporal cat has a same form as the Lind zeta function up to a rescaling:

$$\begin{aligned} 1/\zeta(0, z) &= \exp\left[-\sum_{L=1}^{\infty} \sum_{T=1}^{\infty} \sum_{S=0}^{L-1} \frac{N_{[L \times T]_S}}{LT} (ze^{-\langle \lambda \rangle})^{LT}\right] \\ &= 1/\zeta_{Lind}(t), \quad t = ze^{-\langle \lambda \rangle}. \end{aligned} \quad (139)$$

If we use the stability exponents of finite periodic states $\langle \lambda_c \rangle$ (106) instead of the stability exponents of infinite periodic states $\langle \lambda \rangle$, the spatiotemporal zeta function can be evaluated analytically, due to the fundamental fact:

$$\begin{aligned} 1/\zeta(0, z) &= \exp \left[- \sum_{L=1}^{\infty} \sum_{T=1}^{\infty} \sum_{S=0}^{L-1} \frac{N_{[L \times T]_S}}{LT} \left(\frac{z}{e^{\langle \lambda_c \rangle}} \right)^{LT} \right] \\ &= \exp \left(- \sum_{L=1}^{\infty} \sum_{T=1}^{\infty} \sum_{S=0}^{L-1} \frac{z^{LT}}{LT} \right) \\ &= \prod_{n=1}^{\infty} (1 - z^n) = \phi(z), \end{aligned} \quad (140)$$

where $\phi(z)$ is the Euler function (129).

The spatiotemporal zeta function of section 7.2 is the main result of this paper. However, there are still a couple of questions of general nature that alert reader is likely to ask.

(i) How is this global, high-dimensional orbit stability related to the stability of the conventional low-dimensional, forward-in-time evolution? The two notions of stability are related by Hill's formulas (also known as the Gel'fand-Yaglom theorem [61, 99], for continuous spacetime), relations that are in our formulation equally applicable to energy conserving systems, as to viscous, dissipative systems. We derive them in [93, 94]. From the field-theoretic perspective, Hill determinants are fundamental, forward-in-time evolution is merely one of the methods for computing them.

(ii) The convergence cycle-expansions is accelerated by shadowing of long orbits by shorter periodic orbits [10]. Are d -dimensional tori (primitive cells) that periodic states live on also shadowed smaller tori periodic states? In section 8 we check numerically that spatiotemporal cat periodic states that share finite spatiotemporal mosaics indeed shadow each other to exponential precision.

8. Shadowing

In ergodic theory 'shadowing lemma' –a true time-trajectory is said to shadow a numerical solution if it stays close to it for a time interval [19, 114]– is often invoked to justify collecting statistics from numerical trajectories for integration times much longer than system's Lyapunov time [145]. In periodic orbit theory, the issue is neither the Lyapunov time, nor numerical accuracy: all periodic orbits are 'true' in the sense that in principle they can be computed to arbitrary accuracy [44]. Here 'shadowing' refers to the shortest distance between two orbits decreasing exponentially with the length of the shadowing time interval. Long orbits being shadowed by shorter ones leads to controllable truncations of cycle expansions [10], and computation of expectation values of observables of dynamical systems to exponential accuracy [40].

Field configurations are points in state space (3), with the separation of two periodic states Φ , Φ' given by the state space vector $\Phi - \Phi'$, so we define 'distance' as the average

site-wise state space Euclidean distance-squared between field configurations Φ, Φ' , i.e., by the Birkhoff average (22)

$$|\Phi - \Phi'|^2 = \frac{1}{N_{\mathbb{A}}} \sum_{z \in \mathbb{A}} (\phi'_z - \phi_z)^2 \quad (141)$$

This notion of distance is intrinsically spatiotemporal, it does not refer to time-evolving unstable trajectories separating in time. For spatiotemporal cat we have an explicit formula for pairwise separations: If two spatiotemporal cat periodic states Φ, Φ' share a common sub-mosaic \mathbf{M} , they are site-fields separated by

$$\phi_z - \phi'_z = \sum_{z' \notin \mathbf{M}} g_{zz'} (m - m')_{z'} \pmod{1}, \quad (142)$$

where matrix $g_{zz'}$ is the spatiotemporal cat Green's function (62).

It was shown numerically by Gutkin *et al* [70, 71] that pairs of interior alphabet (65) spatiotemporal cat periodic states of a fixed spatial width L that share sets of sub-mosaics, shadow each other when evolved forward-in-time. Here, in section 8.2, we check numerically spatiotemporal cat shadowing for arbitrary periodic states, without alphabet restrictions, and without any time evolution. Intuitively, if two unstable periodic states Φ, Φ' share a common sub-mosaic \mathbf{M} of volume $N_{\mathbf{M}}$, they shadow each other with exponential accuracy of order of $\propto \exp(-\lambda N_{\mathbf{M}})$. In time-evolution formulation, λ is the leading Lyapunov exponent. What is it for spatiotemporal systems?

We first explain how the exponentially small distances follow for the one-dimensional case.

8.1. Shadowing, one-dimensional temporal cat

As the relation between the mosaics \mathbf{M} and the corresponding periodic states $\Phi_{\mathbf{M}}$ is linear, for \mathbf{M} an admissible mosaic, the corresponding periodic state $\Phi_{\mathbf{M}}$ is given by the Green's function

$$\Phi_{\mathbf{M}} = \mathbf{g} \mathbf{M}, \quad \mathbf{g} = \frac{1}{-r + s \mathbb{1} - r^{-1}}. \quad (143)$$

The Green's function (143) decays exponentially with the distance from the origin, a fact that is essential in establishing the 'shadowing' between periodic states sharing a common sub-mosaic \mathbf{M} . For an infinite temporal lattice $t \in \mathbb{Z}$, the lattice field at site t is determined by the sources $m_{t'}$ at all sites t' , by the Green's function $g_{tt'}$ for one-dimensional discretized heat equation [106, 115],

$$\phi_t = \sum_{t'=-\infty}^{\infty} g_{tt'} m_{t'}, \quad g_{tt'} = \frac{1}{\Lambda - \Lambda^{-1}} \frac{1}{\Lambda^{|t-t'|}}, \quad (144)$$

with Λ the expanding stability multiplier, the positive Lyapunov exponent $\lambda > 0$, and discriminant $D = \mu^2(\mu^2 + 4)$,

$$\begin{aligned} \Lambda^{\pm 1} &= e^{\pm \lambda} = \frac{1}{2}(s \pm \sqrt{D}) \\ \mu^2 &= \Lambda + \Lambda^{-1} - 2 = 2 \cosh(\lambda) - 2 \\ \sqrt{D} &= \mu^2 \sqrt{1 + 4/\mu^2} = \Lambda - \Lambda^{-1} = 2 \sinh(\lambda). \end{aligned} \quad (145)$$

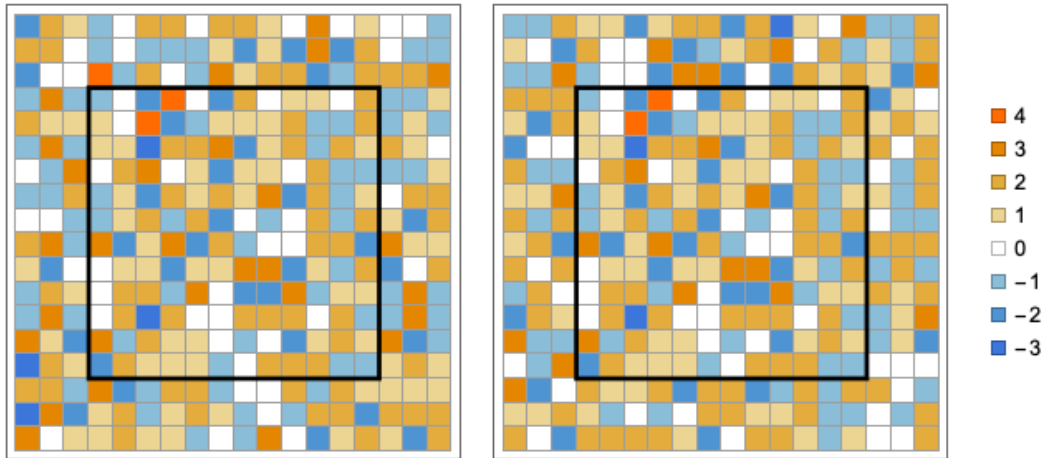


Figure 11. (Color online) Mosaics (45) of two $[18 \times 18]_0$ spatiotemporal cat periodic states which share the sub-mosaic within the $[12 \times 12]$ region enclosed by the black square, and have different, essentially random symbols outside the squares. Color coded 8-letter alphabet (64) for $\mu^2 = 1$. Continued in figure 12.

8.2. Shadowing, two-dimensional spatiotemporal cat

Following [70, 71], consider families of spatiotemporal orbits that share a sub-mosaic shadow each other in the corresponding spatiotemporal region. As the grammar of admissible mosaics is not known, the periodic states used in numerical examples were restricted to those whose mosaics used only the interior, always admissible, alphabet (65). Here we shall check numerically spatiotemporal cat shadowing for general periodic states, with no alphabet restrictions.

The two-dimensional $\mu^2 = 1$ spatiotemporal cat (58), periodic states are labelled by two-dimensional mosaics, 8-letter alphabet (64), as in figure 11.

To test the spatiotemporal cat spatiotemporal shadowing properties, we generated 500 periodic states of $\mu^2 = 1$, two-dimensional spatiotemporal cat with periodicity $[18 \times 18]_0$, all sharing the same $[12 \times 12]$ mosaic, with the symbols outside the common sub-mosaic essentially random, see figure 11. As we do not know the two-dimensional spatiotemporal cat grammar rules, we generated these 500 periodic states by taking a periodic state with the $[12 \times 12]$ mosaic, using it as a starting guess for the next periodic state by randomly changing the lattice site symbols outside the $[12 \times 12]$ mosaic, finding the new periodic state by solving the spatiotemporal cat Euler-Lagrange equation (57), and keeping only those solutions that still had the same $[12 \times 12]$ mosaic.

The spatiotemporal shadowing suggests that for periodic states with identical sub-mosaics of symbols, the distance between the corresponding field values decrease exponentially with the size of the shared mosaics.

To find the rate of decrease of distances between shadowing periodic states, we compute the mean point-wise distances of field values of the 250 pairs of periodic states over each lattice site in their primitive cells. The exponential shadowing of periodic

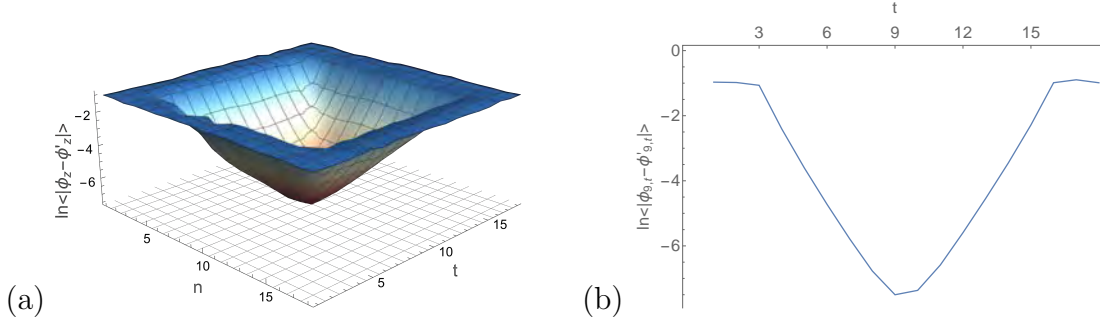


Figure 12. (Color online) $\mu^2 = 1$ spatiotemporal cat. (a) The log of mean of point-wise field value distances $|\phi_z - \phi'_z|$ over all lattice sites of $z \in [18 \times 18]$ primitive cell, averaged over the 250 pairs of periodic states, like the pair of figure 11. (b) The log of mean point-wise distances $|\phi_{9,t} - \phi'_{9,t}|$ evaluated across the strip $z = (9, t)$, $t = 1, 2, \dots, 18$, going through the center of the primitive cell. The decrease from edge to the center is approximately linear, with slope ≈ -1.079 .

states is shown in figure 12. The distances between field values of two periodic states $|\phi_z - \phi'_z|$ decrease exponentially as z approaches the center of the common sub-mosaic. Figure 12 (a) is the log plot of the mean distances. The logarithm of the mean distances across the center of the primitive cell is plotted in figure 12 (b), where the decrease is approximately linear, with a slope of -1.079 . What determines this slope?

8.3. Green's function of two-dimensional spatiotemporal cat

Mosaic \mathbf{M} is admissible (see section 1.9) if field configuration $\Phi_{\mathbf{M}}$ is a periodic state, i.e., all lattice site fields are confined to (63), the compact boson hypercube state space $\phi_z \in [0, 1)$.

The Green's function measures the correlation between two lattice sites in the spacetime. In our problem the distances between the shadowing periodic states can be interpreted using the Green's function, which gives variations of field values ϕ_t induced by a 'source', in this example by change of a letter $m_{t'}$ at lattice site z' . The decrease of the differences between field values of shadowing periodic states is a result of the decay of correlations. The Green's function for two-dimensional square lattice (62) has been extensively studied [49, 70, 72, 104]. But to understand qualitatively the exponential falloff of spacetime correlations, it suffices to consider the large spacetime primitive cell (small lattice spacing) continuum limit:

$$(-\square + \mu^2)\phi(x) = m(x), \quad x \in \mathbb{R}^2$$

whose Green's function is the radially symmetric

$$G(x, x') = \frac{1}{2\pi} K_0(\mu|x - x'|), \quad (146)$$

where K_0 is the **modified Bessel function of the second kind**. For large spacetime separations, $|x - x'| \rightarrow \infty$, the asymptotic form of the Green's function is

$$G(x, x') \sim \sqrt{\frac{1}{8\pi\mu r}} e^{-\mu r}, \quad r = |x - x'|. \quad (147)$$

In the numerical example of section 8.2, we have set Klein-Gordon mass $\mu = 1$, so the Green's function of the continuum screened Poisson equation is a good approximation to the discrete spatiotemporal cat Green's function, where the rate of decrease of correlations computed from the figure 12(b) is approximately $\exp(-\mu' r)$, where $\mu' = -1.079$ is the slope computed from the log plot of the mean distances of field values between shadowing periodic states.

8.4. Convergence of evaluations of observables

Computed on primitive cells \mathbb{A} of increasing volume $N_{\mathbb{A}}$, the expectation value of an observable (section 1.6) converges towards the exact, infinite Bravais lattice value (section 6.4). As the simplest case of such sequence of primitive cell approximations, take a rectangular primitive cell $[L \times T]_0$, and evaluate stability exponents $\langle \lambda \rangle_{[rL \times rT]}$ (section 6.3) for the sequence of primitive cell repeats $[rL \times rT]_0$ of increasing r .

That the convergence of such series of primitive cell approximations is a shadowing calculation can be seen by inspection of figure 5. The exact stability exponent $\langle \lambda \rangle$ is obtained by integration over the bands (smooth surfaces in the figures). A shadowing approximation $\langle \lambda \rangle_{[L \times T]_S}$ is a finite sum over primitive cells $[L \times T]_S$, black dots in the figures, that shadows the curved surface, with increasing accuracy as the primitive cell volume $N_{\mathbb{A}}$ increases. Here shadowing errors are Hipparchus' errors (77) of replacing arcs by cords, as in approximating 2π by the perimeter of a regular n -gon. The sense in which such shadowing or 'curvature' errors are exponentially small for one-dimensional, temporal lattice chaotic systems is explained in [10–12]. We have not extended such error estimates to the spatiotemporal case, so here we only present numerical evidence that they are exponentially small.

As a concrete example, we evaluate numerically the exact $\mu^2 = 1$ spatiotemporal cat stability exponent $\langle \lambda \rangle$ for the infinite Bravais lattice orbit Jacobian operator (112),

$$\langle \lambda \rangle = 1.507983 \dots, \quad (148)$$

and investigate the convergence of its finite primitive cell estimates $\langle \lambda \rangle_{[rL \times rT]}$. For the unit cell $[1 \times 1]_0$ sequence, plotted in figure 13, the logarithm of the difference $\langle \lambda \rangle - \langle \lambda \rangle_{[L \times L]_0}$ decreases linearly as the side length L increases. A linear fit has slope

$$\ln(\langle \lambda \rangle - \langle \lambda \rangle_{[L \times L]_0}) = -1.05538 L - 2.04611. \quad (149)$$

For various primitive cell sequences of rectangular shapes $[L \times T]_0$, the stability exponents of repeat primitive cells $[rL \times rT]_0$ also converge to $\langle \lambda \rangle$ exponentially, with the same convergence rate $\approx 1.055 \dots$. We have no theoretical estimate of this rate, but it appears to be as close to the Klein-Gordon mass $\mu = 1$ value as the shadowing errors of section 8.2.

Above error estimate is deeper than what it might appear at the first glance. In fluid dynamics, pattern recognition, neuroscience, field theory and other high or ∞ -dimensional settings, distances between 'close' spacetime field configurations (let's say pixel images of two faces in a face recognition code, or field theorists's field

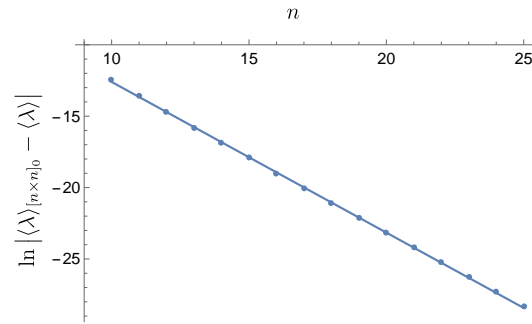


Figure 13. The distance $\langle \lambda \rangle - \langle \lambda \rangle_{\mathbb{A}}$ of the stability exponent of a finite primitive cell to the exact, infinite Bravais lattice value (148), for square primitive cells $[L \times L]_0$ sequence (149). Straight line is the linear fit of the logarithm of the distance as a function of the side length $L = 10, 11, \dots, 25$, with slope -1.05538 .

momenta expectation values $\langle \phi^m \rangle$) are almost always measured using some arbitrary yardstick, let's say a Euclidean L_2 norm, a distance that changes under general fields reparametrizations. Not so in the periodic orbit theory: here $1/|\text{Det } \mathcal{J}|$ weights lead to *intrinsic, coordinatization and norm independent* measure of the distance between close spatiotemporal field configurations.

9. Summary and discussion

The deterministic field theory developed here looks nothing like the textbook exposition [3, 40, 42, 81, 113, 122, 136] of temporally chaotic, few degrees-of-freedom dynamical systems. There one is given an *initial state*, which then evolves in time, much like in mechanics, where given an initial phase-space point, the integration of Hamilton's equations for traces out a phase-space trajectory.

In contrast, the deterministic field theory formulation is “Lagrangian,” in the sense that its building blocks are *orbits*, global field configurations that satisfy systems defining equations everywhere over the spacetime. Here there are no sketches of diverging trajectories and strange attractors, because in the deterministic field theory, spatiotemporal formulation of turbulence there is *no evolution* in time.

the theory is formulated in terms of prime orbits, minimal tilings of spacetime.

The measure concept here is akin to the statistical mechanics understanding of the Ising model - what is the likelihood of occurrence of a given spacetime configuration?

How is the deterministic chaotic field theory different from the

One might wonder why do we focus so much on computing periodic states over every small primitive cell, omitting none? You never see that anywhere in the literature.

There are at least two reasons. First, that what the theory demands: the support of a deterministic field theory is on *all* saddles, as sketched in figure 3.

And second –the beauty of the periodic orbit theory of chaos– due to the shadowing of longer periods unstable periodic states by shorter periods ones, the smallest periodicities periodic states dominate, the longer ones come in only as corrections.

How is a deterministic chaotic field theory different from a conventional field theory? By “spontaneous breaking of the symmetry” in a conventional theory one means that a solution does not satisfy a symmetry such as $\phi \rightarrow -\phi$; we, however, always work in the “broken-symmetry” regime, as almost every ‘turbulent’, spatiotemporally chaotic deterministic solution breaks all symmetries.

We work ‘beyond perturbation theory’, in the anti-integrable, strong coupling regime, in contrast to much of the literature that focuses on weak coupling expansions around a ‘ground state’.

And, in contrast to [18, 69, 105, 123, 148], our ‘far from equilibrium’ field theory has no added dissipation, and is not driven by external noise. All chaoticity is due to the intrinsic unstable deterministic dynamics, and our trace formulas (41) are exact, not merely saddle points approximations to the exact theory.

Acknowledgments

The work of H. L. was fully supported, and of P. C. was in part supported by the family of late G. Robinson, Jr.. This research was initiated during the KITP UC Santa Barbara 2017 *Recurrent Flows: The Clockwork Behind Turbulence* program, supported in part by the National Science Foundation under Grant No. NSF PHY-1748958. No actual cats, graduate or undergraduate were harmed during this research.

Appendix A. Spatiotemporal cat: History

The temporal lattice (59) (studied in companion paper I [93]), the one-dimensional case of spatiotemporal cat was studied by Percival and Vivaldi [115] as a Lagrangian reformulation of the Hamiltonian Thom-Anosov-Arnol’d-Sinai ‘cat map’ [8, 42, 137]. In two spacetime dimensions, the five-term recurrence relation (60) was introduced by Gutkin and Osipov [71].

In the Hamiltonian, forward-in-time temporal evolution formulation, the dynamics is generated by iterations of a linear cat *map*. In the spatiotemporal formulation there is *no map*, only the Euler-Lagrange equation, in form of a recurrence condition, so we refer to the three-term recurrence (59) as the ‘temporal cat’, and to the recurrence condition (57) in higher spatiotemporal dimensions as the ‘spatiotemporal cat’.

The d -dimensional spatiotemporal cat (57) is a generalization of the temporal cat (59) obtained by considering a $(d-1)$ -dimensional spatial lattice where each site field couples to its nearest spatial neighbors, in addition to its nearest past and future field values. If the spatial coupling strength is taken to be the same as the temporal coupling strength, one obtains the Euclidean, space \Leftrightarrow time-interchange symmetric difference equation (57).

A massive free boson over a square lattice is arguably the simplest field theory one can think of, studied by many, recently for example in [27, 28, 128]. It is a linear theory, with a Gaussian partition function, easy to evaluate. In contrast, spatiotemporal cat

is a *compact* boson theory (see section 2.1), a theory (indeed, any theory in which a neighborhood of a state space point is approximated by a local d -dimensional piecewise-linear chart) that is nonlinear in the sense that it is not defined globally by a single linear relation, such as the free-field theory (53), but by a set of distinct maps, such as the spatiotemporal cat (54).

Without compactification of the fields to a circle, Euler-Lagrange equation (57) is known as the discretized *screened Poisson equation* [45, 54], with parameter μ the reciprocal screening length in the Debye-Hückel or Thomas-Fermi approximations. In the homogeneous, free-field case (53), the screened Poisson equation is also known as the time-independent Yukawa or *Klein-Gordon equation* for a free boson of mass μ . Gutkin and Osipov [71] –for reasons that make sense in context of N -body quantum systems– refer to defining condition (60) as a ‘non-perturbed coupled cat map’. We, however, find the name ‘spatiotemporal cat’ [70] more descriptive.

Green’s functions for massive free-boson on integer lattices have been studied by many [7, 13, 23, 26–28, 30, 34, 49, 55, 65, 75, 76, 82–84, 98, 104, 106, 108, 109, 115, 128, 135, 147]. Variants of semi-classical (section 1.7) and deterministic (section 1.8) partition functions had been computed, by wildly different methods, in different contexts, by many [28, 78, 102], always on a given finite primitive cell (‘geometry’), but never on the infinite Bravais lattice, as we do here. We find Ivashkevich *et al* [78] partition function on torus with twisted boundary conditions the most informative. Campos *et al* [28] give explicit formula for the massless boson partition function in terms of a Dedekind eta function, and an analytic formula for the stability exponent. In mathematical physics, what we call orbit Jacobian operator \mathcal{J} (70), is called a ‘Jacobi matrix’, or discrete Schrödinger operator [24, 130–132]. We add prefix ‘orbit’ to make a distinction between the global stability, and the forward-in-time stability.

Elizalde *et al* [51] evaluate the Hill determinant using zeta function regularization.

Kittens live here. The screened Poisson equation is of the same form as the inhomogeneous Helmholtz equation, the only difference being the sign of μ^2 , with the oscillatory sin, cos replaced by the hyperbolic sinh, cosh, and exponentials [67]. Spatiotemporal cat is a lattice of hyperbolic ‘anti’ or ‘inverted’ oscillators [138, 141] on each site, coupled to their nearest neighbors. Think of the usual discretized Helmholtz-type field theory as a spring mattress [149]: you push it, and it pushes back, it oscillates. Spatiotemporal cat, on the other hand, has a ‘cat’ (a ‘rotor’) at every lattice site: you push it, and the cat runs away, but, thanks to the compact boson condition (57), it eventually has to come back. Chaos issues. Our task is to herd these cats over all of the spacetime.

In statistical mechanics, lattice discretized Helmholtz equation is known as the ‘Gaussian model’ [57, 80, 103, 127]. In his *Statistical Physics* textbook [80], Leo Kadanoff draws the Gaussian model phase diagram, explains the physics within the oscillatory $[-K, K]$ window, with K a real spring stiffness parameter, but dares not venture into imaginary K , real boson mass μ lands, as “dragons live here”. In this series of papers,

we have breached into this domain hitherto reputed unreachable [117], and report back that only kittens live here.

Appendix B. Examples of spatiotemporal cat periodic states

Explicitly verifying the Hill determinant formulas for two-dimensional spatiotemporal cat examples is now in order. The simplest examples of periodic states, illustrated by spatiotemporal mosaic tilings of figure 10, are (i) spacetime equilibria over $[1 \times 1]_0$, (ii) space-equilibria over $[1 \times T]_0$, (iii) time-equilibria over $[L \times 1]_0$, and (iv) time-relative equilibria over $[L \times 1]_S$, $S \neq 0$, stationary patterns in a time-reference frame [118] moving with a constant velocity S/T .

For explicit values of Hill determinants, we take the lowest integer value of the Klein-Gordon mass, $\mu^2 = 1$, throughout the paper.

Examples of square-lattice spatiotemporal cat primitive cells' Hill determinants.

(Continuation of calculations of section 3.1.) Consider first the family of primitive cells of temporal period one, $T = 1$ in (110),

$$\text{Det } \mathcal{J}_{[L \times 1]_0} = \mu^2 \prod_{m_1=1}^{L-1} \left[p \left(\frac{2\pi}{L} m_1 \right)^2 + \mu^2 \right]. \quad (\text{B.1})$$

This is the one-dimensional temporal cat Hill determinant, with calculations carried out as in (78). The steady state Hill determinant is

$$\text{Det } \mathcal{J}_{[1 \times 1]_0} = \mu^2 = 1, \quad (\text{B.2})$$

the period-2 periodic state Hill determinant is

$$\text{Det } \mathcal{J}_{[2 \times 1]_0} = \mu^2(\mu^2 + 4) = 5, \quad (\text{B.3})$$

and so on. However, for the simplest relative-periodic state, with slant $S/T = 1$, the Hill determinant is already more surprising, it is larger than $\text{Det } \mathcal{J}_{[2 \times 1]_0} = 5$:

$$\text{Det } \mathcal{J}_{[2 \times 1]_1} = \mu^2 [p(\pi)^2 + p(-\pi)^2 + \mu^2] = \mu^2(\mu^2 + 8) = 9. \quad (\text{B.4})$$

The spatiotemporal spatiotemporal cat calculations proceed as in example (98):

$$\text{Det } \mathcal{J}_{[2 \times 2]_0} = \mu^2(\mu^2 + 4)^2(\mu^2 + 8) = 225.$$

The Hill determinant formula (110) for the $[3 \times 2]_0$ periodic states,

$$\begin{aligned} \text{Det } \mathcal{J}_{[3 \times 2]_0} &= \prod_{m_1=0}^2 \prod_{m_2=0}^1 \left[p \left(\frac{2\pi}{3} m_1 \right)^2 + p \left(\frac{2\pi}{2} m_2 \right)^2 + \mu^2 \right] \\ &= 5120, \end{aligned} \quad (\text{B.5})$$

is in agreement with the fundamental fact count (C.5). Consider next the primitive cell $[3 \times 2]_1$ of figure 2(a), 6(a) and figure 7(b). We have computed

Table B1. The numbers of spatiotemporal cat periodic states for primitive cells $\mathbb{A} = [L \times T]_S$ up to $[3 \times 3]_2$. Here $N_{\mathbb{A}}(\mu^2)$ is the number of periodic states, $M_{\mathbb{A}}(\mu^2)$ is the number of prime orbits, and $R_{\mathbb{A}}$ is the number of prime orbits in the D_4 point-group orbit. The Klein-Gordon mass μ^2 can take only integer values.

\mathbb{A}	$N_{\mathbb{A}}(\mu^2)$	$M_{\mathbb{A}}(\mu^2)$	R
$[1 \times 1]_0$	μ^2	μ^2	1
$[2 \times 1]_0$	$\mu^2(\mu^2 + 4)$	$\mu^2(\mu^2 + 3)/2$	2
$[2 \times 1]_1$	$\mu^2(\mu^2 + 8)$	$\mu^2(\mu^2 + 7)/2$	
$[3 \times 1]_0$	$\mu^2(\mu^2 + 3)^2$	$\mu^2(\mu^2 + 2)(\mu^2 + 4)/3$	2
$[3 \times 1]_1$	$\mu^2(\mu^2 + 6)^2$	$\mu^2(\mu^2 + 5)(\mu^2 + 7)/3$	
$[4 \times 1]_0$	$\mu^2(\mu^2 + 2)^2(\mu^2 + 4)$	$\mu^2(\mu^2 + 1)(\mu^2 + 3)(\mu^2 + 4)/4$	2
$[4 \times 1]_1$	$\mu^2(\mu^2 + 4)^2(\mu^2 + 8)$	$\mu^2(\mu^2 + 3)(\mu^2 + 4)(\mu^2 + 5)/4$	
$[4 \times 1]_2$	$\mu^2(\mu^2 + 4)(\mu^2 + 6)^2$	$\mu^2(\mu^2 + 4)(\mu^2 + 5)(\mu^2 + 7)/4$	
$[4 \times 1]_3$	$\mu^2(\mu^2 + 4)^2(\mu^2 + 8)$	$\mu^2(\mu^2 + 3)(\mu^2 + 5)(\mu^2 + 8)/4$	
$[5 \times 1]_0$	$\mu^2(\mu^4 + 5\mu^2 + 5)^2$	$\mu^2(\mu^2 + 1)(\mu^2 + 2)(\mu^2 + 3)(\mu^2 + 4)/5$	2
$[5 \times 1]_1$	$\mu^2(\mu^4 + 10\mu^2 + 23)^2$	$\mu^2(\mu^2 + 3)(\mu^2 + 7)(\mu^4 + 10\mu^2 + 19)/5$	
$[2 \times 2]_0$	$\mu^2(\mu^2 + 4)^2(\mu^2 + 8)$	$\mu^2(\mu^2 + 3)/2 \times (\mu^4 + 13\mu^2 + 38)/2$	1
$[2 \times 2]_1$	$\mu^2(\mu^2 + 4)(\mu^2 + 6)^2$	$\mu^2(\mu^2 + 7)/2 \times (\mu^2 + 4)(\mu^2 + 5)/2$	
$[3 \times 2]_0$	$\mu^2(\mu^2 + 3)^2(\mu^2 + 4)(\mu^2 + 7)^2$	$\mu^2(\mu^2 + 3)(\mu^2 + 4)(\mu^6 + 17\mu^4 + 91\mu^2 + 146)/6$	2
$[3 \times 2]_1$	$\mu^2(\mu^2 + 4)^3(\mu^2 + 6)^2$	$\mu^2(\mu^2 + 3)(\mu^2 + 5)(\mu^6 + 16\mu^4 + 85\mu^2 + 151)/6$	
$[3 \times 3]_0$	$\mu^2(\mu^2 + 3)^4(\mu^2 + 6)^4$		1
$[3 \times 3]_1$	$\mu^2(\mu^2 + 3)^2(\mu^6 + 15\mu^4 + 72\mu^2 + 111)^2$		
$[3 \times 3]_2$	$\mu^2(\mu^2 + 3)^2(8s^3 + 3(\mu^2 + 4)^2 - 1)^2$		

the eigenvalues of its Laplacian in (98), so the corresponding Hill determinant (105) is

$$\text{Det } \mathcal{J}_{[3 \times 2]_1} = \mu^2(\mu^2 + 4)^3(\mu^2 + 6)^2 = 6125. \quad (\text{B.6})$$

For a list of such two-dimensional spatiotemporal cat Hill determinants, see table B1, and the list of the spatiotemporal cat Hill determinants evaluated for $\mu^2 = 1$, for primitive cells up to $[3 \times 3]_1$, see table B2.

For $\mu^2 = 1$ spatiotemporal cat the pruning turns out to be very severe. Only 52 of the prime $[2 \times 2]_0$ mosaics are admissible. As for the repeats of smaller mosaics, there are 2 admissible $[1 \times 2]_0$ mosaics repeating in time and 2 $[2 \times 1]_0$ mosaics repeating in space. There are 4 admissible 1/2-shift periodic boundary $[1 \times 2]_0$ mosaics. And there is 1 admissible mosaic which is a repeat of letter 0. The total number of $[2 \times 2]_0$ of periodic states is obtained by all cyclic permutations of admissible prime mosaics,

$$\begin{aligned} N_{[2 \times 2]_0} &= 225 \\ &= 52 [2 \times 2]_0 + 2 [2 \times 1]_0 + 2 [1 \times 2]_0 + 4 [2 \times 1]_1 + 1 [1 \times 1]_0, \end{aligned} \quad (\text{B.7})$$

summarized in table B2. This explicit list of admissible prime orbits verifies the Hill determinant formula (110).

Table B2. The numbers of the $\mu^2 = 1$ spatiotemporal cat $[L \times T]_S$ periodic states: $N_{[L \times T]_S}$ is the number of periodic states, $M_{[L \times T]_S}$ is the number of prime orbits, and $R_{[L \times T]_S}$ is the number of prime orbits in the D_4 symmetries orbit.

$[L \times T]_S$	M	N	R
$[1 \times 1]_0$	1	1	1
$[2 \times 1]_0$	2	$5 = 2 [2 \times 1]_0 + 1 [1 \times 1]_0$	2
$[2 \times 1]_1$	4	$9 = 4 [2 \times 1]_1 + 1 [1 \times 1]_0$	
$[3 \times 1]_0$	5	$16 = 5 [3 \times 1]_0 + 1 [1 \times 1]_0$	
$[3 \times 1]_1$	16	$49 = 16 [3 \times 1]_1 + 1 [1 \times 1]_0$	
$[4 \times 1]_0$	10	$45 = 10 [4 \times 1]_0 + 2 [2 \times 1]_0 + 1 [1 \times 1]_0$	
$[4 \times 1]_1$	54	$225 = 54 [4 \times 1]_1 + 4 [2 \times 1]_1 + 1 [1 \times 1]_0$	
$[4 \times 1]_2$	60	$245 = 60 [4 \times 1]_2 + 2 [2 \times 1]_0 + 1 [1 \times 1]_0$	
$[2 \times 2]_0$	52	$225 = 52 [2 \times 2]_0 + 2 [2 \times 1]_0 + 2 [1 \times 2]_0 + 4 [2 \times 1]_1 + 1 [1 \times 1]_0$	1
$[2 \times 2]_1$	60	$245 = 60 [2 \times 2]_1 + 2 [1 \times 2]_0 + 1 [1 \times 1]_0$	
$[3 \times 2]_0$	850	$5120 = 850 [3 \times 2]_0 + 5 [3 \times 1]_0 + 2 [1 \times 2]_0 + 1 [1 \times 1]_0$	
$[3 \times 2]_1$	1012	$6125 = 1012 [3 \times 2]_1 + 16 [3 \times 1]_2 + 2 [1 \times 2]_0 + 1 [1 \times 1]_0$	
$[3 \times 3]_0$	68281	$614656 = 68281 [3 \times 3]_0 + 5 [3 \times 1]_0 + 16 [3 \times 1]_1 + 16 [3 \times 1]_2 + 5 [1 \times 3]_0 + 1 [1 \times 1]_0$	1
$[3 \times 3]_1$	70400	$633616 = 70400 [3 \times 3]_1 + 5 [1 \times 3]_0 + 1 [1 \times 1]_0$	

Appendix B.1. Determining spatiotemporal cat periodic states

As we now show, the mosaic $\mathbf{M} = \{m_{nt} \in \mathcal{A}, (n, t) \in \mathbb{Z}^2\}$ can be used as a two-dimensional symbolic representation of the lattice system state. By the linearity of equation (57), every solution Φ can be uniquely recovered from its symbolic representation \mathbf{M} . Inverting (57) we obtain

$$\phi_z = \sum_{z' \in \mathbb{Z}^2} g_{zz'} m_{z'}, \quad g_{zz'} = \left(\frac{1}{-\square + \mu^2} \right)_{zz'}, \quad (\text{B.8})$$

where $g_{zz'}$ is the Green's function for the two-dimensional discretized screened Poisson equation. However, a given mosaic \mathbf{M} is *admissible* if and only if all $\phi_z \in \Phi$ given by (B.8) fall into the interval $[0, 1)$.

For a given admissible source mosaic \mathbf{M} , the periodic field can be computed by:

$$\Phi_{i_1 j_1} = \sum_{i_2=0}^2 \sum_{j_2=0}^1 \mathfrak{g}_{i_1 j_1, i_2 j_2} \mathbf{M}_{i_2 j_2}.$$

For example, if the source \mathbf{M} is:

$$\mathbf{M} = \begin{bmatrix} 0 & 2 & 0 \\ -1 & 0 & 0 \end{bmatrix},$$

the corresponding field is:

$$\Phi_{\mathbf{M}} = \begin{bmatrix} \phi_{01} & \phi_{11} & \phi_{21} \\ \phi_{00} & \phi_{10} & \phi_{20} \end{bmatrix} = \frac{1}{35} \begin{bmatrix} 5 & 17 & 6 \\ -1 & 5 & 3 \end{bmatrix}.$$

Substitute this solution into figure 7 (b) we can see that (60) is satisfied everywhere.

Appendix C. Spatiotemporal cat: Fundamental fact


As shown in the companion paper I [93], for one-dimensional lattice temporal cat Hill determinants count the numbers of period- n periodic states,

$$N_n = |\text{Det } \mathcal{J}|. \quad (\text{C.1})$$

We now show that for a spatiotemporal cat Hill determinant counts the number of periodic states in any spatiotemporal dimension d .

Spatiotemporal cat periodic state $\Phi_{\mathbf{M}}$ over primitive cell \mathbb{A} is a point within the unit hypercube $[0, 1)^{N_{\mathbb{A}}}$, where $N_{\mathbb{A}}$ is the primitive cell volume (8). Visualize now what spatiotemporal cat Euler-Lagrange equation (58)

$$\mathcal{J}_{\mathbb{A}} \Phi_{\mathbf{M}} - \mathbf{M} = 0$$

means geometrically. The $[N_{\mathbb{A}} \times N_{\mathbb{A}}]$ orbit Jacobian matrix $\mathcal{J}_{\mathbb{A}}$ stretches the state space unit hypercube $\Phi \in [0, 1)^{N_{\mathbb{A}}}$ into an $N_{\mathbb{A}}$ -dimensional *fundamental parallelepiped* (or parallelogram), and maps the periodic state $\Phi_{\mathbf{M}}$ into a point on integer lattice $\mathbb{Z}^{N_{\mathbb{A}}}$ within it, in the $N_{\mathbb{A}}$ -dimensional configuration state space (7). This point is then translated by integer winding numbers \mathbf{M} into the origin. What Baake *et al* [17] call the ‘*fundamental fact*’ follows: 

$$N_{\mathbb{A}} = |\text{Det } \mathcal{J}_{\mathbb{A}}|, \quad (\text{C.2})$$

the number of periodic states equals the number of integer lattice points within the fundamental parallelepiped.

For the history of ‘fundamental fact’ see *Appendix A. Historical context* of the companion paper I [93]. Reader might also want to check the figures of a few fundamental parallelepipeds there, but we know of no good way of presenting them visually for primitive cells of interest here, with $N_{\mathbb{A}} > 3$.

It is a peculiarity of the spatiotemporal cat that it involves two *distinct* integer lattices. (i) The spacetime *coordinates* (2) are discretized by integer lattice \mathbb{Z}^d . The primitive cell \mathbb{A} (6) is an example of a fundamental parallelepiped, and we use the fundamental fact when we express the volume (8) of the primitive cell, i.e. the determinant of the matrix \mathbb{A} , as the number of lattice sites within the primitive cell. (ii) For a spatiotemporal cat the lattice site *field* ϕ_z (57) is compactified to the unit circle $[0, 1)$, imparting integer lattice structure to the configuration *state space* (7): the orbit Jacobian matrix $\mathcal{J}_{\mathbb{A}}$ maps a periodic state $\Phi_{\mathbf{M}} \in [0, 1)^{N_{\mathbb{A}}}$ to a $\mathbb{Z}^{N_{\mathbb{A}}}$ integer lattice site \mathbf{M} . Nothing like that, and no ‘fundamental fact’ applies to general nonlinear field theories of section 2.

Example: Fundamental parallelepiped evaluation of a Hill determinant.

As a concrete example consider periodic states of two-dimensional spatiotemporal cat with periodicity $[3 \times 2]_0$, i.e., space period $L = 3$, time period $T = 2$ and tilt $S = 0$. Periodic states within the primitive cell and their corresponding mosaics can be written as two-dimensional $[3 \times 2]$ arrays:

$$\Phi_{[3 \times 2]_0} = \begin{bmatrix} \phi_{01} & \phi_{11} & \phi_{21} \\ \phi_{00} & \phi_{10} & \phi_{20} \end{bmatrix}, \quad \mathbf{M}_{[3 \times 2]_0} = \begin{bmatrix} m_{01} & m_{11} & m_{21} \\ m_{00} & m_{10} & m_{20} \end{bmatrix}.$$

Reshape the periodic states and mosaics into vectors:

$$\Phi_{[3 \times 2]_0} = \begin{pmatrix} \phi_{01} \\ \phi_{00} \\ \phi_{11} \\ \phi_{10} \\ \phi_{21} \\ \phi_{20} \end{pmatrix}, \quad \mathbf{M}_{[3 \times 2]_0} = \begin{pmatrix} m_{01} \\ m_{00} \\ m_{11} \\ m_{10} \\ m_{21} \\ m_{20} \end{pmatrix}. \quad (\text{C.3})$$

The reshaped orbit Jacobian matrix acting on these periodic states is a block matrix:

$$\mathcal{J}_{[3 \times 2]_0} = \left(\begin{array}{cc|cc|cc} 2s & -2 & -1 & 0 & -1 & 0 \\ -2 & 2s & 0 & -1 & 0 & -1 \\ \hline -1 & 0 & 2s & -2 & -1 & 0 \\ 0 & -1 & -2 & 2s & 0 & -1 \\ \hline -1 & 0 & -1 & 0 & 2s & -2 \\ 0 & -1 & 0 & -1 & -2 & 2s \end{array} \right). \quad (\text{C.4})$$

The fundamental parallelepiped generated by the action of orbit Jacobian matrix $\mathcal{J}_{[3 \times 2]_0}$ on the state space unit hypercube (57) is spanned by 6 primitive vectors, the columns of the orbit Jacobian matrix (C.4). The ‘fundamental fact’ now expresses the Hill determinant, i.e., the number of periodic states within the fundamental parallelepiped, as a polynomial of order $N_{\mathbb{A}}$ in the stretching factor s , or Klein-Gordon mass μ^2 (71),

$$\begin{aligned} N_{[3 \times 2]_0} &= |\text{Det } \mathcal{J}_{[3 \times 2]_0}| = 64s^6 - 288s^4 - 32s^3 + 288s^2 - 72s \\ &= \mu^2(\mu^2 + 3)^2(\mu^2 + 4)(\mu^2 + 7)^2, \end{aligned} \quad (\text{C.5})$$

without recourse to any explicit diagonalization, such as the reciprocal lattice diagonalization (110). For $\mu^2 = 1$ this agrees with the reciprocal lattice evaluation (B.5). For a list of the numbers of spatiotemporal cat periodic states for primitive cells $[L \times T]_S$ up to $[3 \times 3]_2$, see table B1.

Appendix D. Spectra of orbit Jacobian operators for nonlinear field theories

The simplicity of the spatiotemporal cat orbit Jacobian operator band spectrum (81), plotted in figure 4(a) and figure 5(a), is a bit misleading. As explained in section 3.2,

the uniform stretching factor s describes only the stability of a constant periodic state solution, for any field theory. To get a feeling for the general case, in section 10 of paper I [93] we compute the stability of a period-2 periodic state for two nonlinear field theories. Here we outline such calculations, to illustrate the essential difference between the very special spatiotemporal cat, and the general, nonlinear case. The first non-constant solution, a period-2 periodic state, suffices to illustrate the general case.

Appendix D.1. A one-dimensional temporal lattice

As an example of nonlinear field theory, consider the ϕ^3 theory (55)

$$-\square \phi_z + \mu^2 (1/4 - \phi_z^2) = 0.$$

In one spatiotemporal dimension, this field theory is a temporal lattice reformulation of the forward-in-time Hénon map, where large numbers of periodic solutions can be easily computed [68]. The theory has one period-2 prime orbit, conventionally labelled $\overline{LR} = \{\Phi_{LR}, \Phi_{RL}\}$:

$$\begin{bmatrix} \phi_0 \\ \phi_1 \end{bmatrix} = \begin{bmatrix} \bar{\phi} - \sqrt{\frac{1}{2} - \bar{\phi}^2} \\ \bar{\phi} + \sqrt{\frac{1}{2} - \bar{\phi}^2} \end{bmatrix}. \quad (\text{D.1})$$

where $\bar{\phi} = (\phi_0 + \phi_1)/2 = 2/\mu^2$ is the Birkhoff average (22) of the field ϕ_t .

The Bloch theorem (21) yields two bands of eigenfunctions,

$$\Lambda_{LR,\pm}(k) = -2 \pm \sqrt{\mu^4 - 12 - p(2k)^2}, \quad (\text{D.2})$$

plotted in the $k \in (-\pi/2, \pi/2]$ Brillouin zone in figure 4(b). For a finite primitive cell of even period, tiled by m th repeat of the period-2 periodic state Φ_p , the eigenvalues of its orbit Jacobian matrix are $\Lambda_{LR,\pm}(k)$ evaluated at k restricted to a discrete set of wave vectors k multiple of π/m : third and fourth repeats are plotted in figure 4(b).

Appendix D.2. A two-dimensional spatiotemporal lattice

Analytic eigenvalue formulas, such as (D.2), are feasible only for a few shortest period periodic states; in general, periodic states and the associated orbit Jacobian operator spectra are evaluated numerically. Consider spatiotemporal ϕ^4 lattice field theory (56) as an example. For Klein-Gordon mass-squared $\mu^2 = 5$, spatiotemporal ϕ^4 has a $[2 \times 1]_0$ prime orbit Φ_p :

$$\Phi_p = \left(0.447214, 0.894427 \right). \quad (\text{D.3})$$

The Bravais lattice orbit Jacobian operator has eigenstates which are products of plane waves and periodic functions (21), the two bands plotted in figure 5(b). For any finite primitive cell tiled by repeats of the prime orbit Φ_p , eigenstates of the orbit Jacobian matrix have a discrete set of wave vectors k . As an example, eigenvalues of a $[6 \times 4]_0$ periodic state tiled by 12 repeats of Φ_p have wave vectors k marked by black dots in figure 5(b).

For more such calculations, see paper III [146], where we study stabilities of large sets of nonlinear field theories periodic states.

Appendix E. Orbit Jacobian matrices as block matrices

By reshaping the d -dimensional periodic states as vectors the tensors, the multi-index orbit Jacobian matrices \mathcal{J} can be rewritten as block matrices. For example consider a $[L \times T]_0$ periodic state Φ_c of a two-dimensional spatiotemporal ϕ^4 theory (56). Reshape the spatiotemporal periodic state as a temporal periodic state with the spatial dependence treated as a multicomponent field at each temporal lattice site. Then the orbit Jacobian matrix is a $[T \times T]$ block matrix,

$$\mathcal{J}_A = \begin{pmatrix} \mathbf{s}_0 & -\mathbb{1} & & -\mathbb{1} \\ -\mathbb{1} & \mathbf{s}_1 & -\mathbb{1} & \\ & \ddots & \ddots & \ddots \\ & & -\mathbb{1} & \mathbf{s}_{T-2} & -\mathbb{1} \\ -\mathbb{1} & & & -\mathbb{1} & \mathbf{s}_{T-1} \end{pmatrix}, \quad (\text{E.1})$$

with $[L \times L]$ matrix block \mathbf{s}_t

$$\mathbf{s}_t = \begin{pmatrix} s_{0,t} & -1 & & -1 \\ -1 & s_{1,t} & -1 & \\ & \ddots & \ddots & \ddots \\ & & -1 & s_{L-2,t} & -1 \\ -1 & & & -1 & s_{L-1,t} \end{pmatrix}, \quad (\text{E.2})$$

and $\mathbb{1}$ a $[L \times L]$ identity matrix. For a periodic state with periodicity $[L \times T]_S$ the orbit Jacobian matrix is still a tri-diagonal block matrix, but with relative periodic boundary conditions, imposed by the non-zero shift S :

$$\mathcal{J} = \begin{pmatrix} \mathbf{s}_0 & -\mathbb{1} & & -\mathbf{r}_1^S \\ -\mathbb{1} & \mathbf{s}_1 & -\mathbb{1} & \\ & \ddots & \ddots & \ddots \\ & & -\mathbb{1} & \mathbf{s}_{T-2} & -\mathbb{1} \\ -\mathbf{r}_1^S & & & -\mathbb{1} & \mathbf{s}_{T-1} \end{pmatrix}, \quad (\text{E.3})$$

where \mathbf{r}_1 is a $[L \times L]$ cyclic shift matrix $(\mathbf{r}_1)_{n,n'} = \delta_{n+1,n'}$.

A spatiotemporal lattice field theory which couples adjacent field values by discrete Laplace operator (50) has orbit Jacobian matrices with tri-diagonal form similar to (E.1). For example, a $[L \times T]_0$ periodic state of a uniform stretching systems such as the two-dimensional spatiotemporal cat (54) has orbit Jacobian matrix (E.1)–(E.2) but $s_{l,t}$ is a constant $2s$ that does not depend on the field values at each lattice site. The spatiotemporal-translation invariance allows one to compute the eigenvalues of the orbit Jacobian matrix using the discrete Fourier transform.

Appendix F. Examples of prime primitive cells

The square lattice unit primitive cell,

$$\mathbb{A} = \begin{bmatrix} 1 & 0 \\ 0 & 1 \end{bmatrix}, \quad N_{\mathbb{A}} = 1, \quad (\text{F.1})$$

$[1 \times 1]_0$ -periodic field configuration, or the constant lattice field

$$\Phi = \begin{bmatrix} \phi_{00} \end{bmatrix}$$

is the unit cell of a square \mathbb{Z}^2 integer lattice.

$[2 \times 1]_0$ -periodic field configuration

$$\Phi = \begin{bmatrix} \phi_{00} & \phi_{10} \end{bmatrix},$$

$[1 \times 2]_0$ -periodic field configuration

$$\Phi = \begin{bmatrix} \phi_{01} \\ \phi_{00} \end{bmatrix}$$

have ‘bricks’ stacked atop each other, see mosaics of figure 10 (a) and (b).

$[2 \times 1]_1$ -periodic field configuration

$$\Phi = \begin{bmatrix} \phi_{00} & \phi_{10} \end{bmatrix}$$

has layers of ‘bricks’ stacked atop each other, but with a relative-periodic boundary condition, with layers shifted by $S = 1$, as in figure 7 (a).

The boundary conditions for the above three kinds of primitive cells can be illustrated by repeats of the three ‘bricks’, on top, sideways, and on top and shifted:

$$[2 \times 1]_0 \simeq \begin{bmatrix} \phi_{00} & \phi_{10} \\ \phi_{00} & \phi_{10} \end{bmatrix}, \quad [1 \times 2]_0 \simeq \begin{bmatrix} \phi_{01} & \phi_{01} \\ \phi_{00} & \phi_{00} \end{bmatrix}, \quad [2 \times 1]_1 \simeq \begin{bmatrix} & \phi_{00} & \phi_{10} \\ \phi_{00} & \phi_{10} & \end{bmatrix}.$$

$[3 \times 2]_1$ -periodic field configuration can be presented as a field over the *parallelepiped-shaped* tilted primitive cell of figure 2 (a),

$$[3 \times 2]_1 = \begin{bmatrix} & \phi_{11} & \phi_{21} & \phi_{01} \\ \phi_{00} & \phi_{10} & \phi_{20} & \end{bmatrix},$$

or as an $[3 \times 2]$ rectangular array an $[3 \times 2]$ rectangular array

$$\Phi = \begin{bmatrix} \phi_{01} & \phi_{11} & \phi_{21} \\ \phi_{00} & \phi_{10} & \phi_{20} \end{bmatrix}, \quad (\text{F.2})$$

with the Bravais lattice relative-periodicity imposed by a shift boundary condition, as in figure 7 (b) and the mosaic of figure 10 (f).

Appendix G. Enumeration of prime orbits

Here we show how to enumerate the total numbers of distinct periodic states in terms of prime orbits.

The enumeration of spatiotemporal cat doubly-periodic states proceeds in 3 steps:

- (i) Construct a hierarchy of two-dimensional Bravais lattices \mathcal{L} , starting with the smallest primitive cells, list Bravais lattices by increasing $[L \times T]_S$, one per each set related by translation symmetries (83) (here we are ignoring discrete point group D_4).
- (ii) For each $\mathcal{L} = [L \times T]_S$ Bravais lattice, compute $N_{\mathcal{L}}$, the number of doubly-periodic spatiotemporal cat periodic states, using the ‘fundamental fact’ $N_{\mathcal{L}} = |\text{Det } \mathcal{J}(\mathcal{L})|$.
- (iii) We have defined the *prime orbit* in section 5.4.

The total number of (doubly) periodic mosaics is the sum of all cyclic permutations of prime mosaics,

$$N_{\mathcal{L}} = \sum_p N_p [L_p \times T_p]_{S_p}$$

where the sum goes over prime tilings of the $[L \times T]_S$ mosaic.

$$M_n = \frac{1}{n} \left(N_n - \sum_{d|n}^{d < n} d M_d \right), \quad (\text{G.1})$$

where d 's are all divisors of n .

The number of prime orbits is given recursively by (see (G.1)),

$$M_p = \frac{1}{LT} \left(N_p - \sum_{p'} L_{p'} T_{p'} M_{p'} \right), \quad (\text{G.2})$$

where the sum is over p' , the prime divisors of p that satisfy tiling conditions.

Appendix G.1. Prime lattice field configurations

$$\begin{aligned} \sum_{L=1} N_{[L \times 1]_0} z^L &= \frac{s - 2z}{1 - sz + z^2} - \frac{2}{1 - z} \\ &= (s - 2) + (s - 2)z + (s - 2)(s + 2)z^2 + (s - 2)(s + 1)^2 z^3 \\ &\quad + (s - 2)(s + 2) s^2 z^4 + (s - 2)(s^2 + s - 1)^2 z^5 \\ &\quad + \dots, \end{aligned} \quad (\text{G.3})$$

Appendix H. Spectra of orbit Jacobian operators

Appendix H.1. Temporal lattice

Appendix H.2. Orbit Jacobian operator stability exponents

Hill determinants of finite-dimensional orbit Jacobian matrices can be computed as products of their eigenvalues. Hill determinants of the infinite-dimensional orbit Jacobian operators are not finite. To evaluate the stability of periodic states on the infinite lattice, we define the *stability exponent* $\langle \lambda_c \rangle$ (106) of periodic state c .

For an infinite repeat of a finite prime orbit, the stability exponent is computed as an integral of the logarithm of the eigenvalue function over wave vector k in the Brillouin zone. Consider spatiotemporal cat (58) as an example. The stability exponent $\langle \lambda \rangle$ of an infinite periodic state is:

$$\langle \lambda \rangle = \frac{1}{4\pi^2} \int_{-\pi}^{\pi} dk_1 \int_{-\pi}^{\pi} dk_2 \ln (2s - 2 \cos k_1 - 2 \cos k_2) . \quad (\text{H.1})$$

References

- [1] M. Akila, D. Waltner, B. Gutkin, P. Braun, and T. Guhr, “Semiclassical identification of periodic orbits in a quantum many-body system”, *Phys. Rev. Lett.* **118**, 164101 (2017).
- [2] M. Akila, D. Waltner, B. Gutkin, and T. Guhr, “Particle-time duality in the kicked Ising spin chain”, *J. Phys. A* **49**, 375101 (2016).
- [3] K. T. Alligood, T. D. Sauer, and J. A. Yorke, *Chaos, An Introduction to Dynamical Systems* (Springer, New York, 1996).
- [4] S. Anastassiou, “Complicated behavior in cubic Hénon maps”, *Theoret. Math. Phys.* **207**, 572–578 (2021).
- [5] S. Anastassiou, A. Bountis, and A. Bäcker, “Homoclinic points of 2D and 4D maps via the parametrization method”, *Nonlinearity* **30**, 3799–3820 (2017).
- [6] S. Anastassiou, A. Bountis, and A. Bäcker, “Recent results on the dynamics of higher-dimensional Hénon maps”, *Regul. Chaotic Dyn.* **23**, 161–177 (2018).
- [7] W. N. Anderson and T. D. Morley, “Eigenvalues of the Laplacian of a graph”, *Lin. Multilin. Algebra* **18**, 141–145 (1985).
- [8] V. I. Arnol’d and A. Avez, *Ergodic Problems of Classical Mechanics* (Addison-Wesley, Redwood City, 1989).
- [9] M. Artin and B. Mazur, “On periodic points”, *Ann. Math.* **81**, 82–99 (1965).
- [10] R. Artuso, E. Aurell, and P. Cvitanović, “Recycling of strange sets: I. Cycle expansions”, *Nonlinearity* **3**, 325–359 (1990).
- [11] R. Artuso, E. Aurell, and P. Cvitanović, “Recycling of strange sets: II. Applications”, *Nonlinearity* **3**, 361–386 (1990).
- [12] R. Artuso, H. H. Rugh, and P. Cvitanović, “Why does it work?”, in *Chaos: Classical and Quantum*, edited by P. Cvitanović, R. Artuso, R. Mainieri, G. Tanner, and G. Vattay (Niels Bohr Inst., Copenhagen, 2023).

- [13] J. H. Asad, “Differential equation approach for one- and two-dimensional lattice green’s function”, *Mod. Phys. Lett. B* **21**, 139–154 (2007).
- [14] N. W. Ashcroft and N. D. Mermin, *Solid State Physics* (Holt, Rinehart and Winston, 1976).
- [15] S. Aubry, “Anti-integrability in dynamical and variational problems”, *Physica D* **86**, 284–296 (1995).
- [16] S. Aubry and G. Abramovici, “Chaotic trajectories in the standard map. The concept of anti-integrability”, *Physica D* **43**, 199–219 (1990).
- [17] M. Baake, J. Hermisson, and A. B. Pleasants, “The torus parametrization of quasiperiodic LI-classes”, *J. Phys. A* **30**, 3029–3056 (1997).
- [18] E. Balkovsky, G. Falkovich, I. Kolokolov, and V. Lebedev, “Intermittency of Burgers’ turbulence”, *Phys. Rev. Lett.* **78**, 1452–1455 (1997).
- [19] E. Barreto, “Shadowing”, *Scholarpedia* **3**, 2243 (2008).
- [20] R. J. Baxter, “Some comments on developments in exact solutions in statistical mechanics since 1944”, *J. Stat. Mech.* **2010**, P11037 (2010).
- [21] J. Bell, Euler and the pentagonal number theorem, 2005.
- [22] E. H. Berger, *Die geographischen Fragmente des Hipparch* (Teubner, 1869).
- [23] H. S. Bhat and B. Osting, “Diffraction on the two-dimensional square lattice”, *SIAM J. Appl. Math.* **70**, 1389–1406 (2010).
- [24] T. Bountis and R. H. G. Helleman, “On the stability of periodic orbits of two-dimensional mappings”, *J. Math. Phys* **22**, 1867–1877 (1981).
- [25] L. Brillouin, “Les électrons libres dans les métaux et le role des réflexions de Bragg”, *J. Phys. Radium* **1**, 377–400 (1930).
- [26] B. L. Buzbee, G. H. Golub, and C. W. Nielson, “On direct methods for solving Poisson’s equations”, *SIAM J. Numer. Anal.* **7**, 627–656 (1970).
- [27] M. Campos, E. López, and G. Sierra, “Integrability and scattering of the boson field theory on a lattice”, *J. Phys. A* **54**, 055001 (2021).
- [28] M. Campos, G. Sierra, and E. López, “Tensor renormalization group in bosonic field theory”, *Phys. Rev. B* **100**, 195106 (2019).
- [29] J. L. Cardy, “Operator content of two-dimensional conformally invariant theories”, *Nucl. Phys. B* **270**, 186–204 (1986).
- [30] M. Chen, “On the solution of circulant linear systems”, *SIAM J. Numer. Anal.* **24**, 668–683 (1987).
- [31] M. Cheng and N. Seiberg, Lieb-Schultz-Mattis, Luttinger, and ’t Hooft – anomaly matching in lattice systems, 2022.
- [32] S.-N. Chow, J. Mallet-Paret, and W. Shen, “Traveling waves in lattice dynamical systems”, *J. Diff. Equ.* **149**, 248–291 (1998).

- [33] S.-N. Chow, J. Mallet-Paret, and E. S. Van Vleck, “Pattern formation and spatial chaos in spatially discrete evolution equations”, *Random Comput. Dynam.* **4**, 109–178 (1996).
- [34] F. Chung and S.-T. Yau, “Discrete Green’s functions”, *J. Combin. Theory A* **91**, 19–214 (2000).
- [35] D. Cimasoni, “The critical Ising model via Kac-Ward matrices”, *Commun. Math. Phys.* **316**, 99–126 (2012).
- [36] H. Cohen, *A Course in Computational Algebraic Number Theory* (Springer, Berlin, 1993).
- [37] M. M. P. Couchman, D. J. Evans, and J. W. M. Bush, “The stability of a hydrodynamic Bravais lattice”, *Symmetry* **14**, 1524 (2022).
- [38] P. Cvitanović, *Field Theory*, Notes prepared by E. Gyldenkerne (Nordita, Copenhagen, 1983).
- [39] P. Cvitanović, “Counting”, in *Chaos: Classical and Quantum* (Niels Bohr Inst., Copenhagen, 2023).
- [40] P. Cvitanović, R. Artuso, R. Mainieri, G. Tanner, and G. Vattay, *Chaos: Classical and Quantum* (Niels Bohr Inst., Copenhagen, 2023).
- [41] P. Cvitanović and H. Liang, *A chaotic lattice field theory in two dimensions*, In preparation, 2023.
- [42] R. L. Devaney, *An Introduction to Chaotic Dynamical systems*, 2nd ed. (Westview Press, Cambridge, Mass, 2008).
- [43] X. Ding, H. Chaté, P. Cvitanović, E. Siminos, and K. A. Takeuchi, “Estimating the dimension of the inertial manifold from unstable periodic orbits”, *Phys. Rev. Lett.* **117**, 024101 (2016).
- [44] X. Ding and P. Cvitanović, “Periodic eigendecomposition and its application in Kuramoto-Sivashinsky system”, *SIAM J. Appl. Dyn. Syst.* **15**, 1434–1454 (2016).
- [45] F. W. Dorr, “The direct solution of the discrete Poisson equation on a rectangle”, *SIAM Rev.* **12**, 248–263 (1970).
- [46] M. S. Dresselhaus, G. Dresselhaus, and A. Jorio, *Group Theory: Application to the Physics of Condensed Matter* (Springer, New York, 2007).
- [47] H. R. Dullin and J. D. Meiss, “Generalized Hénon maps: the cubic diffeomorphisms of the plane”, *Physica D* **143**, 262–289 (2000).
- [48] D. S. Dummit and R. M. Foote, *Abstract Algebra* (Wiley, 2003).
- [49] E. N. Economou, *Green’s Functions in Quantum Physics* (Springer, Berlin, 2006).
- [50] E. Elizalde, *Ten Physical Applications of Spectral Zeta Functions*, 2nd ed. (Springer, Berlin, 2012).
- [51] E. Elizalde, K. Kirsten, N. Robles, and F. Williams, “Zeta functions on tori using contour integration”, *Int. J. Geom. Methods M.* **12**, 1550019 (2015).

- [52] T. Engl, J. D. Urbina, and K. Richter, “Periodic mean-field solutions and the spectra of discrete bosonic fields: Trace formula for Bose-Hubbard models”, *Phys. Rev. E* **92**, 062907 (2015).
- [53] L. Fazza and T. Sulejmanpasic, “Lattice quantum Villain Hamiltonians: compact scalars, $U(1)$ gauge theories, fracton models and quantum Ising model dualities”, *J. High Energy Phys.* **2023**, 17 (2023).
- [54] A. L. Fetter and J. D. Walecka, *Theoretical Mechanics of Particles and Continua* (Dover, New York, 2003).
- [55] M. Fiedler, “Algebraic connectivity of graphs”, *Czech. Math. J* **23**, 298–305 (1973).
- [56] G. Floquet, “Sur les équations différentielles linéaires à coefficients périodiques”, *Ann. Sci. Ec. Norm. Sér* **12**, 47–88 (1883).
- [57] E. Fradkin, *Field Theories of Condensed Matter Physics* (Cambridge Univ. Press, Cambridge UK, 2013).
- [58] M. I. Freidlin and A. D. Wentzel, *Random Perturbations of Dynamical Systems* (Springer, Berlin, 1998).
- [59] S. Friedland and J. Milnor, “Dynamical properties of plane polynomial automorphisms”, *Ergodic Theory Dynam. Systems* **9**, 67–99 (1989).
- [60] P. Gaspard, *Chaos, Scattering and Statistical Mechanics* (Cambridge Univ. Press, Cambridge, 1997).
- [61] I. M. Gel’fand and A. M. Yaglom, “Integration in functional spaces and its applications in quantum physics”, *J. Math. Phys.* **1**, 48–69 (1960).
- [62] É. Ghys and J. Leys, “Lorenz and modular flows: a visual introduction”, *Amer. Math. Soc. Feature Column* (2006).
- [63] G. Giacomelli, S. Lepri, and A. Politi, “Statistical properties of bidimensional patterns generated from delayed and extended maps”, *Phys. Rev. E* **51**, 3939–3944 (1995).
- [64] F. Ginelli, P. Poggi, A. Turchi, H. Chaté, R. Livi, and A. Politi, “Characterizing dynamics with covariant Lyapunov vectors”, *Phys. Rev. Lett.* **99**, 130601 (2007).
- [65] J. I. Glaser, “Numerical solution of waveguide scattering problems by finite-difference Green’s functions”, *IEEE Trans. Microwave Theory Tech.* **18**, 436–443 (1970).
- [66] C. Godsil and G. F. Royle, *Algebraic Graph Theory* (Springer, New York, 2013).
- [67] I. S. Gradshteyn and I. M. Ryzhik, *Tables of Integrals, Series and Products*, 8th ed. (Elsevier LTD, Oxford, New York, 2014).
- [68] M. N. Gudorf, *Orbithunter: Framework for Nonlinear Dynamics and Chaos*, tech. rep. (School of Physics, Georgia Inst. of Technology, 2021).
- [69] V. Gurarie and A. Migdal, “Instantons in the Burgers equation”, *Phys. Rev. E* **54**, 4908–4914 (1996).

- [70] B. Gutkin, L. Han, R. Jafari, A. K. Saremi, and P. Cvitanović, “Linear encoding of the spatiotemporal cat map”, *Nonlinearity* **34**, 2800–2836 (2021).
- [71] B. Gutkin and V. Osipov, “Classical foundations of many-particle quantum chaos”, *Nonlinearity* **29**, 325–356 (2016).
- [72] A. J. Guttmann, “Lattice Green’s functions in all dimensions”, *J. Phys. A* **43**, 305205 (2010).
- [73] M. C. Gutzwiller, *Chaos in Classical and Quantum Mechanics* (Springer, New York, 1990).
- [74] G. W. Hill, “On the part of the motion of the lunar perigee which is a function of the mean motions of the sun and moon”, *Acta Math.* **8**, 1–36 (1886).
- [75] T. Horiguchi, “Lattice Green’s function for the simple cubic lattice”, *J. Phys. Soc. Jpn.* **30**, 1261–1272 (1971).
- [76] T. Horiguchi and T. Morita, “Note on the lattice Green’s function for the simple cubic lattice”, *J. Phys. C* **8**, L232 (1975).
- [77] S. Isola, “ ζ -functions and distribution of periodic orbits of toral automorphisms”, *Europhys. Lett.* **11**, 517–522 (1990).
- [78] E. V. Ivashkevich, N. S. Izmailian, and C.-K. Hu, “Kronecker’s double series and exact asymptotic expansions for free models of statistical mechanics on torus”, *J. Phys. A* **35**, 5543–5561 (2002).
- [79] N. S. Izmailian, K. B. Oganessian, and C.-K. Hu, “Exact finite-size corrections for the square-lattice Ising model with Brascamp-Kunz boundary conditions”, *Phys. Rev. E* **65**, 056132 (2002).
- [80] L. P. Kadanoff, *Statistical Physics: Statics, Dynamics and Renormalization* (World Scientific, Singapore, 2000).
- [81] A. Katok and B. Hasselblatt, *Introduction to the Modern Theory of Dynamical Systems* (Cambridge Univ. Press, Cambridge, 1995).
- [82] S. Katsura and S. Inawashiro, “Lattice Green’s functions for the rectangular and the square lattices at arbitrary points”, *J. Math. Phys.* **12**, 1622–1630 (1971).
- [83] S. Katsura, S. Inawashiro, and Y. Abe, “Lattice Green’s function for the simple cubic lattice in terms of a Mellin-Barnes type integral”, *J. Math. Phys.* **12**, 895–899 (1971).
- [84] S. Katsura, T. Morita, S. Inawashiro, T. Horiguchi, and Y. Abe, “Lattice Green’s function. Introduction”, *J. Math. Phys.* **12**, 892–895 (1971).
- [85] J. P. Keating, “The cat maps: quantum mechanics and classical motion”, *Nonlinearity* **4**, 309–341 (1991).
- [86] C. Kittel, *Introduction to Solid State Physics*, 8th ed. (Wiley, 2004).
- [87] S. Lang, *Linear Algebra* (Addison-Wesley, Reading, MA, 1987).
- [88] S. Lepri, A. Politi, and A. Torcini, “Chronotopic Lyapunov analysis. I. A detailed characterization of 1D systems”, *J. Stat. Phys.* **82**, 1429–1452 (1996).

- [89] S. Lepri, A. Politi, and A. Torcini, “Chronotopic Lyapunov analysis. II. Towards a unified approach”, *J. Stat. Phys.* **88**, 31–45 (1997).
- [90] S. Levit and U. Smilansky, “A new approach to Gaussian path integrals and the evaluation of the semiclassical propagator”, *Ann. Phys.* **103**, 198–207 (1977).
- [91] S. Levit and U. Smilansky, “A theorem on infinite products of eigenvalues of Sturm-Liouville type operators”, *Proc. Amer. Math. Soc.* **65**, 299–299 (1977).
- [92] M.-C. Li and M. Malkin, “Bounded nonwandering sets for polynomial mappings”, *J. Dynam. Control Systems* **10**, 377–389 (2004).
- [93] H. Liang and P. Cvitanović, “A chaotic lattice field theory in one dimension”, *J. Phys. A* **55**, 304002 (2022).
- [94] H. Liang and P. Cvitanović, *A derivation of hill’s formulas*, In preparation, 2024.
- [95] T. M. Liaw, M. C. Huang, Y. L. Chou, S. C. Lin, and F. Y. Li, “Partition functions and finite-size scalings of Ising model on helical tori”, *Phys. Rev. E* **73**, 041118 (2006).
- [96] D. A. Lind, “A zeta function for Z^d -actions”, in *Ergodic Theory of Z^d Actions*, edited by M. Pollicott and K. Schmidt (Cambridge Univ. Press, 1996), pp. 433–450.
- [97] D. A. Lind and B. Marcus, *An Introduction to Symbolic Dynamics and Coding* (Cambridge Univ. Press, Cambridge, 1995).
- [98] R. de la Llave, *Variational methods for quasiperiodic solutions of partial differential equations*, in *Hamiltonian Systems and Celestial Mechanics (HAMSYS-98)*, edited by J. Delgado, E. A. Lacomba, E. Pérez-Chavela, and J. Llibre (2000).
- [99] M. Ludewig, “Heat kernel asymptotics, path integrals and infinite-dimensional determinants”, *J. Geom. Phys.* **131**, 66–88 (2018).
- [100] J. Mallet-Paret and S.-N. Chow, “Pattern formation and spatial chaos in lattice dynamical systems. I”, *IEEE Trans. Circuits Systems I Fund. Theory Appl.* **42**, 746–751 (1995).
- [101] J. Mallet-Paret and S.-N. Chow, “Pattern formation and spatial chaos in lattice dynamical systems. II”, *IEEE Trans. Circuits Systems I Fund. Theory Appl.* **42**, 752–756 (1995).
- [102] A. Maloney and E. Witten, “Quantum gravity partition functions in three dimensions”, *J. High Energy Phys.* **2010**, 029 (2010).
- [103] E. C. Marino, *Quantum Field Theory Approach to Condensed Matter Physics* (Cambridge Univ. Press, Cambridge UK, 2017).
- [104] P. A. Martin, “Discrete scattering theory: Green’s function for a square lattice”, *Wave Motion* **43**, 619–629 (2006).
- [105] P. C. Martin, E. D. Siggia, and H. A. Rose, “Statistical dynamics of classical systems”, *Phys. Rev. A* **8**, 423–437 (1973).

- [106] B. D. Mestel and I. Percival, “Newton method for highly unstable orbits”, *Physica D* **24**, 172 (1987).
- [107] I. Montvay and G. Münster, *Quantum Fields on a Lattice* (Cambridge Univ. Press, Cambridge, 1994).
- [108] T. Morita, “Useful procedure for computing the lattice Green’s function - square, tetragonal, and bcc lattices”, *J. Math. Phys.* **12**, 1744–1747 (1971).
- [109] T. Morita and T. Horiguchi, “Calculation of the lattice Green’s function for the bcc, fcc, and rectangular lattices”, *J. Math. Phys.* **12**, 986–992 (1971).
- [110] G. Münster, “Lattice quantum field theory”, *Scholarpedia* **5**, 8613 (2010).
- [111] G. Münster and M. Walzl, *Lattice gauge theory - A short primer*, 2000.
- [112] Y. Okabe, K. Kaneda, M. Kikuchi, and C.-K. Hu, “Universal finite-size scaling functions for critical systems with tilted boundary conditions”, *Phys. Rev. E* **59**, 1585–1588 (1999).
- [113] E. Ott, *Chaos and Dynamical Systems* (Cambridge Univ. Press, Cambridge, 2002).
- [114] K. Palmer, “Shadowing lemma for flows”, *Scholarpedia* **4**, 7918 (2009).
- [115] I. Percival and F. Vivaldi, “A linear code for the sawtooth and cat maps”, *Physica D* **27**, 373–386 (1987).
- [116] H. Poincaré, “Sur les déterminants d’ordre infini”, *Bull. Soc. Math. France* **14**, 77–90 (1886).
- [117] H. Poincaré, *New Methods in Celestial Mechanics* (Springer, New York, 1992).
- [118] A. Politi and A. Torcini, “Periodic orbits in coupled Hénon maps: Lyapunov and multifractal analysis”, *Chaos* **2**, 293–300 (1992).
- [119] A. Politi, A. Torcini, and S. Lepri, “Lyapunov exponents from node-counting arguments”, *J. Phys. IV* **8**, 263 (1998).
- [120] M. Pollicott, Dynamical zeta functions, in *Smooth Ergodic Theory and Its Applications*, Vol. 69, edited by A. Katok, R. de la Llave, Y. Pesin, and H. Weiss (2001), pp. 409–428.
- [121] K. Richter, J. D. Urbina, and S. Tomsovic, “Semiclassical roots of universality in many-body quantum chaos”, *J. Phys. A* **55**, 453001 (2022).
- [122] R. C. Robinson, *An Introduction to Dynamical Systems: Continuous and Discrete* (Amer. Math. Soc., New York, 2012).
- [123] V. Rosenhaus and M. Smolkin, *Feynman rules for wave turbulence*, 2022.
- [124] D. Ruelle, “Generalized zeta-functions for Axiom A basic sets”, *Bull. Amer. Math. Soc* **82**, 153–157 (1976).
- [125] D. Ruelle, “Zeta-functions for expanding maps and Anosov flows”, *Inv. Math.* **34**, 231–242 (1976).
- [126] D. Ruelle, *Thermodynamic Formalism: The Mathematical Structure of Equilibrium Statistical Mechanics*, 2nd ed. (Cambridge Univ. Press, Cambridge, 2004).

- [127] R. Shankar, *Quantum Field Theory and Condensed Matter* (Cambridge Univ. Press, Cambridge UK, 2017).
- [128] Y. Shimizu, “Tensor renormalization group approach to a lattice boson model”, *Mod. Phys. Lett. A* **27**, 1250035 (2012).
- [129] C. L. Siegel and K. Chandrasekharan, *Lectures on the Geometry of Numbers* (Springer Berlin Heidelberg, Berlin, Heidelberg, 1989).
- [130] B. Simon, Almost periodic schröder operators: a review.
- [131] B. Simon, “Almost periodic Schrödinger operators: A review”, *Adv. Appl. Math.* **3**, 463–490 (1982).
- [132] S. Simons, “Analytical inversion of a particular type of banded matrix”, *J. Phys. A* **30**, 755 (1997).
- [133] E. M. Stein and R. Shakarchi, *Complex Analysis* (Princeton Univ. Press, Princeton, 2003).
- [134] D. Sterling and J. D. Meiss, “Computing periodic orbits using the anti-integrable limit”, *Phys. Lett. A* **241**, 46–52 (1998).
- [135] I. Stewart and D. Gökaydin, “Symmetries of quotient networks for doubly periodic patterns on the square lattice”, *Int. J. Bifur. Chaos* **29**, 1930026 (2019).
- [136] S. H. Strogatz, *Nonlinear Dynamics and Chaos* (Westview Press, Boulder, CO, 2014).
- [137] R. Sturman, J. M. Ottino, and S. Wiggins, *The Mathematical Foundations of Mixing* (Cambridge Univ. Press, 2006).
- [138] V. Subramanyan, S. S. Hegde, S. Vishveshwara, and B. Bradlyn, “Physics of the inverted harmonic oscillator: From the lowest Landau level to event horizons”, *Ann. Phys.* **435**, 168470 (2021).
- [139] M. Toda, *Theory of Nonlinear Lattices* (Springer, Berlin, 1989).
- [140] J. H. Van Vleck, “The correspondence principle in the statistical interpretation of quantum mechanics”, *Proc. Natl. Acad. Sci.* **14**, 178–188 (1928).
- [141] G. Vattay, “Noise and quantum corrections to trace formulas”, in *Chaos: Classical and Quantum*, edited by P. Cvitanović, R. Artuso, R. Mainieri, G. Tanner, and G. Vattay (Niels Bohr Inst., Copenhagen, 1997).
- [142] Y. Colin de Verdière, “Spectrum of the Laplace operator and periodic geodesics: thirty years after”, *Ann. Inst. Fourier* **57**, 2429–2463 (2007).
- [143] Wikipedia contributors, [Index of a subgroup](#) — Wikipedia, The Free Encyclopedia, 2022.
- [144] Wikipedia contributors, [Chord \(geometry\)](#) — Wikipedia, The Free Encyclopedia, 2023.
- [145] Wikipedia contributors, [Lyapunov time](#) — Wikipedia, The Free Encyclopedia, 2023.

- [146] S. V. Williams, X. Wang, H. Liang, and P. Cvitanović, *Nonlinear chaotic lattice field theory*, In preparation, 2023.
- [147] W. L. Wood, “Periodicity effects on the iterative solution of elliptic difference equations”, *SIAM J. Numer. Anal.* **8**, 439–464 (1971).
- [148] H. W. Wyld, “Formulation of the theory of turbulence in an incompressible fluid”, *Ann. Phys.* **14**, 143–165 (1961).
- [149] A. Zee, *Quantum Field Theory in a Nutshell*, 2nd ed. (Princeton Univ. Press, Princeton NJ, 2010).
- [150] R. M. Ziff, C. D. Lorenz, and P. Kleban, “Shape-dependent universality in percolation”, *Physica A* **266**, 17–26 (1999).